

Université de Montréal

Implication de la voie de dégradation ubiquitine-dépendante dans la  
pathologie des maladies de surcharge lysosomale

par

Panojot Bifsha

11627719

Département de Biochimie

Faculté de Médecine

Mémoire présenté à la Faculté des études supérieures  
en vue de l'obtention du grade de  
Maître ès sciences  
en Biochimie

Mai, 2005

© Panojot Bifsha, 2005

Université de Montréal  
Faculté des études supérieures



W  
4  
U58  
2005  
V.113

## **AVIS**

L'auteur a autorisé l'Université de Montréal à reproduire et diffuser, en totalité ou en partie, par quelque moyen que ce soit et sur quelque support que ce soit, et exclusivement à des fins non lucratives d'enseignement et de recherche, des copies de ce mémoire ou de cette thèse.

L'auteur et les coauteurs le cas échéant conservent la propriété du droit d'auteur et des droits moraux qui protègent ce document. Ni la thèse ou le mémoire, ni des extraits substantiels de ce document, ne doivent être imprimés ou autrement reproduits sans l'autorisation de l'auteur.

Afin de se conformer à la Loi canadienne sur la protection des renseignements personnels, quelques formulaires secondaires, coordonnées ou signatures intégrées au texte ont pu être enlevés de ce document. Bien que cela ait pu affecter la pagination, il n'y a aucun contenu manquant.

## **NOTICE**

The author of this thesis or dissertation has granted a nonexclusive license allowing Université de Montréal to reproduce and publish the document, in part or in whole, and in any format, solely for noncommercial educational and research purposes.

The author and co-authors if applicable retain copyright ownership and moral rights in this document. Neither the whole thesis or dissertation, nor substantial extracts from it, may be printed or otherwise reproduced without the author's permission.

In compliance with the Canadian Privacy Act some supporting forms, contact information or signatures may have been removed from the document. While this may affect the document page count, it does not represent any loss of content from the document.

Université de Montréal  
Faculté des études supérieures

Ce mémoire intitulé :  
Implication de la voie de dégradation ubiquitine-dépendante dans la  
pathologie des maladies de surcharge lysosomale

présenté par :  
Panojot Bifsha

a été évalué par un jury composé des personnes suivantes :

Président-rapporteur : Alain Moreau  
Directeur de recherche : Alexei Pchejetski  
Membre du jury : Marie-Josée Hébert

Mémoire accepté le :

## ACKNOWLEDGEMENTS

This work was supported in part by the operating grant from Canadian Institutes of Health Research MT-38107, Genome Canada/Genome Quebec grant and by the equipment grant from Canadian Foundation for Innovation to Dr Alexey V. Pshezhetsky. It is also worth mentioning the contribution of Dr Rob Sladek and the Genome Quebec Microarray Facility for the gene microarray studies. First and foremost, many thanks to Dr Pshezhetsky for offering me a position in his prestigious laboratory, for his relentless efforts towards my supervision and his overall support in conducting research. I greatly appreciate the predoctoral summer studentship offered by the Canadian Society for Mucopolysaccharide and Related Disease, which allowed me to initiate these studies. This work would not have been possible without the contribution of every laboratory team member and the collaboration of select members of the scientific community, who provided helpful suggestions and who were willing to share their results. Consequently, I would like to thank Mme Karine Landry for helping me to integrate into the lab and for her enormous contribution in the realization of this project in biochemistry techniques (immunocytochemistry, westerns, Real-time PCR). Dr Volkan Seyrantepe supervised me in matters of molecular biology such as gene cloning techniques (UCH-L1 subcloning and siRNA studies). Dr Mila Ashmarina helped in the interpretation of microarray results and the elaboration of the main hypothesis. Mme Stéphanie Trudel helped in the mass spectrometry analysis of mouse brains and Mme Christianne Quiniou in the westerns of apoptotic proteins. Dr Roy Gravel, of the University of Calgary, provided Sandhoff mouse brains. I apologize if the name of certain individuals could not be included herein, but I will never cease to recognize their benevolence. Lastly, I would like to thank my parents for their encouragement in pursuing graduate studies.

## **Table of contents**

<b>LIST OF FIGURES.....</b>	<b>vi</b>
<b>LIST OF TABLES.....</b>	<b>vii</b>
<b>ABBREVIATIONS.....</b>	<b>viii</b>
<b>ABSTRACT.....</b>	<b>1</b>
<b>RÉSUMÉ.....</b>	<b>2</b>
<b><u>LITERATURE REVIEW.....</u></b>	<b>3</b>
<b>LYSOSOMAL STORAGE DISORDERS.....</b>	<b>3</b>
-Endosomal-lysosomal system.....	4
-Concept of lysosomal storage.....	7
-Pathological features.....	9
-Cellular pathology.....	11
-Animal models of lysosomal storage disorders.....	14
-Diagnosis and strategies of treatment.....	17
<b>PROGRAMMED CELL DEATH (APOPTOSIS).....</b>	<b>18</b>
-Apoptotic protease activation.....	18
-Regulators of apoptosis.....	19
-Two pathways of caspase activation.....	20
-The consequences of caspase activation.....	23
-Caspase-independent pathways.....	23
<b>UBIQUITIN-PROTEASOMAL SYSTEM (UPS).....</b>	<b>24</b>
-Deubiquitinating enzymes and UCH-L1.....	25
-Animal model for UCH-L1 deficiency (GAD mouse).....	27
-Role of ubiquitination in apoptosis.....	29
-Involvement of UPS in neurodegeneration.....	32
<b>INTRODUCTION.....</b>	<b>37</b>
<b><u>MATERIALS AND METHODS.....</u></b>	<b>41</b>
-Cell culture.....	41
-mRNA quantification by real-time PCR.....	41
-Confocal immunofluorescence microscopy.....	42
-Enzymatic assays.....	44
-Western blotting.....	45
-Proteasomal activity assays.....	46
·UCH-L1 overexpression studies and apoptosis detection.....	47
-Quantification of UCH-L1 protein in brain extracts by tandem mass spectrometry.....	48

-UCH-L1 small interfering RNA gene silencing in human skin fibroblasts.....	50
-Detection of pro- and anti-apoptotic proteins in UCH-L1 siRNA-treated cells.....	53
<b>RESULTS AND DISCUSSION.....</b>	<b>54</b>
<b>UCH-L1 AND LYSOSOMAL STORAGE.....</b>	<b>54</b>
-Reduced UCH-L1 mRNA levels in fibroblasts from LSD patients and Sandhoff mouse brains.....	54
-Reduced ubiquitin hydrolase activity and UCH-L1 protein levels in fibroblasts of LSD patients.....	58
-Reduced UCH-L1 protein levels in Sandhoff mouse brains.....	59
-E-64-induced lysosomal storage results in reduced expression of UCH-L1.....	62
<b>UBIQUITIN-PROTEASOME PATHWAY IN LYSOSOMAL STORAGE.....</b>	<b>64</b>
-Decreased proteasomal activity in human fibroblasts with lysosomal storage.....	64
-Impaired proteasomal activity in Sandhoff mouse brains.....	67
-Lysosomal storage induces formation of ubiquitin protein aggregates and reduced level of free ubiquitin.....	67
<b>APOPTOSIS AND LYSOSOMAL STORAGE.....</b>	<b>69</b>
-Fibroblasts with lysosomal storage display higher apoptosis rates.....	71
-Overexpression of UCH-L1 in fibroblasts with lysosomal storage rescues them from apoptosis.....	73
-Suppression of UCH-L1 in normal fibroblasts induces caspase-mediated apoptosis.....	74
-Apoptotic proteins bax, bcl-2 and p53 are increased in UCH-L1 suppressed fibroblasts.....	79
<b>CONCLUSIONS AND PERSPECTIVES.....</b>	<b>82</b>
<b>REFERENCES.....</b>	<b>88</b>

## **LIST OF FIGURES**

<b>FIGURE 1: The lysosomal network.....</b>	<b>6</b>
<b>FIGURE 2: Molecular elements of the apoptotic cascade.....</b>	<b>21</b>
<b>FIGURE 3: Generic mass spectrometry (MS)-based proteomics experiment.....</b>	<b>49</b>
<b>FIGURE 4: Mechanism of RNA interference (RNAi).....</b>	<b>52</b>
<b>FIGURE 5: Lysosomal storage bodies in the cells of patients affected with sialidosis and sialic acid storage disease.....</b>	<b>55</b>
<b>FIGURE 6: Suppression of UCH-L1 in cultured fibroblasts obtained from LSD patients.....</b>	<b>56</b>
<b>FIGURE 7: Immunohistochemical detection of UCH-L1 in control cells and cells obtained from LSD patients.....</b>	<b>57</b>
<b>FIGURE 8: Ubiquitin hydrolase activity in control cells and cells of LSD patients.....</b>	<b>58</b>
<b>FIGURE 9: Comparison of UCH-L1 cDNA and protein levels in total brains of Sandhoff mouse model.....</b>	<b>59</b>
<b>FIGURE 10: Western blots for UCH-L1 in Sandhoff mouse brains.....</b>	<b>60</b>
<b>FIGURE 11: Identification and quantification of UCH-L1 protein in brain lysates of Sandhoff mouse model by tandem mass spectrometry.....</b>	<b>61</b>
<b>FIGURE 12: Ubiquitinated lysosomal storage bodies in cultured skin fibroblasts treated with E-64.....</b>	<b>63</b>
<b>FIGURE 13: Decrease of proteosomal activity in cultured skin fibroblasts from LSD patients.....</b>	<b>65</b>
<b>FIGURE 14: Decrease of proteosomal activity in brain tissues of Sandhoff mice.....</b>	<b>66</b>
<b>FIGURE 15: Detection of ubiquitinated proteins in cells with lysosomal storage.....</b>	<b>68</b>
<b>FIGURE 16: Ubiquitin western blot of fibroblasts of LSD patients.....</b>	<b>69</b>
<b>FIGURE 17: Development of lysosomal storage, UCH-L1 deficiency and apoptosis in cultured skin fibroblasts treated with E-64.....</b>	<b>70</b>
<b>FIGURE 18: E-64-treated fibroblasts show decreased UCH-L1 protein and increased apoptosis.....</b>	<b>72</b>
<b>FIGURE 19: Development of apoptosis in cultured skin fibroblasts from LSD patients.....</b>	<b>73</b>
<b>FIGURE 20: Suppression of E-64-induced apoptosis in cultured skin fibroblasts.....</b>	<b>75</b>
<b>FIGURE 21: Inhibition of UCH-L1 expression in cultured human skin fibroblasts by siRNA.....</b>	<b>77</b>
<b>FIGURE 22: Induction of apoptosis by siRNA-induced inhibition of UCH-L1 expression.....</b>	<b>78</b>
<b>FIGURE 23: Expression of pro- and anti-apoptotic proteins in cultured skin fibroblasts treated with UCH-L1 siRNA.....</b>	<b>81</b>
<b>FIGURE 24: Proposed scheme of UCH-L1-mediated apoptosis following lysosomal storage.....</b>	<b>85</b>



**LIST OF TABLES**

<i>TABLE I: Non-exhaustive list of LSD with defective enzyme(s) and corresponding metabolite accumulation.....</i>	<i>8</i>
<i>TABLE II: Clinicopathological LSD phenotypes.....</i>	<i>10</i>
<i>TABLE III: Non-exhaustive list of mouse models of human LSD.....</i>	<i>15</i>
<i>TABLE IV: Neurodegenerative disorders with ubiquitin-immunoreactivity in cell inclusions.....</i>	<i>34</i>
<i>TABLE V: Major groups of proteins whose expression was changed in both SIASD and sialidosis fibroblasts.....</i>	<i>40</i>
<i>TABLE VI: PCR primers and conditions used to measure concentration of UCH-L1 mRNA in cultured fibroblasts and mouse brain.....</i>	<i>42</i>
<i>TABLE VII: siRNA primers used to downregulate UCH-L1 in cultured fibroblasts.....</i>	<i>50</i>

**ABBREVIATIONS**

AD	Alzheimer's disease
AMC	7-amido-4-methylcoumarin
CAS	Caspase
DAPI	4,6-diamidino-2-phenylindole;
DMSO	Dimethylsulfoxide
DTT	Dithiothreitol
E-64	(epoxysuccinyl-leucylamido-(4-guanidino)butane
EDTA	Ethylenediaminetetraacetic acid
FMK	Fluoromethylketone
GAPDH	Glyceraldehyde-3-phosphate dehydrogenase
GI	Gaucher disease type I
GII	Gaucher disease type II
GM1	GM1-gangliosidosis
GS	Galactosialidosis
HEX	Hexosaminidase
HPLC	High performance liquid chromatography
LC-MS/MS	Liquid chromatography-tandem mass spectrometry
LSD	Lysosomal storage disorder/disease
MA	Morquio syndrome type A
MB	Morquio syndrome type B
MEM	Minimum essential medium
PAGE	Polyacrylamide gel electrophoresis
PBS	Phosphate-buffered saline
PD	Parkinson's disease
SDS	Sodium dodecyl sulfate
SIASD	Sialic acid storage disease
SL	Sialidosis
TBS	Tris buffered saline
UCH-L1	Ubiquitin C-terminal hydrolase L1 (PGP 9.5)
UPS	Ubiquitin-proteasome system

## **ABSTRACT**

Increased programmed cell death is an important pathological feature underlying the tissue and organ malfunction seen in lysosomal storage disorders (LSD). Using expression microarrays, differentially expressed genes that were common to cultured fibroblasts from patients affected with several different LSDs were identified. These studies, confirmed by biochemical experiments, demonstrated that lysosomal storage is associated with down-regulation of the most abundant cellular ubiquitin C-terminal hydrolase, UCH-L1 (PGP 9.5), in cultured fibroblasts of patients representing 8 different LSDs as well as in the brain tissues of a mouse model of Sandhoff disease with a disrupted hexosaminidase B gene. Induction of lysosomal storage by treatment of cultured fibroblasts with the lysosomal cysteine protease inhibitor E-64 reduced UCH-L1 transcripts, protein levels and enzyme activity. All cells and tissues exhibiting lysosomal storage contained ubiquitinated protein aggregates, and showed reduced levels of free ubiquitin, decreased proteasomal activity, and increased numbers of apoptotic cells. The increased rate of apoptosis seen in E64-treated fibroblasts was reversed by transient transfection with a UCH-L1 expression vector. In contrast, siRNA mediated down-regulation of UCH-L1 resulted in high apoptosis rates with concomitant increase in the expression of pro-apoptotic proteins such as Bax and p53. Taken together, these data suggest that UCH-L1 deficiency and partial impairment of the ubiquitin-dependent protein degradation pathway may represent a common mechanism for the pathogenesis of lysosomal storage disorders.

Keywords: Lysosome, proteasome, UCH-L1, ubiquitin, apoptosis, inclusions, neurodegeneration

## RÉSUMÉ

La mort programmée accrue de cellules est un dispositif pathologique important sous-tendant les défauts de fonctionnement du tissu et de l'organe dans les désordres de surcharge lysosomale (SL). Nous montrons que l'apoptose dans les cellules avec de la SL se réalise par l'entremise d'un affaiblissement partiel de la voie de dégradation ubiquitine-dépendante. En utilisant des micropuces d'expression, nous avons évalué les changements secondaires des profils d'ARN messenger dans les fibroblastes cultivés de patients affectés avec plusieurs différentes maladies de SL et avons identifié les gènes différentiellement exprimés qui étaient communs à ces conditions. Ces études, confirmées par des expériences biochimiques, ont démontré que la SL est associée avec la sous-régulation de la plus abondante hydrolase d'ubiquitine C-terminale, soit UCH-L1 (PGP 9.5), dans tous les patients représentant huit désordres de SL différents. Les niveaux de transcrits UCH-L1, de protéine et d'activité ont été également réduits dans des cellules normales en lesquelles la SL a été induite par l'inhibiteur lysosomal de cystéine protéases, E-64. Toutes les cellules montrant de la SL contenaient des agrégats de protéines ubiquitinées, en plus des niveaux réduits d'ubiquitine libre, inhibition partielle de l'activité du proteasome et un nombre accru de cellules apoptotiques. Le taux d'apoptose accru observé chez les fibroblastes traités avec E-64 a pu être reversé lors d'une transfection temporaire avec le vecteur d'expression pour UCH-L1. D'autre part, la suppression de UCH-L1 par interférence d'ARN dans des fibroblastes normaux a précipité ces derniers vers l'apoptose avec une élévation concomitante de l'expression des protéines pro-apoptotiques Bax et p53. Nous spéculons que l'insuffisance en UCH-L1 ainsi que la dérégulation partielle de la voie de dégradation ubiquitine-dépendante représentent un mécanisme commun pour la pathogénèse des maladies de surcharge lysosomale.

Mots-clés : Lysosome, protéasome, UCH-L1, ubiquitine, apoptose, inclusions, neurodégénération

## LITERATURE REVIEW

### LYSOSOMAL STORAGE DISORDERS

Cellular composition is determined by the maintenance of a balance between degradation and synthesis of intracellular components. This homeostasis can be perturbed when either process is impaired especially during adaptive changes, leading to cell and tissue deregulation. Component turnover is not only important for the sake of salvaging damaged or unnecessary by-products, but is also essential in the redirection of ongoing processes toward new needs. For example, protein degradation rates are increased during muscle hypertrophy and liver regeneration.

In lysosomal storage disorders (LSD), defects in lysosomal enzymes, in lysosomal transmembrane transporters, in hydrolase cofactors or in the biogenesis of the organelle itself, causes the sequestration of the corresponding unprocessed substrates inside the lysosomes and renders virtually impossible the further reutilization of the monomeric components. This affects the architecture and function of the cells, tissues and organs (extralysosomal effects) even though in very few cases the accumulated substrate may be directly cytotoxic. The signs associated with LSDs are often neurological, but can also be multisystemic, with skeletal, CNS, cardiovascular and ocular defects.

The clinical course of these diseases is chronic and progressive, very often lethal before or in early adulthood. Over 40 types of lysosomal storage diseases have been identified, with a collective incidence of 1 in 7000-8000 (Winchester et al, 2000) live births, and they have been grouped according to similarities in the biochemistry of accumulated materials, the clinical presentation and the enzymatic deficiencies. In terms of the storage material, LSDs can be divided into three large groups, the sphingolipidoses, mucopoly-

saccharidoses, glycoproteinoses and several other individual entities (Table I, p.8). The inheritance is autosomal recessive for most LSDs, except for MPS II and Fabry disease. Most of the LSDs can be diagnosed by the assay of enzymes in circulating leucocytes, biopsy material or cultured skin fibroblasts. Almost all of the genes responsible for the variety of LSDs have been cloned and this information is being used for genotype-phenotype correlation, genetic counseling and selection of patients for novel forms of therapy.

### *Endosomal-lysosomal system*

Lysosomes are organelles specialized for the intracellular digestion of macromolecules and are filled with hydrolytic enzymes operating optimally at an acidic pH of about 5.0. Lysosomes contain about 40 types of hydrolytic enzymes or acid hydrolases, including proteases, nucleases, glycosidases, lipases, phospholipases, phosphatases, and sulfatases. The internal pH of the lysosome is consequently maintained low by an integral lysosomal membrane ATP-driven hydronium ion ( $H^+$ ) pump. The limiting membrane of the lysosome or late endosome contains also a set of highly glycosylated integral membrane proteins, designated as lysosomal-associated membrane proteins (LAMPs) (such as LAMP-1, LAMP-2, and CD63/LAMP-3), lysosomal membrane glycoproteins (LGPs) and lysosomal integral membrane proteins (LIMPs) (Eskelinen et al, 2003). Additional lysosomal membrane proteins mediate transport of ions, amino acids, and other solutes across the lysosomal membrane and contribute to the maintenance of an acidic luminal pH in the range of 4.6 -5.0. Similar to all other secretory proteins, lysosomal enzymes or acid hydrolases are synthesized in the endoplasmic reticulum and transported to the Golgi apparatus where they undergo a variety of post-translational modifications, of which is the attachment of terminal mannose-

6-phosphate groups to specific oligo-saccharide side chains that can be recognized by M6P receptors found on the inner surface of the Golgi membrane, and then carried from the trans Golgi network to late endosomes by means of clathrin-coated transport vesicles.

Lysosomes are morphologically heterogeneous, often resembling other organelles of the endocytic and secretory pathways including melanosomes, lytic granules, major histocompatibility complex (MHC) class II compartments, platelet dense granules, basophil granules, and neutrophil azurophil granules. Therefore, lysosomes are currently distinguished from other organelles on the basis of an operational definition, which describes them as membrane-bound acidic organelles that contain mature acid-dependent hydrolases and LAMPs, but lack mannose 6-phosphate receptors (MPRs) (Kornfeld and Mellman, 1989).

In all eukaryotic cells, there are two major pathways of membrane traffic reaching lysosomes, the endocytic pathway (heterophagy) and autophagy (Fig. 1, p.6). The former delivers cargo from outside of the cell and plasma membrane, while the latter transports materials in the cytoplasm and into lysosomes. Endosomes also relay newly synthesized lysosomal enzymes from the secretory pathway to lysosomes (biosynthetic pathway).

It is well known that receptors endocytosed from the plasma membrane are either recycled to cell surface or transported to lysosomes for degradation. This sorting event, which takes place in the endosomes, is critical, since it acts as a filter of cellular signal transduction (Yoshimori, 2002). Ligand-mediated endocytosis is characteristically an early response in the signaling pathways triggered by a diverse group of cell surface receptors, including hetero-trimeric guanine nucleotide-binding protein (G protein)-coupled receptors (GPCRs), receptor tyrosine kinases (RTKs) and cytokine receptors.

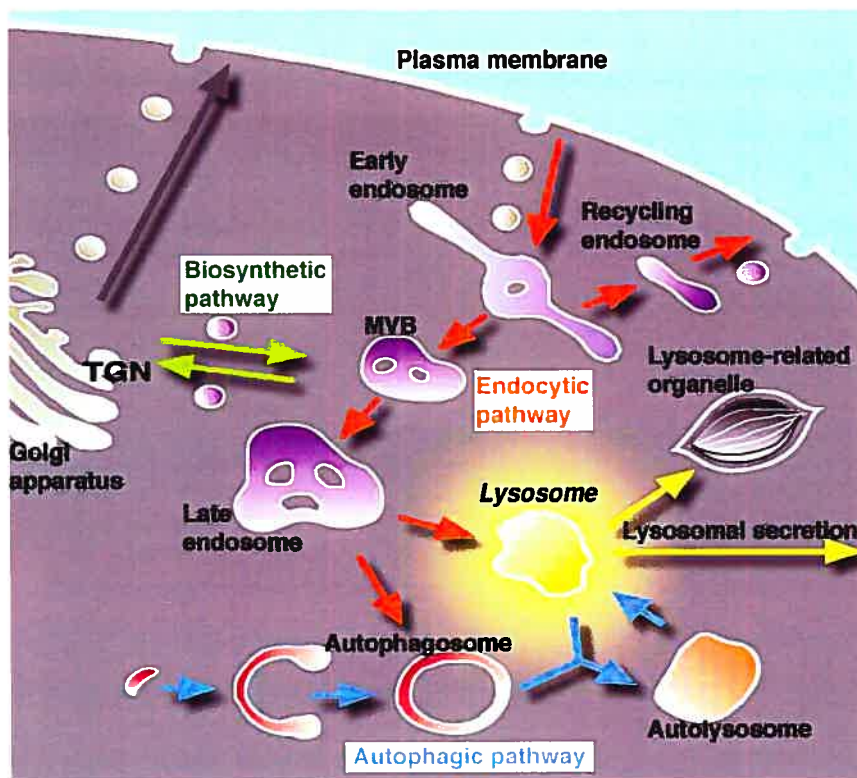


**FIGURE 1** The lysosomal network.

From the cell surface, the endocytic pathway extends to lysosomes. The biosynthetic pathway bridges the secretory pathway and the endocytic pathway. Autophagy delivers materials from the cytoplasm to lysosomes. Lysosomes are usually meeting places where several streams of intracellular traffic converge. Endocytosed molecules are initially delivered in vesicles to small, irregularly shaped intracellular organelles called **early endosomes**. Some of these ingested molecules are selectively retrieved and recycled to the plasma membrane, while others pass on into the mildly acidic (pH ~6) **late endosomes** to be digested by lysosomal hydrolases. These are progressively delivered to the endosome from the Golgi apparatus. **Mature lysosomes** form from the late endosomes, accompanied by a further decrease in internal pH. Lysosomes are thought to be produced by a gradual maturation process, during which endosomal membrane proteins are selectively retrieved from the developing lysosome by transport vesicles that deliver these proteins back to endosomes or the trans Golgi network. A second pathway to degradation in lysosomes is used in all cell types for the disposal of obsolete parts of the cell itself, a process called autophagy. The process seems to begin with the enclosure of an organelle by membranes of unknown origin, creating an **autophagosome**, which then fuses with a lysosome (or a late endosome). Professional phagocytes (macrophages and neutrophils in vertebrates) engulf objects to form a phagosome, which is then converted to a lysosome in the manner of the autophagosome. Lysosomal secretion (also called defecation) of the undigested contents is a minor pathway that enables all cells under stress to eliminate indigestible debris. Some cell types, however, contain specialized lysosomes such as melanocytes that have acquired the necessary machinery for fusion with the plasma membrane.



### *Concept of lysosomal storage*

In general, the distribution of the stored material, and hence which organs are affected in LSDs, is determined by two interrelated factors: (1) the tissue where most of the material to be degraded is found and (2) the location where most of the degradation normally occurs (Winchester et al, 2000). For example, the brain is rich in glycosphingolipids due to their presence in neuronal membranes, and hence defective hydrolysis of these molecules, as occurs in GM1 and GM2 gangliosidoses such as Krabbe, Niemann- Pick and Gaucher diseases, results primarily in storage within neurons and neurologic symptoms. In contrast, glycosaminoglycans (mucopolysaccharides) are primarily structural molecules produced by most cells and are found mainly on the surface of cells and in the matrix. Thus, defects in the degradation of mucopolysaccharides affect virtually every organ because they are widely distributed in the body. Cells of the mononuclear phagocyte system are involved in the degradation of a variety of substrates through the lysosomal pathway and organs rich in phagocytic cells, such as the spleen and liver, are frequently enlarged in several forms of LSDs.

Normally, LSDs show allelic variation (different mutations of the same gene) and significant clinical heterogeneity. The severity of the disease, which influences the time of onset and the pace of the regression, appears to be correlated with the residual enzyme activity, which itself depends on the nature of the molecular defect (even though clear genotype-phenotype correlations have often not been established, suggesting the existence of "modifying" genes). Such a model, elaborated by Conzelmann and Sandhoff (1983-1984) has found experimental support in several sphingolipidoses.

**TABLE I** Non-exhaustive list of LSD with defective enzyme(s) and corresponding metabolite accumulation

Disease	Enzyme Deficiency	Major Accumulating Metabolites
Glycogenosis		
Type 2 – Pompe disease	$\alpha$ -1,4-Glucosidase (lysosomal glucosidase)	Glycogen
Sphingolipidoses		
GM <sub>1</sub> gangliosidosis	GM <sub>1</sub> ganglioside $\beta$ -galactosidase	GM <sub>1</sub> ganglioside, galactose-containing oligosaccharides
GM <sub>2</sub> gangliosidosis	Hexosaminidase- $\alpha$ subunit	GM <sub>2</sub> ganglioside
Tay-Sachs disease	Hexosaminidase- $\beta$ subunit	GM <sub>2</sub> ganglioside, globoside
Sandhoff disease	Ganglioside activator protein	GM <sub>2</sub> ganglioside
GM <sub>2</sub> gangliosidosis, variant AB		
Sulfatidoses		
Metachromatic leukodystrophy	Arylsulfatase A	Sulfatide
Multiple sulfatase deficiency	Arylsulfatases A, B, C; steroid sulfatase; iduronate sulfatase; heparan N-Sulfatide, steroid sulfatase, dermatan sulfate	Sulfatide, steroid sulfatase, heparan sulfate, dermatan sulfate
Krabbe disease	Galactosylceramidase	Galactocerebroside
Fabry disease	$\alpha$ -Galactosidase A	Ceramide trihexoside
Gaucher disease	Glucocerebrosidase	Glucocerebroside
Niemann-Pick disease: types A and B	Sphingomyelinase	Sphingomyelin
Mucopolysaccharidoses (MPS)		
MPS I H (Hurler)	$\alpha$ -L-Iduronidase	Dermatan sulfate, heparan sulfate
MPS II (Hunter)	L-Iduronosulfate sulfatase	
Mucopolipidoses (ML)		
I-cell disease (ML II) and pseudo-Hurler polydystrophy	Deficiency of phosphorylating enzymes essential for the formation of mannose-6-phosphate recognition marker; acid hydrolases lacking the recognition marker cannot be targeted to the lysosomes but are secreted extracellularly	Mucopolysaccharide, glycolipid
Other Diseases of Complex Carbohydrates		
Fucosidosis	$\alpha$ -Fucosidase	Fucose-containing sphingolipids and glycoprotein fragments
Mannosidosis	$\alpha$ -Mannosidase	Mannose-containing oligosaccharides
Aspartylglycosaminuria	Aspartylglycosamine amide hydrolase	Aspartyl-2-deoxy-2-acetamido-glycosylamine
Other Lysosomal Storage Diseases		
Wolman disease	Acid lipase	Cholesterol esters, triglycerides
Acid phosphate deficiency	Lysosomal acid phosphatase	Phosphate esters

Twenty percent of normal enzyme activity is usually adequate to carry out cellular function. Consequently, heterozygotes (carriers of LSDs) whose enzyme activity is about 50 percent of normal are clinically unaffected (Grabowski and Hopkin, 2003). Symptoms develop when residual enzyme activity falls below a threshold of 15 to 20 percent. Therefore, mutations that leave no residual enzyme activity cause severe, early-onset illness. Milder mutations cause insidious, late- or adult-onset illness. But, what is the link between (specific) substrate storage in the lysosomes and tissue lesions? Although no well-established mechanism has yet been put forward to answer this question, it is likely that LSDs are accompanied by dysregulated cell growth or death.

### *Pathological features*

Manifestations of neurological deterioration associated with many LSDs begin in infancy or childhood. Very often it begins with a delay and then arrest of psychomotor development, neurological regression, blindness, and seizures. Inexorable progression leads to a vegetative state. LSDs have diverse and distinct clinical manifestations. Some of them share certain clinical and pathological features grouped into four basic clinical-pathological phenotypes: leukodystrophy, mucopolysaccharidosis, storage histiocytosis and neuronal lipidosis, the latter being the most prevalent phenotype (Table II, p.10).

The pathology, in the neuronal lipidosis phenotype, primarily involves the gray matter. Storage causes neuronal ballooning and torpedo-like swellings of proximal axons and dendrites. This process leads to loss of neurons and their axons, but myelin is not primarily affected (Neufeld and Muenzer, 2001). Storage in retinal ganglion cells causes blindness. Other cells

and organs that do not process large amounts of gangliosides are either normal or show mild storage without cell damage. The prototype of the

PHENOTYPE	PATHOLOGY	CLINICAL FINDINGS	LSDs
NEURONAL LIPIDOSIS	Storage in the neuronal body and processes	Neurological regression, seizures, blindness	Gangliosidoses, mucopolysaccharidoses, neuronal ceroid lipofuscinoses
LEUKODYSTROPHY	Storage in oligodendrocytes and Schwann cells	Neurological regression, spasticity, peripheral neuropathy	Gangliosidoses (metachromatic leukodystrophy, Krabbe's disease)
MUCOPOLYSACCHARIDOSIS	Storage in extraneural tissues	Visceromegaly, soft tissue swelling, skeletal dysplasia, heart disease	Mucopolysaccharidoses, glycoproteinoses, GM1 gangliosidosis
STORAGE HISTIOCYTOSIS	Storage in histiocytes	Hepatosplenomegaly, hematopoietic abnormalities	Gangliosidoses (Gaucher disease, Niemann-Pick disease)

neuronal lipidosis phenotype is Tay-Sachs disease, a form of GM2 gangliosidosis prevalent among Ashkenazi Jews, first described more than 100 years ago (Neufeld and Muenzer, 2001). Some LSDs impair enzymes that are important for turnover of myelin lipids and damage myelin-producing cells. This results in loss of myelin (leukodystrophy) manifested by neurological deterioration and spasticity. The mucopolysaccharidoses and glycoproteinoses affect neurons as well but have also severe skeletal and visceral manifestations, which constitute the mucopolysaccharidosis phenotype. In general, the cells that are most severely affected by LSDs are neurons, because they process large amounts of gangliosides and once lost they cannot be replaced, and histiocytes, because their main function is lysosomal degradation, and they decompensate if their lysosomal enzymes are deficient. Several LSDs show lipid storage in histiocytes throughout the lymphoid and hematopoietic tissues. Such storage histiocytosis causes hepatosplenomegaly, bone marrow depression, bone damage and other

manifestations. In some LSDs, notably Gaucher disease, storage histiocytosis is the main abnormality.

### *Cellular pathology*

The major classes of storage diseases can be distinguished by the ultrastructural appearance of their storage material. Glycosphingolipidoses present membranous swirls, mucopolysaccharidoses with multilamellar stacks ("zebra bodies"), fucosidosis and mannosidosis with watery or wispy material ("open" inclusions), and so forth (Suzuki, 1976). On electron microscopic examination, the stored products are membrane-bound because they are contained within lysosomes. The explanation for the characteristic appearances of storage bodies was that the accumulation of undegraded cell material past a certain critical point was believed to lead to physicochemical interactions with other components within the lysosome (e.g., cholesterol) and to formation of the characteristic morphological appearance of the residual or storage body for a given disease (Suzuki, 1976). Early studies have shown that residual bodies in storage diseases like Tay-Sachs and other neurolipidoses contained acid phosphatase activity, suggesting a lysosomal status (Walkley, 1998). Arguments that the storage bodies sometimes lacked histochemical evidence of lysosomal enzymes, or even lysosomal-like delimiting membranes, and thus might not be lysosomal, were eventually interpreted as simply late disease-associated alterations in the lysosome.

Cytotoxicity following mechanical disruption of cells has often been invoked as a plausible explanation for the cell dysfunction in lysosomal diseases. Given the observations that there are cell-selective consequences of the storage disease process, it was reasonable to assume that significant extra-lysosomal events are set in motion by deficiencies of single lysosomal enzymes. At least four possible mechanisms that reach beyond the mere

mechanical disruption hypothesis can be cited (Walkley, 1998): (i) Material stored within the lysosome may escape and in turn have deleterious effects elsewhere in the cell, either by direct toxicity or by impinging on other metabolic pathways to alter cell function. (ii) The massive accumulation of unprocessed compounds within the lysosome (e.g., gangliosides) may deprive the cell of certain precursor molecules, leading to a compensatory upregulation or dysfunction of other metabolic pathways or organelles. (iii) Abnormalities of the lysosomal system may lead to a reduced entry of materials into lysosomes and to subsequent increases of this compound elsewhere in the cell, with detrimental consequences. For example, plasma membrane receptor endocytosis is partially disrupted and the related signaling pathway remains activated. (iv) Defective lysosomal enzyme activity may adversely effect the normal functioning of other related organelles, most notably endosomes and the whole lysosomal network dynamics (Fig. 1, p.6).

Generally exacerbated apoptosis has been observed in cells or tissues from patients or animals affected with neuropilidoses; that is, in Tay-Sachs, Sandhoff (Huang et al, 1997; Wada et al, 2000), and Krabbe diseases (Taniike et al, 1999; Jatana et al, 2002), prosaposin deficiency (Tohyama et al, 1999), neuronal ceroid lipofuscinoses (Lane et al, 1996) and metachromatic leukodystrophy (Coenen et al, 2001). Although the molecular mechanism of this increased (neuronal) cell death is not yet established, it has been postulated that lysosphingolipids, which accumulate in the affected cells, may mediate cytotoxicity, possibly through inhibition of protein kinase C (Hannun et al, 1987). Interestingly, cellular sphingosine levels are elevated in Niemann-Pick disease type C mice, in which increased neuronal cell death has been also observed (Wu et al, 1999). Although the exact contribution of sphingolipids to apoptosis needs further characterization (mostly in terms of enzymes

involved and cellular targets), evidence has accumulated that some of these lipidic molecules act as bioregulators of cell growth and death. There is little information regarding possible alterations in the apoptotic program in the visceral forms of lysosomal disorders. Nevertheless, increased apoptosis has been described in chondrocytes from animals affected with mucopolysaccharidosis type VI (Simonaro et al, 2001). Cystinotic cells also exhibit an increased sensitivity to apoptosis (Park et al, 2002) that might be related to the (thiol-related) redox status of these cells.

Neurons in storage diseases not only exhibit somatic swelling secondary to accumulation of material, but they reveal a number of other somatic, dendritic and axonal changes. In Tay-Sachs disease for example, cortical neurons were described as being swollen and having enlargements within the basilar dendrites, but spinal motoneurons only exhibited swelling without dendritic changes (Walkley et al, 1998). This concept of neuron type-specific changes was extended to the other storage diseases. Two distinct types of cellular alterations emerged as characteristic of many storage diseases, namely meganeurites and axonal spheroids. Meganeurites were parasomatic enlargements within the axon hillock and appeared to occur secondary to storage as part of a volume expansion by the neuron. They were found only on certain types of neurons while other types appeared to undergo simple somatic enlargement secondary to storage. There are really two classes of meganeurites (Walkley et al, 1987; Walkley et al, 1988), named spiny and aspiny. Spiny and aspiny meganeurites can occur on specific populations of neurons, whereas in other diseases, like Batten disease, only aspiny meganeurites were found. On the other hand, axonal spheroids are enlargements of the distal segment of the axon that contain storage material inconsistent with the specific defective lysosomal hydrolase, as opposed to meganeurite storage material composition. The ultrastructural appearance of

spheroid material is the same across many types of storage disorders. The close similarity of accumulated material in studies of a distal crush or low temperature lesions in axons to that of spheroids in storage disease (Parton et al, 1992) suggests that the latter may be secondary to a block in retrograde transport. Spheroids are capable of causing significant interference with the efficacy or timing of action potential propagation (Walkley et al, 1991). In animal models of GM1 and GM2 gangliosidosis, Niemann- Pick disease,  $\alpha$ -mannosidosis, and mucopolysaccharidosis, there is a striking correlation between the location and incidence of axonal spheroids and the type and severity of clinical neurological disease (March et al, 1997).

#### *Animal models of lysosomal storage disorders*

The animal models of the LSDs should be defined as those in which the genes that are orthologous to the genes that cause human lysosomal disorders are functionally defective. This is to make the distinction with models generated by exogenous administration of metabolites in high doses to artificially induce a lysosomal storage condition by perturbing the balance of substrate influx over its efflux. Although spontaneously occurring genetic lysosomal storage diseases are as rare in other mammalian species as in man, the advent of gene targeting technology has revolutionized the state of animal models of genetic diseases and nearly all lysosomal storage diseases have been duplicated in the mouse (Table III, p.15). These animal models can overcome many of the limitations inherent in studies of human patients such as rarity of the disease, extremely complex genetic background and logistical and ethical constraints in the design and execution of experiments with human subjects.



**TABLE III** Non-exhaustive list of mouse models of human LSD

<b>Inactivated gene</b>	<b>Equivalent human disease</b>
Sphingomyelinase	Niemann-Pick, types A and B
Glucosylceramidase	Gaucher
$\alpha$ -Galactosidase A	Fabry
Arylsulphatase A (sulphatidase)	Metachromatic leukodystrophy (MLD)
$\beta$ -Hexosaminidase a subunit	Tay-Sachs
$\beta$ -Galactosidase	GM1-gangliosidosis
$\beta$ -Hexosaminidase $\beta$ subunit	Sandhoff
$\beta$ -Hexosaminidase $\alpha$ and $\beta$ subunits	Sandhoff
GM2 activator	GM2-gangliosidosis AB variant
Sphingolipid activator (prosaposin)	Total sphingolipid activator deficiency
$\beta$ -gal/sialidase protective protein/Cathepsin A	Galactosialidosis
Acid phosphatase	Unknown
N-acetyl- $\alpha$ -galactosaminidase	Schindler
Cation-dependent mannose 6-phosphate receptor	Unknown
Cation-independent mannose 6-phosphate receptor	Unknown
Mannose 6-phosphate receptors, double-knockout	Unknown
Acid lipase	Wolman disease & cholesteryl ester storage
Lysosomal $\alpha$ -neuraminidase	Sialidosis
$\alpha$ -1,4-Glucosidase	Glycogen storage II
Glucose-6-phosphatase	Glycogen storage Ia
$\alpha$ -Iduronidase	Hurler-Scheie (MPS I)
$\alpha$ -N-Acetylglucosaminidase	MPS IIIB (Sanfilippo's syndrome)
Arylsulphatase B	Maroteaux-Lamy (MPS VI)
Palmitoyl-protein thioesterase 1	Infantile neuronal ceroid lipofuscinosis (CLN1)
Glycosylasparaginase	Aspartylglycosaminuria

Adapted from J. Inher. Metab. Dis. 21 540-547 and J Gene Med 2004; 6: 481-506

Genetic lysosomal diseases have been known to occur spontaneously in many mammalian species, but most of them occur among larger animals that cannot be easily amenable to genetic manipulation such as mice or rats. Only two spontaneous mouse models of well-delineated genetic lysosomal diseases are known;  $\beta$ -glucuronidase deficiency (mucopolysaccharidosis VII) and the twitcher mutant (galactosylceramidase deficiency, Krabbe disease). These models have been well characterized and closely duplicate the

respective human defects in all aspects (Ellinwood et al, 2004) and so happens with some of the induced mutants, such as acid sphingomyelinase deficiency,  $\beta$ -hexosaminidase  $\beta$ -subunit (Sandhoff disease), galactosialidosis and total sphingolipid activator deficiency. Conversely, a subgroup of those induced mouse models shows minor deviations from human disease, including the acid  $\beta$ -galactosidase deficiency and  $\beta$ -hexosaminidase  $\alpha$ -subunit deficiency (Tay-Sachs disease) among others.

While mouse models have become necessary in the clarification of the pathogenetic mechanism of disease and the exploration of therapeutic approaches, species differences in the brain development and metabolic pathways must be always remembered if the ultimate goal of the study is application to human patients. When mouse models exhibit phenotypic differences to those of human diseases, several factors are considered as the underlying mechanism of those differences. Of primary importance is the lag in developmental processes that occur at different time intervals between humans and mice, notably the absolute and relative time scales with respect to the lifespan, and the variability in metabolic pathways (Suzuki et al, 1998). For example, neuronal proliferation and arborization in mice are initiated 7-8 days after birth, as opposed to prenatal completion in humans. At the same time period, human newborn brains are already well into the active phase of myelination in the telencephalon. An excellent example that illustrates the effect of metabolic differences on the displayed phenotype is the Tay-Sachs disease, which shows dramatically different clinical manifestations between human and the genetically equivalent mouse disease. In humans, the gangliosides containing a single sialic acid residue, known as GM1 and GM2, are degraded almost exclusively by hydrolysis of the respective terminal sugars, galactose and N-acetylgalactosamine. These reactions are catalyzed by lysosomal  $\beta$ -galactosidase and  $\beta$ -hexosaminidase-A, in the presence of

their substrate specific cofactors saposin-B and GM2-activator protein, respectively (Huang et al, 1997). In contrast, in the mouse, GM1- and GM2-gangliosides are readily degraded also by sialidase through sialic acid removal to the respective derivatives, GA1 and GA2, thus providing an alternative route for their catabolism.

### *Diagnosis and strategies of treatment*

Theoretically, two approaches can be envisaged in order to restrict the amount of stored material inside the lysosome. First, we can provide the missing enzyme either by direct administration, gene therapy or bone marrow transplantation. Second, we can alleviate the amount of undigested substrate by pharmacologically decreasing its rate of synthesis or by restricting its flow to the lysosome. In case of a lysosomal transporter defects, equally valid would be the possibility to divert the transport of products or by enhancing their export from the lysosome. For example, in cystinosis, there is an intra-lysosomal accumulation of cysteine. Intralysosomal cysteine levels can be decreased by oral administration of high doses of cysteamine, a basic compound that reacts with the accumulated cysteine to form a mixed disulfide resembling the structure of lysine, which is further transported outside of the lysosome by the corresponding lysine amino acid transporter (Winchester et al, 2003).

The most widely used procedure for the diagnosis of LSDs is enzyme assay and for most LSDs, this can be performed on leukocytes with fast turnaround (Neufeld et al, 2001). Cultured fibroblasts are required in a few LSDs. Cultured amniocytes or chorionic villus cells may be used for prenatal diagnosis. Biochemical determination of storage products is cumbersome, but has some applications. For instance, demonstration of glucosaminoglycans (GAG) in urine is a useful screening test for GAG storage. Storage of

abnormal products can be detected in the cells of the patient by light and electron microscopy. In addition to neurons, gangliosides and ceroid-lipofuscin are stored in somatic cells and may be detected by nerve, muscle, skin, conjunctival, and other biopsies. Tissue diagnosis (detection of specific storage materials by electron microscopy) is still the standard for some NCLs because biochemical assays of the affected proteins are not yet available. The gene mutations of LSDs can be detected by DNA analysis. Mutation analysis is used mainly for carrier detection and prognosis.

### **PROGRAMMED CELL DEATH (APOPTOSIS)**

Cell death is a part of normal physiology for most metazoan species. During development, redundant or unwanted cells are removed through programmed cell death, making important contributions to morphogenesis, organogenesis and other processes. However, excessive apoptosis, for example, has been implicated in neurodegenerative diseases such as Alzheimer's disease, Parkinson's disease, amyotrophic lateral sclerosis and several hereditary diseases that are caused by extended polyglutamine repeats (Yuan et al, 2000). Among the features of cells undergoing apoptosis, as opposed to necrosis, are chromatin condensation, nuclear fragmentation, plasma membrane blebbing, cell shrinkage and ultimately shedding of membrane-delimited cell fragments known as apoptotic bodies (Arends and Wyllie, 1991).

#### ***Apoptotic protease activation***

The biochemical events that occur during apoptosis are the result of hydrolysis of cellular proteins by a family of cysteine proteases called caspases, which cleave specific target proteins at aspartic acid residues. Of the 11 human caspases, 7 have definite (caspases 3, 6, 8, and 9) or probable

(caspases 2, 7, and 10) roles in apoptosis, whereas the remainder is thought to be involved in cytokine processing and the regulation of inflammation (Honig et al, 2000). Active caspases are tetrameric enzymes consisting of two large 17- to 37-kDa and two small 10- to 12-kDa subunits. Caspases are normally held in an inactive form by an integral inhibitory domain that becomes the target of proteolysis upon their activation. Each caspase is synthesized as a single-chain zymogen that contains an N-terminal prodomain followed by one large and one small subunit. Maturation of the procaspases involves cleavage at critical aspartate residues, that is, at the same type of bonds that caspases themselves cleave. This feature of caspase activation provides the opportunity for autoactivation as well as the possibility of caspase cascades. The advantage to the cell of this strategy is that no protein synthesis is required to activate the apoptotic pathway given that all the components are already present.

### *Regulators of apoptosis*

The Bcl-2 family of proteins comprises both anti-apoptotic and pro-apoptotic members and has a pivotal role in controlling programmed cell death by regulating mitochondrial integrity and mitochondria-mediated caspase activation (Adams et al, 2001). There are at least 17 family members, which can be divided into three groups based on the presence or absence of four conserved Bcl-2 homology (BH) domains. The N-terminal BH4 domain is present in all anti-apoptotic family members, including Bcl-2, Bcl-w, Bcl-xL, Mcl-1, A-1, Boo/Diva, and Nrf3. Pro-apoptotic family members, all of which lack the BH4 domain, fall into one of two categories. Either they are small family members containing only the BH3 domain (e.g., Bid, Bad, Bik, Bim, Blk, Bmf, Hrk, Bnip3, Nix, Noxa, and PUMA) or are larger and resemble Bcl-2 more closely but merely lack the BH4 domain (e.g., Bax, Bak, and Bok). The

pro-apoptotic “BH3 only” proteins present in higher eukaryotes (e.g., Bid, Bim, Bmf) translocate from cytoplasmic sites to the outer surfaces of mitochondria in response to apoptotic stimuli. The ratio between anti-apoptotic and pro-apoptotic Bcl-2 members is a crucial factor that helps to determine the susceptibility of a cell to a death signal (Hengartner, 2000).

In addition to Bcl-2 family members, a family of polypeptides called IAP (inhibitor of apoptosis) proteins also regulates apoptotic processes (Deveraux et al, 1999; Salvesen et al, 2002). Human members of this family include cIAP1, cIAP2, XIAP, NAIP and livin. Common structural features include one or more baculovirus inhibitor repeat (BIR) motifs and RING domains. The zinc finger-like BIR domains bind the surfaces of caspases, allowing sequences between the BIRs to block the caspase active site. In this manner, XIAP, cIAP1, and cIAP2 are able to block caspase 8- and 9- initiated events *in vitro* and to inhibit the activities of purified caspases 3, 7, and 9. The RING domain acts as an ubiquitin ligase and presumably facilitates proteasome-mediated degradation of whatever these IAP proteins bind (Kaufmann et al, 2001).

### *Two Pathways of Caspase Activation*

Apoptosis-signaling pathways can be categorized into three phases: initiation and caspase activation, mitochondrial commitment and effector events (Fig. 2, p.21). According to current understanding, there are at least two major pathways of apoptotic caspase activation (Hengartner, 2000). One, called the “death receptor” or “extrinsic” pathway, utilizes caspase 8 and/or 10 as the initiator caspase in a protease cascade. The other, called the “mitochondrial” or “intrinsic” pathway, involves caspase 9. Though the initiation and early spectrum of caspase activation differ between these two

pathways, both these signal transduction pathways converge at the activation of caspases 3 and 6, which are the two widely studied effector caspases.

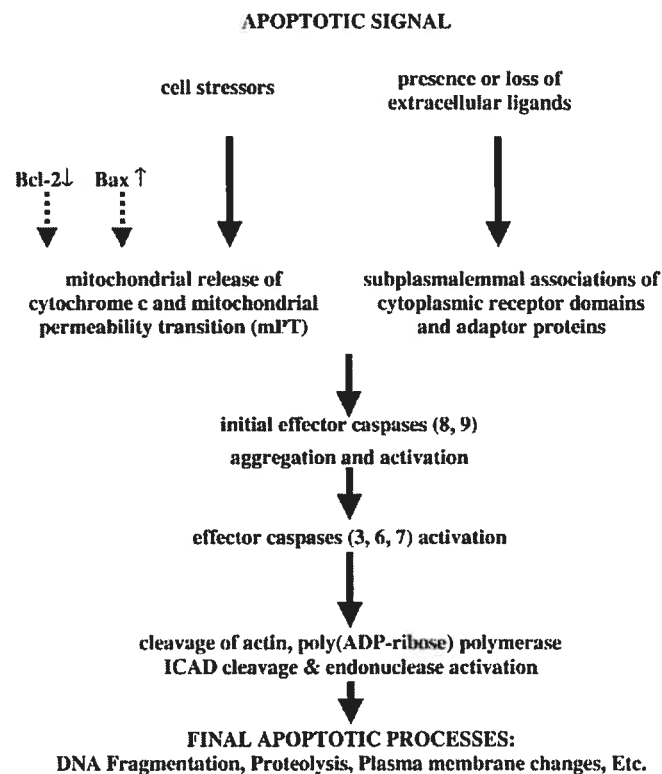


**FIGURE 2** Molecular elements of the apoptotic cascade (Honig et al, 2000)

The “extrinsic” or “death receptor” pathway begins with ligation of specific cell surface receptors. In the case of Fas, binding of its cognate ligand (Fas ligand) results in an alteration of the so-called “death domain” in the cytoplasmic tail of the receptor to permit binding of the death domain-containing adaptor molecule FADD. As a consequence of this binding, the “death effector domain” of FADD acquires the ability to bind homologous domains in procaspase 8, thereby drawing this zymogen to the site. Molecular interactions within this assembly, which is called a DISC, result in cleavage of procaspase 8 and release of mature caspase 8 to the cytosol, where

it cleaves both procaspase 3 and the small “BH3 only” Bcl-2 family member Bid (Hacker, 2000). Depending on the ratio of these cleavages, apoptosis might be triggered directly or might depend on activation of the mitochondrial pathway (intrinsic pathway).

Induction of apoptosis by a variety of toxic insults, including radiation and chemotherapeutic agents, is accompanied by changes in mitochondrial function. These stimuli cause several mitochondrial changes, including decreases of mitochondrial membrane potential and the release of polypeptides that normally reside in the mitochondrial inter-membrane space. Among the polypeptides released is cytochrome *c*. Once in the cytoplasm, this protein binds to a scaffolding protein called apoptotic protease-activating factor-1 (Apaf-1). In the presence of cytochrome *c* and dATP, Apaf-1 undergoes a conformational change that facilitates binding of a protein interaction domain called a caspase recruitment domain (CARD) on Apaf-1 to a similar motif present in the prodomain of procaspase 9. The result is the formation of a *Mr* ~700,000 complex called an apoptosome that has enhanced ability to cleave pro-caspases 3 and 7 to active enzymes (Dimmeler et al, 1999). These caspases then contribute to the characteristic apoptotic phenotype. Another mechanism that triggers apoptosis in response to cell stress operates through the transcription factor p53, which is a major player in the events of cell cycle control mainly in response to DNA damage. DNA repair mechanisms are activated, but so is transcription of the gene for another bcl-2 family protein called Bax. Like Bad, Bax allows cytochrome *c* to escape from mitochondria, so if the DNA is not repaired in time, BAX concentrations increase, cytochrome *c* escapes, and apoptosis ensues.



### *The Consequences of Caspase Activation*

In the last stages of apoptosis, once caspase 3 has been activated, biochemical changes that characterize the apoptotic phenotype begin to occur. First, caspase 3 directly participates in endonuclease activation. The nuclease caspase-activated deoxyribonuclease (CAD/DFF40) is a constitutively expressed nuclear protein that is ordinarily complexed with its inhibitor ICAD. Caspase 3-mediated cleavage of ICAD results in the liberation of CAD, which begins to digest the chromatin (Hacker, 2000). Because chromatin in the linker regions is more accessible than chromatin wound around histones, the net result is a characteristic internucleosomal pattern of DNA degradation. This internucleosomal degradation is accompanied by chromatin condensation, another hallmark of apoptosis. Caspase 3 also cleaves procaspase 6, liberating the active form of this enzyme. Together, caspases 3 and 6 cleave structural proteins of the nucleus (lamins and NuMA), facilitating nuclear fragmentation. In addition, these two proteases (primarily caspase 3) cleave more than 200 other cellular substrates, thereby inhibiting DNA repair and cell cycle progression, inactivating signal transduction pathways that are critical for survival, and activating a series of enzymes that are thought to participate in cellular disassembly.

### *Caspase-Independent Pathways*

Even though caspases appear to be critical for cleavage of key substrates during apoptosis, other effector molecules might also contribute to the apoptotic phenotype. For example, apoptosis-inducing factor (AIF) is an oxidoreductase that is released from mitochondria into the cytosol during apoptosis (Daugas et al., 2000). It subsequently localizes to nuclei, where it is capable of generating large (>50 kb) DNA fragments and inducing chromatin condensation by unknown mechanisms. It is also important to recognize that

some caspase-independent cell deaths appear to be necrotic, that is, to involve ATP depletion and loss of membrane integrity. When caspases are inhibited, the primary lesions induced by various treatments (e.g., microtubule disruption or DNA damage) and the cytochrome *c* release that follows still occurs. These changes might be sufficiently disruptive to cellular metabolism so that cells will ultimately die even if they cannot activate caspases.

Attempts have been made to order caspase-independent cell death according to the cellular organelles involved such as the mitochondria, lysosomes and the endoplasmic-reticulum (Ferri et al, 2001). Interestingly, active participation of lysosomal proteases such as cathepsins B and D has been observed in cell death induced by several stimuli, including oxidative stress, TNF- $\alpha$ , bile salt-induced apoptosis and chemotherapeutic drugs (Broker et al, 2005). Indeed, cathepsin B has been shown to act as an effector protease, downstream of caspases in certain cell types (Foghsgaard et al, 2001), and is capable of executing cell death independent of the apoptotic machinery in WEHI-S fibrosarcoma and non-small cell lung cancer (NSCLC) cells (Broker et al, 2005). Other reports have shown that lysosomal proteases can promote cell death more indirectly by triggering mitochondrial dysfunction and subsequent release of mitochondrial proteins probably through Bid translocation after lysosomal disruption by lysosomotropic agents (Cirman et al, 2004). Finally, lysosomal proteases have been reported to directly cleave and activate caspases, thereby confirming that lysosomal permeabilization often is an early event in the apoptotic cascade (Ferri et al, 2001).

## UBIQUITIN-PROTEASOMAL SYSTEM (UPS)

Protein degradation by the ubiquitin/proteasome system plays a primordial role in a broad array of basic cellular processes such as the cell cycle, signal transduction and development. Considering these numerous processes, it is not surprising that the system has been implicated in the pathogenesis of many diseases such as Parkinson's disease, Alzheimer's disease, ischaemia reperfusion injury, aging in the central nervous system and diabetes. Proteins modified by multiubiquitin chains are the preferred substrates for degradation by the 26S proteasome, a multicatalytic protease complex. The proteasome is a massive complex consisting of more than 20 protein subunits and having a sedimentation coefficient of 26 (26S) (Ciechanover et al., 2000). It has a cap and barrel structure, with the cap (referred to as the 19S component of the proteasome) being the part that orients the ubiquitinated proteins in preparation for degradation by the 20S barrel component, which contains the proteases. This multicatalytic protease is characterized by three major activities, that is the tryptic, chymotryptic and peptidylglutamyl hydrolytic activities.

Ubiquitination of proteins is a complex ATP-dependent process in which ubiquitin is sequentially activated by ubiquitin-activating enzymes (E1), transferred to ubiquitin-conjugating enzymes (E2) and then ligated to protein substrates by ubiquitin ligases (E3). Ubiquitin is joined to the substrate through the formation of an isopeptide bond between the C terminus of ubiquitin (Gly76) and the side-chain of a lysine residue of the substrate. An additional conjugation factor, named E4, was recently described and is involved in polyubiquitin chain elongation of at least a subset of substrates in conjunction with E1, E2 and E3.

Although targeting proteins for destruction by the proteasome is the best-characterized task of ubiquitin, other functions are being discovered at a

rapid rate. Examples for such proteolysis-independent functions are ubiquitin-dependent endocytosis, transcriptional control and DNA repair (Varshavsky, 1997). Many of these are regulated by alternative types of ubiquitin modification, such as monoubiquitylation (in which only one ubiquitin moiety is added), or by a non-canonical multiubiquitin chain. The proteasome also plays an essential role in maintaining cell homeostasis by degrading many rate limiting enzymes and critical regulatory proteins.

### *Deubiquitinating enzymes and UCH-L1*

Deubiquitinating enzymes (DUB) are proteases that specifically hydrolyse ester, thiol ester and amide bonds to the carboxyl group of glycine residue 76 of ubiquitin (Wing, 2003). These enzymes, in analogy with the role of phosphatases in reversible phosphorylation, perform the reversible ubiquitination of proteins and can have important regulatory functions. They are involved in processing of ubiquitin gene products, in negatively regulating the functions of ubiquitination, in regenerating free ubiquitin after protein degradation by the proteasome or the lysosome and in salvaging ubiquitin from possible intracellular adduct formation (Wilkinson, 1997). All eukaryotes contain DUBs encoded by at least two gene families, the ubiquitin carboxyl-terminal hydrolase (UCH) and the ubiquitin-specific processing protease (UBP) families, which comprise in total more than 60 known members. The products of the UCH family were named for their activity in hydrolysing small amides and esters at the C-terminus of ubiquitin and have also been shown to remove peptides and small proteins, whereas the UBPs are responsible for ubiquitin proprotein and ubiquitin fusion protein processing.

Three human UCH isozymes have been cloned and they exhibit marked tissue specificity. For instance, UCH-L3 is an isoform specifically

expressed in hematopoietic cells, whereas UCH-L1 is highly expressed in neurons (Doran et al, 1983) and to cells of the diffuse neuroendocrine system and their tumors. Day and Thompson (1987) cloned UCH-L1 cDNA and the deduced protein, which they called PGP9.5, contains 212 amino acids. Day et al. (1990) determined that the UCH-L1 gene contains 9 exons and spans 10 kb. The 5-prime region contains elements common to many genes and other elements that are shared with the 5-prime regions of the genes encoding neurofilament neuron-specific enolase (ENO2) and THY1 antigen. By Northern blot analysis, Leroy et al. (1998) detected a 1.3-kb transcript expressed only in brain and further confirmed the gene structure. Examination of specific brain regions revealed expression in all areas tested, particularly in the substantia nigra. Ubiquitin C-terminal hydrolase L1 represents 1 to 2% of total soluble brain proteins (Wilkinson et al., 1989).

Its occurrence in Lewy bodies and its function in the proteasome pathway made UCH-L1 a compelling candidate gene in Parkinson disease. In a German family with Parkinson disease, Leroy et al. (1998) identified a missense mutation in the UCH-L1 gene, ile93 to met (I93M), which caused a partial loss of the catalytic activity of this thiol protease. They suggested that this could lead to aberrations in the proteolytic pathway and aggregation of proteins. In other studies, Lincoln et al. (1999) sequenced the entire coding region of the UCH-L1 gene in 11 families with a pattern of Parkinson's disease consistent with autosomal dominant inheritance. Although they found polymorphisms in noncoding regions, the only amino acid change was S18Y. The S18Y allele was found in approximately 20% of chromosomes in a Caucasian population, suggesting that it is unlikely to be pathogenic. Lincoln et al. (1999) concluded that the I93M variant must be a rare cause of Parkinson's disease or a harmless substitution whose occurrence in the family reflected chance. However, Liu et al. (2002) found that UCH-L1, especially

variants linked to higher susceptibility to Parkinson disease, caused the accumulation of alpha-synuclein in cultured cells, an effect that could not be explained by its recognized hydrolase activity. Therefore, UCH-L1 exhibited an additional dimerization-dependent ubiquityl ligase activity. Interestingly, the polymorphic variant of UCH-L1 associated with decreased risk for Parkinson disease, ser18 to tyr (S18Y), had reduced ligase activity compared with the wildtype enzyme, but it had comparable hydrolase activity. The authors concluded that the ligase and hydrolase activities of UCH-L1 may play roles in proteasomal protein degradation, a process critical for neuronal health. Osaka et al. (2003) recently demonstrated that monoubiquitin is stabilized by its direct association to UCH-L1. This team investigated the effect of a UCH-L1 loss of function on ubiquitin levels, as in the *gad* (gracile axonal dystrophy) mouse, where neuronal monoubiquitin levels were reduced compared to wild-type.

#### ***Animal model for UCH-L1 deficiency (GAD mouse)***

The gracile axonal dystrophy (*gad*) mouse is an autosomal recessive mutant that shows sensory ataxia at an early age, followed by motor ataxia later (Yamazaki et al, 1988). Pathologically, the mutant is characterized by 'dying-back' type axonal degeneration and formation of spheroid bodies in nerve terminals. Pathologic observations in the human have associated brain aging and neurodegenerative diseases with progressive accumulation of ubiquitinated protein conjugates. In *gad* mice, accumulation of amyloid- $\beta$  protein and ubiquitin-positive deposits occur retrogradely along the sensory and motor nervous systems.

Suh et al. (1995) showed that the *gad* mutation is located on mouse chromosome 5. Later, Saigoh et al. (1999) found that the *gad* mutation is caused by an in-frame deletion including exons 7 and 8 of the UCH-L1 gene,

encoding the ubiquitin carboxy-terminal hydrolase selectively expressed in the nervous system and testis. The *gad* allele encodes a truncated UCH-L1 protein lacking a segment of 42 amino acids containing a catalytic residue. Since this protein is thought to stimulate protein degradation by generating free monomeric ubiquitin, the *gad* mutation appears to affect protein turnover. The findings showed that altered function of the ubiquitin system directly causes neurodegeneration and suggests that the *gad* mouse provides a useful model for investigating human neurodegenerative disorders.

Kurihara et al. (2000) showed that mice homozygous for a targeted deletion of the related UCH-L3 gene are indistinguishable from wildtype. To assess whether the two hydrolases have redundant function, Kurihara et al. (2001) generated mice homozygous for both UCH-L1 (*gad*) and UCH-L3( $\Delta$ 3-7). The double homozygotes weighed 30% less than single homozygotes and displayed an earlier onset of lethality, possibly due to dysphagia. Axonal degeneration of the nucleus tractus solitarius and area postrema of the medulla was noted in these mice. The double homozygotes also displayed a more severe axonal degeneration of the gracile tract of the medulla and spinal cord than had been observed in UCH-L1 (*gad*) single homozygotes. In addition, degeneration of dorsal root ganglia cell bodies was detected in both the double homozygotes and UCH-L3( $\Delta$ 3-7) single homozygotes. Given that both UCH-L1 (*gad*) and UCH-L3( $\Delta$ 3-7) single homozygotes displayed distinct degenerative defects that were exacerbated in the double homozygotes, the authors concluded that UCH-L1 and UCH-L3 may have both separate and overlapping functions in the maintenance of neurons of the gracile tract, nucleus tractus solitarius, and area postrema.

### *Role of ubiquitination in apoptosis*

The relation between ubiquitin and apoptosis was first suggested when increases in ubiquitin expression were observed during programmed cell death in the intersegmental muscle of insects (Schwartz et al, 1990) and mature lymphocytes. This hypothesis was further reinforced by evidence linking proteasome inhibition to the activation of cell death in human leukemic HL60 cells (Drexler, 1997). Today, it is widely accepted that ubiquitin is critically involved in the regulation of molecules at every phase of apoptosis. Important regulators of apoptosis, including the Bcl-2 family of proteins, the IAPs and regulators of the inhibitor of nuclear factor- $\kappa$ B kinase (IKK) have been identified as new substrates of the ubiquitination system. In addition, the tumour suppressor p53 and other cell-cycle proteins that are already known to be substrates of the proteasome have now been assigned specific functions in the regulation of apoptosis. Moreover, IAPs, which are pivotally involved in the negative regulation of pathways that induce death, have themselves been shown to take part in the ubiquitylation of apoptotic substrates.

Despite the amount of work correlating the variation in ubiquitin levels (and ubiquitination pattern), proteasomal subunit composition and proteasomal activity to apoptosis, proteasomal inhibition does not exhibit a clear directional correlation. That is to say that the downstream effects to proteasomal inhibition, in terms of apoptosis, may be either positive or negative in a cell-type dependent manner without negating the possibility that it changes the cell susceptibility to apoptotic stimuli. These seemingly contradictory results might be due to the unspecific nature or concentrations of the inhibitors that were used, or to differences between the cell types (Orlowski et al, 1999). An illustration of the above assertion is that most stages of lymphocytes and most leukemic cell lines become sensitized to



apoptosis following proteasome inhibition, whilst primary thymocytes do not in response to dexamethasone,  $\gamma$ -irradiation, phorbol ester or etoposide treatment (Lee et al, 2003). As a general rule, in most cell lines, proteasome inhibitors trigger apoptosis.

As mentioned earlier, the IAP family inhibits apoptosis primarily by inactivating and degrading pro-apoptotic proteins and presents the only known subset of apoptosis-signaling molecules that contain E3 ligase activity (Deveraux et al, 1999) by the presence of RING domains. The mechanism of IAP-mediated inhibition of apoptosis predominantly lies in its interaction with caspases such as casp 3, casp 7, casp 9, which results in their ubiquitination and subsequent degradation by the UPS.

Ubiquitination of the Bcl-2 proteins is known to target for degradation both pro- or anti-apoptotic family members. Recent reports indicate that the ubiquitin/proteasome system decisively influences the delicate balance between these two fractions of the Bcl-2 family. Degradation of pro-apoptotic members such as Bid, Bax and Bak has been reported to promote cell survival and conversely, apoptotic progression has been found to require poly-ubiquitin-mediated Bcl-2 degradation. Proteasomes have also been noted to modulate apoptosis by affecting the life time of the 'BH3-only' members BH3-interacting-domain death agonist (Bid) and Bcl-2 interacting killer (Bik).

The p53 tumor suppressor protein is one of the best-known pro-apoptotic proteins acting at the transcriptional level and its induction occurs following intrinsic stressors, such as DNA damage, and leads to a halt in cell cycle progression and/or apoptosis activation. Following activation by various stresses, p53 downregulates anti-apoptotic proteins, such as Bcl-2 and the transcription factor  $\beta$ -catenin (Sadot et al, 2001), and upregulates several death-promoting molecules such as the adaptor protein Apaf-1, Bax, Noxa, Puma, etc (Lee and Peter, 2003). The role of each of these proteins in p53-

mediated apoptosis seems to be cell-type dependent. In addition, p53 might also contribute to the induction of apoptosis through transcriptionally independent activities (Ryan et al. 2001). The mechanisms that underlie these functions remain poorly understood, but might point to a direct role for p53 at mitochondria and the relocalization of death receptors to the cell surface. For example, p53 was shown to directly interact with Bax protein leading to its activation and to the subsequent permeabilization of the mitochondrial membrane (Chipuk et al, 2004). The levels of p53 protein are usually quite low, as its rapid degradation prevents the accumulation of p53 in normal proliferating cells. The stability of p53 is highly regulated, primarily by its ability to bind the cellular proto-oncogene Mdm2, which functions as an ubiquitin ligase for p53, mediating its ubiquitination and proteasome degradation. The expression of Mdm2, in turn, is regulated by p53, producing a feedback loop that tightly regulates p53 function.

Several stress-induced signaling pathways leading to the inhibition of MDM2-mediated degradation of p53 have been identified. Kinases activated by genotoxic damage, including ATM and ATR, Chk1, Chk2 as well as other stress-related kinases, have been shown to phosphorylate and thus stabilize p53 (Abraham, 2001). Furthermore, the response to p53 phosphorylation on a particular residue may depend on the specific stress signal initiating the phosphorylation event, underscoring the complexity of p53 phosphorylation and stabilization. Regulation of p53 nuclear localization also plays an important role in controlling p53 function and its ability to transactivate responsive genes. The ability of p53 to be exported from the nucleus is certainly enhanced by Mdm2 ubiquitin ligase activity (Ryan et al, 2001).

Unlike polyubiquitination, the functional consequences of monoubiquitination are diverse and include receptor endocytosis, virus budding, transcription, DNA repair and caspase recruitment during apoptosis.

Concerning apoptosis, four proteins are targeted by monoubiquitination: histone H2A, caspase-3, caspase-7 and DEDD. The role of monoubiquitination of the above proteins in apoptosis remains speculative since this field is still under development, but a current hypothesis is that a lattice formation of ubiquitinated proteins forms and may act as a signaling platform (Lee and Peter, 2003).

### *Involvement of UPS in neurodegeneration*

Genetic data from various species clearly indicate the existence of a link between proteasomal dysfunction and neuronal disorders. Moreover, an increasing body of evidence supports a crucial role for the apoptotic system in the manifestation of many of the neurodegenerative diseases, although our knowledge about the mechanisms that are involved in these disorders is still incomplete.

Neuronal death takes place within hours to days after a stroke, but may occur over years in Alzheimer disease (AD). After a traumatic injury or stroke, neurons die rapidly because of excitotoxicity (typically occurring within 48 h) and apoptosis (typically occurring within 4–14 days) (Honig and Rosenberg, 2000). There can also be extensive apoptosis of astrocytes and oligodendrocytes during this period. In contrast, neuronal death in diseases such as AD or Parkinson disease (PD) occurs over a period of years as a result of necrosis induced by oxidative stress and the accumulation of protein aggregates. The steady accumulation of protein aggregates in late-onset neurodegenerative diseases presents an ongoing insult to neurons that causes steady, progressive injury and steady, progressive cell death. Conversely, preventing the accumulation of toxic protein aggregates appears to be the most effective strategy for inhibiting neurodegeneration in these progressive, late-onset neurodegenerative diseases (Orr et al, 2000). The toxic aggregates

cause ongoing injury, which differs from the time delimited cell death stimulus typically associated with apoptosis. Late-onset neurodegenerative diseases constitute a diverse array of diseases that are all characterized by the loss of specific populations of neurons and the accumulation of particular types of inclusions in each disease (Alves-Rodrigues et al, 1998). **Table IV (p.34)** lists also some of the major neurodegenerative illnesses, the nerve populations that are affected in each illness, and the proteins that make up the inclusions. In some cases, some of the general pathophysiological mechanisms are known, but the specific factors that cause death of a selected population of neurons is poorly understood. There is a growing consensus that oxidative stress plays a key role in both aging and the pathophysiology of most neurodegenerative diseases.

A key factor determining cellular vulnerability to oxidative stress appears to be protein oxidation and protein aggregation (Alves-Rodrigues et al, 1998). Many neurodegenerative diseases contain inclusions characteristic of that disorder. Each inclusion contains a particular type of protein that is present in an aggregated state, often as a fibrillar aggregate. For example, mutations in two proteins, APP or presenilins, which increase production of rapidly aggregating amyloid- $\beta$ , cause familial AD. Expansions of polyglutamine stretches cause proteins such as huntingtin and ScaI to aggregate, which causes Huntington's disease and spinocerebellar ataxia, respectively (Ross, 1995). Mutations in tau protein and  $\alpha$ -synuclein increase the tendency of each of these proteins to aggregate and cause frontotemporal dementia of chromosome 17 and PD, respectively. Accumulating evidence shows that these protein aggregates cause toxicity through a number of different mechanisms.

**TABLE IV Neurodegenerative disorders with ubiquitin-immunoreactivity in cell inclusions**

Inclusions	Diseases	Protein components	Cell type
Cytoplasmic			
Ballooned neurons	Pick's disease, CBD, AD, CJD, ALS, COFS and seizures	Neurofilaments	Neurons
Corpora amylacea	Normal aging and AD	HSP27 and HSP72	Astrocytes
Dystrophic neurites	AD, PD, DLBD, MND	Neurofilaments and proteasome	Neurites
Glial tangles	CBD	Tau in straight filaments	Perikarya
Neuropil grains			Neurons, glia
Gliofibrillary inclusion	After hypoxic stress	Intermediate filaments	Astrocytes
Granulovascular bodies	AD, normal aging	Neurofilaments and tau	Neurons (in vacuoles)
Lewy bodies	PD, DLBD	Neurofilaments $\alpha$ -crystallin, 26S proteasome	Monoaminergic and cholinergic neurons
Lewy body-like inclusions	ALS	Neurofilaments	Motoneurons
Neurofibrillary tangles	AD, PSP	PHF (AD) or straight filaments	Perikarya
Neuropil threads		(PSP), tau and heat shock proteins	Axons, nerve endings
Pick bodies	Pick's disease	PHF with tau	Neurons
Rosenthal fibers	Alexander's disease	$\alpha$ -Crystallin, intermediate filaments	Astrocytes
Endosomal/lysosomal			
Late endosome-like organelles	TSE	Prion protein, cathepsin B	Neurons
Lysosome-related structures	TSE, AD	Prion protein, HSP70	Neurons
Bunina bodies	ALS	Vimentin, HSP70	Motoneurons
Nuclear			
Intranuclear inclusion	Machado-Joseph disease, Huntington's disease	Ataxin 3, huntingtin	Neurons

Abbreviations: AD, Alzheimer's disease; ALS, amyotrophic lateral sclerosis; CBD, corticobasal ganglionic degeneration; CJD, Creutzfeldt-Jacob disease; COFS, cerebro-oculo-facio-skeletal syndrome; DLBD, diffuse Lewy body disease; HSP, heat shock protein; MND, motor neuron disease; PD, Parkinson's disease; PHF, paired helical filaments; PSP, progressive supranuclear palsy; TSE, transmissible spongiform encephalopathies.  
Trends Neurosci. (1998) 21, 516-520

For many years, neuropathologists have noted that the inclusions that form in a neuron are highly ubiquitinated (Table IV, p.34) and immunostaining for ubiquitin represents one of the most sensitive methods of detecting inclusions (Lennox et al., 1989). One reason why ubiquitinated inclusions accumulate is that the UPS is impaired in many neurodegenerative diseases. The significance of ubiquitination only recently became appreciated with the discovery that one of the key disease-related genes, termed parkin, is an E3 ubiquitin ligase (Kitada et al, 1998). The UPS in affected regions of cases of PD and AD shows a decrease in activity of between 30% and 40% (McNaught et al, 2001). The causes of this decrease, though, are somewhat controversial. Although proteasomal activity generally increases in response to oxidative stress, the latter combined with reduced ATP production (associated with cell injury) might reduce UPS activity in neurodegenerative disease (Conconi et al, 1996).

The debate in this area centers on whether the protein aggregates themselves inhibit the UPS. Most recently, many protein aggregates have been shown to inhibit the proteasome, which is a process that causes acute apoptosis in cells grown in culture (Bence et al, 2001; Snyder et al, 2003). Similarly, large protein aggregates that accumulate in the endoplasmic reticulum, termed aggresomes, inhibited the proteasome (Johnston et al, 1998). Aggregates of huntingtin and the CFTR (cystic fibrosis transmembrane conductance regulator) both inhibit the UPS. However, whether UPS inhibition accounts for the mechanism of cell death associated with  $\beta$ -amyloid,  $\alpha$ -synuclein and tau is less clear. For instance,  $\alpha$ -synuclein binds the TBP1 protein of the proteasome, and overexpressing  $\alpha$ -synuclein inhibits the proteasome, but there is no evidence showing that aggregated  $\alpha$ -synuclein inhibits the proteasome more than monomeric  $\alpha$ -synuclein (Snyder et al, 2003).

Together, the overall work in this field suggests that oxidative stress does generally inhibit the UPS in many neurodegenerative diseases but that the contribution of protein aggregates to inhibition of the UPS might vary among different diseases. The concordance of these different lines of evidence leads to the conclusion that protein aggregation is a process that is fundamentally important to the progression of neurodegenerative disease, and therefore investigating the pathophysiology of disease-related aggregates could provide fundamental insights into the pathophysiology of neurodegenerative disease.

## INTRODUCTION

The genetically determined deficiency of lysosomal enzymes and proteins, or of proteins involved in the lysosomal biogenesis results in lysosomal storage disorders (LSD), which are characterized by the accumulation of partially undegraded catabolic products in lysosomes leading to their increased size and number. This severely affects cell turnover causing malfunction of many tissues and organs, and leads to hepatosplenomegaly, corneal clouding, skeletal deformation and central nervous system degeneration. Although rapid progress has been achieved in revealing the genetic basis of many lysosomal storage diseases, much less is known about the mechanisms underlying the disruption of cell metabolic and signalling pathways associated with these conditions.

Multiple studies have demonstrated that the increased occurrence of programmed cell death (apoptosis) in many tissues and organs of patients affected with LSDs as well as in corresponding animal models results in the elimination of entire classes of cells (reviewed in Buccoliero et al, 2002). For example, high levels of apoptosis were detected in neurones, microglia, and Purkinje cells of patients affected with Tay-Sachs disease, Globoid cell leukodystrophy (Krabbe disease), Nieman-Pick disease type C, GM1-gangliosidosis and Gaucher disease (Burek et al, 2001; Erickson & Bernard, 2002; Finn LS et al, 2000; Huang et al, 1997; Im et al, 2001; Jatana et al, 2002; Jeyakumar et al, 2003; Lozano et al, 2001; Zhou et al, 1998). In addition, apoptosis of cartilage cells (chondrocytes) was detected in mucopolysaccharidosis (MPS) Type VI (Simonaro et al, 2001) while apoptosis of muscle cells leading to loss of cardiac muscle mass and cardiomyopathy was found in Pompe disease (Hesselink et al, 2003). Apoptosis was also observed in the cultured fibroblasts and renal tubular epithelial cells from patients affected with cystinosis (Park et al., 2002). In several cases accumulated substrates of



the deficient enzymes (such as psychosine in globoid cell leukodystrophy, or ceramide in Farber disease) were directly shown to be cytotoxic and to induce apoptosis, whereas apoptosis was considered to result from general inflammation in the central nervous system in patients with  $G_{M2}$ - and  $G_{M1}$ -gangliosidoses (Jeyakumar et al, 2003). Taken together these data suggest that a high rate of apoptosis in the tissues affected in LSDs is a general phenomenon that does not depend on the primary genetic defect but rather originates from overfilling of the lysosomes with storage materials.

To identify genes whose expression was altered by the presence of lysosomal storage products, our laboratory previously used oligonucleotide microarrays to compare mRNA transcript levels in cultured skin fibroblasts from normal individuals with those in fibroblasts obtained from patients affected with sialic acid storage disease (SIASD) and sialidosis. Although these conditions are caused by different primary genetic defects and result in the accumulation of different storage products, they are all characterized by significantly increased lysosome number and volume in many cell types (Igdoura et al, 1994; Renlund et al, 1986). A total of 53 probe sets, representing 43 known genes and 6 ESTs were differentially expressed in each of the three patient cell lines. Many of the differentially regulated transcripts were consistent with previously described phenotypes of LSD cells (Table V, p.40). For example, the suppression of numerous proteins and enzymes involved in the formation of the extracellular matrix (transglutaminase 2, different types of collagen; tissue inhibitor of metalloproteinase 3; elastin; aggrecan 1; versican) correlates with the reduced ability of LSD fibroblasts to form elastic fibers (Hinek et al, 2000). On the other hand, the majority of differentially regulated transcripts identified in our microarray studies have not been previously reported in association with LSDs (Table V, p.40). This latter group includes ubiquitin C-terminal hydrolase L1 (UCH-L1), a member of

deubiquitinating enzymes family presumably involved in ubiquitin recycling to maintain pools of monomeric ubiquitin in the cell. Malfunction of the ubiquitin pathway due to UCH-L1 deficiency has previously been associated with neuronal degeneration in a small number of patients with autosomal dominant Parkinson's disease (PARK8) (Leroy et al, 1998). As neuronal death and dystrophy is also a characteristic feature in LSDs, we wished to further characterize the relationship between decreased UCH-L1 expression and LSDs.

Our emerging hypothesis was that lysosomal storage might impair cell function and trigger apoptosis via the inhibition of the ubiquitin-mediated protein degradation pathway. The main objectives of the current project, in a perspective of providing general clues about the pathogenesis of LSDs, were:

1. To characterize the expression pattern of UCH-L1 in a group of lysosomal storage disorders (in human fibroblasts and tissues of LSD mouse models)
2. To study the overall involvement of the ubiquitin-proteasome degradation pathway in the cellular pathogenesis of LSD and its possible implication in the mechanisms of apoptosis.

Table V Major groups of proteins whose expression was changed in both SIASD and sialidosis fibroblasts

	Probe Set	Control 1	Control 2	Control 3	Salla	Salla	Salla	Sialidosis	Fold Change	Accession	Gene	Description
Cell Adhesion and Extracellular Matrix	32112_s_at	29.8	9.5	14.4	425.6	295.8	1852.5	47.9	AI800499	AM1	absent in melanoma 1	
	35829_at	229.1	37.0	486.4	1600.5	912.8	3214.4	7.6	AL080181	IGSF4	immunoglobulin superfamily, member 4	
	32193_at	131.1	23.5	116.0	1067.1	398.5	551.6	7.5	AF030339	PLXNC1	plexin C1	
	36917_at	378.8	573.2	625.1	2182.0	1072.3	1169.0	2.8	Z26653	LAMA2	laminin, alpha 2 (merosin, congenital muscular dystrophy)	
	33127_at	5957.9	1802.1	5454.9	11363.6	6772.6	6670.5	1.9	U89942	LOXL2	lysyl oxidase-like 2	
	38077_at	8703.4	8544.3	9305.9	12643.9	10759.1	8985.9	1.2	X52022	COL6A3	collagen, type VI, alpha 3	
	38126_at	40745.6	37915.2	49246.0	30188.8	19650.4	21133.1	-1.8	J04599	BGN	biglycan	
	36513_at	2871.3	2178.2	2410.2	974.3	1479.0	447.2	-2.6	U37283	MAGP2	microfibril-associated glycoprotein-2	
	36636_at	18696.3	15581.0	8226.3	3797.7	5990.7	6570.0	-2.6	AB003184	ISLR	immunoglobulin superfamily containing leucine-rich repeat	
	38112_g_at	6571.3	9058.7	6721.1	1393.2	4184.7	2289.3	-2.8	X15998	CSPG2	chondroitin sulfate proteoglycan 2 (versican)	
	1034_at	11826.4	16617.4	6886.4	4266.4	4018.2	3198.3	-3.1	U14394	TIMP3	tissue inhibitor of metalloproteinase 3 (Sorsby fundus dystrophy, pseudoinflammatory)	
	39333_at	4733.7	4238.4	7949.4	716.5	1703.1	1834.4	-4.0	M26576	COL4A1	collagen, type IV, alpha 1	
	39098_at	8578.2	1542.5	3617.5	121.9	635.6	792.5	-8.9	X52896	ELN	elastin (supravalvular aortic stenosis, Williams-Beuren syndrome)	
	38965_at	1864.1	1029.6	2129.1	214.9	29.7	62.7	-16.3	M55172	AGC1	agrecan 1 (chondroitin sulfate proteoglycan 1, large aggregating proteoglycan)	
	38545_at	728.9	120.5	559.5	6840.9	2452.1	3243.7	8.9	M31682	IN-HBB	inhibin, beta B (activin AB beta polypeptide)	
34335_at	93.6	274.8	375.8	825.4	894.1	1810.5	4.7	A1765533	EFNB2	ephrin-B2		
39685_at	427.3	424.4	302.7	3021.8	1173.4	1227.9	4.7	U33267	GLRB	glycine receptor, beta		
41419_at	660.2	150.9	677.0	1621.5	1007.6	1340.7	2.7	AL022723	HLA-F	major histocompatibility complex, class I, F		
38379_at	3473.2	3633.3	3397.1	11436.0	5949.4	8633.1	2.5	AL080142	CED-6	CED-6 protein		
41123_s_at	7281.0	6639.4	8029.9	4623.7	4970.5	2151.4	-1.9	X76534	GNM5	glycoprotein (transmembrane) nmb		
2062_at	10533.1	13086.2	16306.5	7146.8	5080.9	4494.4	-2.4	L35594	ENPP2	ectonucleotide pyrophosphatase/phosphodiesterase 2 (autotaxin)		
33705_at	1915.1	1012.6	1137.6	309.3	535.3	407.6	-3.2	L19182	IGFBP7	insulin-like growth factor binding protein 7		
1929_at	4753.7	1430.8	1573.8	730.4	476.3	672.8	-4.1	U83508	ANGPT1	angiotensinogen 1		
38404_at	5428.6	11486.9	3179.2	1016.6	1505.5	2186.2	-4.3	M55153	TGM2	transglutaminase 2 (C polypeptide, protein-glutamine-gamma-glutamyltransferase)		
32521_at	18948.3	9071.5	13745.1	6453.1	673.8	768.5	-5.3	AF056087	SFRP1	secreted frizzled-related protein 1		
38268_at	643.2	449.4	491.7	55.1	21.3	116.4	-8.2	U08989	SLC1A1	solute carrier family 1 (neuronal/epithelial high affinity glutamate transporter, system Xag)		
1495_at	3188.1	1697.8	2818.0	419.1	135.5	281.7	-9.2	M34057	LTBP1	latent transforming growth factor beta binding protein 1		
39593_at	1319.8	194.8	250.4	53.1	27.8	21.1	-17.3	A1432401	FGL2	fibrinogen-like 2		
35729_at	1067.8	510.9	674.2	3981.8	2738.2	1476.2	3.6	AB018270	MYO1D	myosin ID		
39542_at	3003.9	3120.3	2907.3	1261.3	1154.8	1558.8	-2.3	AF059611	ENC1	ectodermal-neural cortex (with BTB-like domain)		
38800_at	10678.7	3829.0	2130.7	1147.3	420.7	944.5	-6.6	D46352	STMN2	stathmin-like 2		
39093_at	3725.4	20552.6	16992.0	167.0	2159.4	1311.0	-11.3	J00073	ACTC	actin, alpha, cardiac muscle		
37391_at	6190.1	5308.6	5777.4	21878.6	7949.7	8526.0	2.2	X12451	CTSL	cathepsin L		
34182_at	2367.3	2674.5	1720.7	5679.3	3895.4	4479.1	2.1	U18932	NDST1	N-deacetylase/N-sulfotransferase (heparan glucosaminyl) 1		
36990_at	5636.1	12166.4	4310.6	674.9	1834.2	1880.8	-5.1	X04741	UCHL1	ubiquitin carboxyl-terminal esterase L1 (ubiquitin thioesterase)		
36308_at	355.1	186.4	13.6	1031.6	577.3	503.0	3.8	D78435	ZIC1	Zic family member 1 (odd-paired homolog, Drosophila)		
41448_at	378.8	367.2	377.6	938.2	478.4	755.1	1.9	AC004080	HOXA10	homeo box A10		
40674_s_at	7930.4	3775.4	4470.5	1216.7	918.9	2157.5	-3.8	S82986	HOXC6	homeo box C6		
39158_at	4517.4	2239.8	1432.4	500.1	403.6	594.7	-5.5	AB021663	AIF5	activating transcription factor 5		
33436_at	3249.7	1680.1	4095.5	224.3	424.6	482.8	-8.0	Z46629	SOX9	SRY (sex determining region Y)-box 9 (campomelic dysplasia, autosomal sex-reversal)		
40813_at	539.4	396.2	282.8	2173.8	978.2	1543.4	3.9	A1768188	FLJ12433	fls		
39614_at	844.8	646.8	810.7	2298.7	1529.2	2089.2	2.6	AB018345	KIAA0802	KIAA0802 protein		
37225_at	1317.2	1123.9	1074.4	651.9	640.0	892.1	-1.6	D79994	KANK	kidney ankyrin repeat-containing protein		
41177_at	2181.1	2021.6	2443.2	1116.8	1371.8	736.6	-2.1	AW024285	FLJ12443	hypothetical protein FLJ12443		
32566_at	5700.5	5420.2	5543.2	1519.4	2389.2	2515.7	-2.6	AA165701	FLJ22678	hypothetical protein FLJ22678		
36686_at	2678.2	1064.5	2197.3	702.3	746.6	243.0	-3.5	U07919	ALDH1A3	aldehyde dehydrogenase 1 family, member A3		
38351_at	667.4	291.7	516.2	45.1	157.4	125.4	-4.5	AL050154	DKFZp568L0120	Homo sapiens mRNA; cDNA DKFZp568L0120		
33241_at	1470.3	1001.8	1271.4	184.2	354.8	155.0	-5.4	KIAA0626	KIAA0626	KIAA0626 gene product		

## **MATERIALS AND METHODS**

### ***Cell culture***

Human skin fibroblasts from patients affected with LSDs (galactosialidosis (GM05076), GM<sub>1</sub>-gangliosidosis (GM05653, GM05335), Morquio syndrome types A (GM00958) and B (GM01602, GM03251) sialidosis (GM01718A, FP2601), Gaucher disease types I and II (GM00852, GM00372), and sialic acid storage disease (FP0421) as well as from normal controls (FP0065, FP0075, FP0996, FP0221, FP0342) were obtained from the NIGMS Human Genetic Mutant Cell Repository and from the Ste-Justine Hospital cell repository. Cells were cultured in MEM supplemented with 10% fetal calf serum. To induce lysosomal storage, cells were treated for 0-48 h with the cysteine protease inhibitor E-64 (epoxysuccinyl-leucylamido-(4-guanidino)butane, Sigma, Saint-Louis, MO) which was added directly to the culture medium at a final concentration of 0.5 mM.

### ***mRNA quantification by real-time PCR***

Total RNA was isolated from cells using Trizol reagent (Invitrogen) according to the manufacturer's instructions. RNA quantity and quality was analyzed spectrophotometrically and by agarose-formaldehyde gel electrophoresis. After the extraction of total RNA, first strand cDNA synthesis was performed in presence of random primers using Superscript II reverse transcriptase (Invitrogen). Removal of RNA complementary to cDNA was achieved by incubating the newly synthesized cDNA with 2 units of *E. coli* RNase H (Invitrogen) at 37°C for 20 min. PCR amplification was performed on a SmartCycler (Cepheid) using the SYBR Green PCR kit (Qiagen). The primer pairs, annealing temperatures, number of PCR cycles, and RNA amounts are shown in (Table VI, p.42), which also shows the

predicted sizes of the resulting PCR products. As positive controls for real-time PCR detection, we used mRNA coding for ribosomal subunit 18S (Ambion) and mouse  $\beta$ -actin.

**Table VI** PCR primers and conditions used to measure concentration of UCH-L1 mRNA in cultured fibroblasts and mouse brain.

Gene	Primers	PCR conditions	Product length
UCH-L1	Forward: <sup>446</sup> GGCCAATGTCGGGTAGATGA Reverse: GAACTGGCGCCATGGTTCA <sup>546</sup>	95°C 900 sec. 45 cycles of: 94°C 15 sec. 60°C 30 sec. 72°C 30 sec.	100 bp
18S rRNA	Universal 18S Internal Standards primers (Ambion, Austin, TX)	95°C 900 sec. 35 cycles of: 94°C 15 sec. 63°C 30 sec. 72°C 15 sec.	315 bp
$\beta$ -actin (mouse)	Forward: <sup>937</sup> ACGTTGACATCCGTAAGACCT Reverse: GCAGTAATCTCCTTCTGCATCC <sup>1036</sup>	95°C 900 sec. 45 cycles of: 94°C 15 sec. 60°C 30 sec. 72°C 30 sec.	100 bp

### *Confocal immunofluorescence microscopy*

Skin fibroblasts of normal controls and of patients affected with LSDs were treated for 1 h with 75 nM LysoTracker Red DND-99 dye (Molecular Probes, Eugene, OR), washed twice with ice-cold PBS and fixed with 3.8% paraformaldehyde in PBS for 30 min. Cells were permeabilized by 0.5% Triton X-100, blocked with 10% goat serum in PBS for 1 h, stained with monoclonal anti-UCH-L1 antibodies, or monoclonal anti-ubiquitin antibodies

both from Novocastra (Newcastle, UK) and counterstained with oregon green 488-conjugated anti-mouse IgG antibodies (Molecular Probes, Eugene, OR). Alternatively cells were double stained with FITC-labeled monoclonal anti-UCH-L1 antibodies, or monoclonal anti-ubiquitin antibodies and Texas Red-labeled monoclonal antibodies against LAMP-2 (Washington Biotechnology Inc., Baltimore). Also, immunocytochemical staining for GAPDH (Ambion) and FLAG tag (Stratagene) was performed using corresponding mouse monoclonal antibodies. Slides were studied on a Zeiss LSM510 inverted confocal microscope (Carl Zeiss Inc., Thornwood).

Apoptosis or programmed cell death was detected immunocytochemically using the in situ cell death detection kit or TUNEL method from Roche. The basis of such method relies upon the labeling of DNA strand breaks resulting from DNA fragmentation, by terminal deoxynucleotidyl transferase enzyme, which catalyzes polymerization of labeled nucleotides to free 3'-OH DNA ends in a template-independent manner. The TUNEL reaction preferentially labels DNA strand breaks generated during apoptosis (emission on the green channel) as opposed to necrosis. After fixation in 3% paraformaldehyde for 45 min, fibroblasts cultured under different conditions were permeabilized for 30 min in 0.1% Triton X-100 (in 0.1 % sodium citrate) and incubated for 1 h at 37°C upon addition of the TUNEL reaction mixture. After blocking with 10 % FBS for 30 min, additional immunocytochemical double or triple staining was performed if necessary.

Programmed cell death was also detected using the sulforhodamine multi-caspase activity kit from Biomol, which detects active caspase enzymes (casp. 1-9) in living cells as the SR-VAD-FMK reagent covalently attaches a fluorescent label to the reactive cysteine residue of the active site exposed upon proteolytic cleavage of the zymogens. Confluent fibroblast cells cultured under given conditions (with or without E-64 treatment, transfected

or not with siRNA for GAPDH and UCH-L1) were incubated for 1 h at 37°C ( under 5% CO<sub>2</sub> ) with the SR-VAD-FMK reagent (Biomol), washed, fixed in 3.8 % paraformaldehyde in PBS for 45 min and permeabilized by 0.5% Triton X-100 for 30 min. The cells were either directly observed under the fluorescence microscope or additionally stained for UCH-L1 and/or DAPI.

### *Enzymatic assays*

Ubiquitin hydrolase activity was assayed using AMC-ubiquitin substrate (BostonBiochem, Cambridge, MA) as described more in detail by Liu et al. (2002). The pellet from harvested cultured cells was resuspended in buffer containing 50 mM Tris-HCl (pH 7.6), 0.5 mM EDTA, 5 mM DTT (UCH buffer ) and, following brief sonication on ice, the rates of substrate hydrolysis were determined from the initial linear portion of the kinetic curves (10 min). The same procedure was followed for mouse brain tissues, which were homogenized in UCH buffer and the lipids removed by filtration in a three-layered cheesecloth.

Caspase-3 activity was measured after determining the initial linear part of the kinetic curves using a fluorogenic caspase-3 substrate II Ac-DEVD-AMC and the caspase-3 inhibitor I Ac-DEVD-CHO both from Calbiochem (Darmstadt, Germany). After treatment of normal fibroblasts with 0.5 mM E-64 for given time intervals or skin fibroblasts taken from LSD patients, the cell pellets were harvested and lysed in buffer containing 0.32 M of sucrose, 10 mM of Tris-HCl (pH 8.0 ), 5 mM EDTA and 1% of TritonX-100 for 30 min on ice. After centrifugation at 10,000 × g for 10 min at 4°C, the supernatant or cell lysate was used for assaying the caspase-3 activity.

The lysosomal enzyme β-hexosaminidase was assayed using the corresponding fluorogenic 4-methylumbelliferyl (Muf)-glycoside derivative as substrate (Pshezhetsky and Potier, 1996). The reaction mixture containing 50

$\mu\text{l}$  of the cellular homogenate, 40  $\mu\text{l}$  of 0.1 M sodium acetate buffer (pH 4.6) and 10  $\mu\text{l}$  of Muf-NANA substrate in the same buffer was incubated at 37 °C for 30 min. The reaction was terminated by the addition of 1.90 ml of 0.4 M glycine buffer (pH 10.5) and the concentration of Muf was assayed fluorometrically.

### ***Western blotting***

Cultured cells from LSD patients, controls and 0.5 mM E64 (Sigma, Saint-Louis, MO) treated cells were harvested and homogenized in Laemmli buffer, which was heated for 3 min at 85°C. Protein concentration was determined spectrophotometrically using the reducing agent and detergent-compatible Biorad protein assay kit. Cellular proteins were resolved by 5-15% PAGE pre-cast gels from Invitrogen and electrotransferred on nitrocellulose membrane. Ponceau's staining of the nitrocellulose membrane and alternative staining for cytoplasmic  $\beta$ -actin using mouse monoclonal  $\beta$ -actin (Abcam) antibodies were used as internal controls to normalize for the amount of protein. In the case of ubiquitin immunoblots, the membranes, after being sandwiched between whatmann filters, were autoclaved in TBS for 30 min at 110° C to increase the sensitivity of the assay as described by Swerdlow et al. (1986) and stained with rabbit/mouse (for UCH-L1, FLAG and GAPDH immunoblots) polyclonal anti-ubiquitin antibodies (Sigma). Subsequently, anti-mouse or anti-rabbit peroxidase-conjugated secondary antibodies were used for the detection with BM chemiluminescence blotting substrate kit from Roche (Penzberg, Germany). The same procedure was performed also for mouse brain homogenates and cultured cells, but using this time antibodies directed against human UCH-L1 (mouse monoclonal, Novocastra), GAPDH (mouse monoclonal, Ambion) and FLAG (mouse monoclonal anti-FLAG-M2, Stratagene), except for the membrane autoclaving.



### *Proteasomal activity assays*

Proteasomal activity was assayed as described by Rodgers et al (2003), where fractionation of the cell lysate by ultrafiltration in conjunction with gel-filtration was used to obtain a proteasome rich fraction almost devoid of contaminating protease activities that derive from low molecular weight intracellular proteases.

Mouse whole brain was trimmed into small pieces on dry ice and homogenized in a buffer containing 50 mM Tris-HCl (pH 7.8), 20 mM KCl, 0.5 mM magnesium acetate, 1 mM DTT (Buffer A) using a glass tube homogenizer. The homogenate was filtered through a three-layered cheesecloth to remove lipids and the filtrate was centrifuged at 12,000xg for 10 min at 4°C. Conversely, human skin fibroblasts were harvested from 150cm<sup>2</sup> flasks and lysed by three freeze-thaw cycles in 1 ml water containing 1 mM DTT and the lysate was centrifuged at 14000 x g for 30 min at 4°C to remove any insoluble material.

The supernatant was diluted 20-fold in freshly prepared buffer A containing 10% (v/v) glycerol and 2 mM ATP, concentrated to original volume using a polyethersulfone ultrafiltration membrane with a cut-off of 500 kDa (Millipore, Bedford, MA) and subjected to FPLC gel-filtration on a Superose 6 HR 10/30 FPLC column (Pharmacia Biotech, Castle Hill, NSW, Australia) equilibrated by the same buffer. The addition of 10% glycerol and ATP to the buffer during the membrane separation was required to maintain proteasome activity.

1-ml fractions were collected and assayed for tryptic and chymotryptic activities using N-Suc-LLVY-AMC (Biomol, Plymouth Meeting, PA) and Boc-LRR-AMC (Bachem, Bubendorf, Switzerland) and in the presence or absence of the proteasome specific inhibitor lactacystin (Calbiochem) as described by Rodgers and Dean (2003).

### ***UCH-L1 overexpression studies and apoptosis detection***

pCMV-Sport6 vector containing full-length human UCH-L1 (PGP 9.5) cDNA was purchased from Invitrogen. To obtain a plasmid coding for UCH-L1-FLAG fusion protein, the cDNA was amplified using modified primers aiming the removal of stop codon (AAGCTTATGCAGCTCAAGCCGATGG and CTCGAGGTAGGCTGCCTTGCAGAGAGC) and containing flanking HindIII and XhoI sites. Following gel purification of the ~670 base-pairs PCR product (Wizard PCR Preps DNA Purification System, Promega), it was cloned into pCR2.1 TOPO vector according to the manufacturers indications (TOPO TA Cloning kit, Invitrogen) and then subcloned as a HindIII/XhoI fragment into pCMV-Tag 4a vector by preserving a continuous open reading frame between PGP 9.5 and the FLAG tag. The construct was entirely sequenced and expressed in COS-7 cells to ensure that FLAG-tagged protein retains catalytic activity.

Normal skin fibroblasts were electroporated with 20  $\mu$ g of pCMV-UCH-L1-FLAG vector in MEM containing 1.25% (v/v) DMSO using Gene Pulser II apparatus (Bio-Rad) set at 290 V and 950  $\mu$ F (0.55 kV/cm). 24 hours after transfection the cells growing on glass slides were treated with 0.5 mM E-64 for an additional 24 h, fixed, stained with monoclonal anti-FLAG peptide antibodies/Texas Red-conjugated anti-mouse IgG antibodies (Molecular Probes, Eugene, OR) and counter-stained for apoptosis using TUNEL (Fluorescein in *Situ* Cell Death Detection) kit from Roche. Alternatively, prior to immunocytochemical studies cells were treated for 1 h with LysoTracker Red prior and counterstained with DAPI (Molecular Probes).

*CAChapter AQuantification of UCH-L1 protein in brain extracts by tandem mass spectrometry*

**DAChapter A**Mass spectrometry (MS) has the ability to identify and to quantify thousands of proteins from complex samples with great sensitivity, speed and accuracy (Aebersold and Mann, 2003) (Fig. 3, p.49). In order to quantify and compare the UCH-L1 protein levels, total brain tissues of HEXB+/+ and HEXB-/- mice were dissolved in Laemmli buffer and analysed by SDS-PAGE. Gels were either stained with Coomassie Blue or transferred to nitrocellulose membrane for western blotting with anti-UCH-L1 antibodies. Gel pieces containing UCH-L1-immunoreactive band were excised from Coomassie-stained gels and subjected to tryptic digestion and peptide extraction as described below. Samples were analyzed on ion-trap LC-MS/MS instrument (Nanoflow proteomic solution, Agilent). Spectra were interpreted and quantified using a Spectrum Mill software (Agilent) interface.

The gel was stained in Coomassie blue/20% methanol/0.5% acetate for 1 h and then destained in 30% methanol until the background was nearly clear. The gel slices of interest, as indicated by the position of the UCH-L1 immunoreactive bands, were cut in a sterile environment and were washed for 1 h in 500  $\mu$ l of 100 mM ammonium bicarbonate prior to the reduction of the sulfhydryl groups with 2.8 mM DTT solution in 100mM ammonium bicarbonate. Alkylation of the proteins was performed by adding 10  $\mu$ l of 100 mM iodoacetamide to the gel plug and standing at room temperature for 30 min in the dark until the gel became partially dehydrated. The supernatant was then removed and the gel slices were washed in 500  $\mu$ l of 50% acetonitrile/100 mM ammonium bicarbonate with shaking for 1 hr. Next, the dehydration step was performed by adding 50  $\mu$ L of acetonitrile to the gel pieces for 15 min and drying to dust-like appearance in the rotary evaporator.

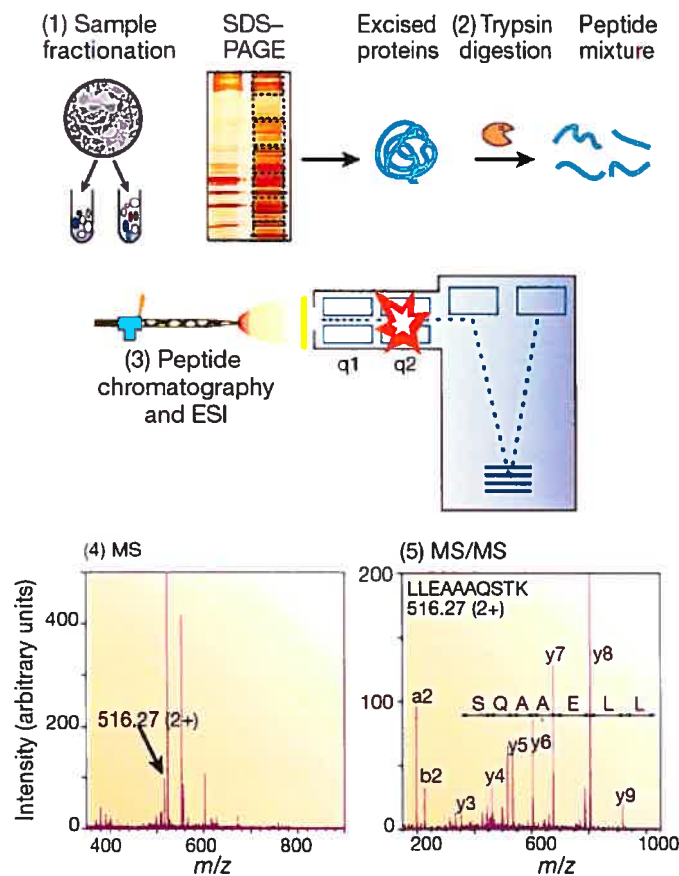


**FIGURE 3** Generic mass spectrometry (MS)-based proteomics experiment.




By definition, a mass spectrometer consists of an ion source, a mass analyser that measures the mass-to-charge ratio ( $m/z$ ) of the ionized analytes, and a detector that registers the number of ions at each  $m/z$  value. Mass spectrometric measurements are carried out in the gas phase on ionized analytes. Electrospray ionization (ESI) and matrix-assisted laser desorption/ionization (MALDI) are the two techniques most commonly used to volatilize and ionize the proteins or peptides for mass spectrometric analysis. The typical proteomics experiment consists of five stages. In **stage 1**, the proteins to be analysed are isolated from cell lysate or tissues by biochemical fractionation (eg. SDS PAGE) or affinity selection. Proteins are degraded enzymatically to peptides in **stage 2**, usually by trypsin, leading to peptides with C-terminally protonated amino acids. In **stage 3**, the peptides are separated by one or more steps of HPLC and eluted into an ESI ion source where they are nebulized in small, highly charged droplets. After evaporation, multiply protonated peptides enter the mass spectrometer and, in **stage 4**, a mass spectrum of the peptides eluting at this time point is taken. The computer generates a prioritized list of these peptides for additional fragmentation and a series of tandem mass spectrometric or 'MS/MS' experiments ensues (**stage 5**). The MS and MS/MS spectra are typically acquired for about one second each and stored for matching against protein sequence databases. The outcome of the experiment is the identity of the peptides and therefore the proteins making up the purified protein population. (Adapted from Aebersold and Mann, 2003)

The gel pieces were swollen or rehydrated with 10  $\mu$ l of 25 mM ammonium bicarbonate containing Promega modified trypsin (sequencing grade) in a substrate to enzyme ratio of 10:1. The digestion reaction was kept at 37°C overnight and the resulting peptides were extracted twice into the organic phase with 50  $\mu$ l of 60% acetonitrile/0.1% TFA for 20 min and then dried in a rotary evaporator. The dried digest extract was redissolved in 20  $\mu$ l of aqueous solvent containing 0.1% of TFA acid for subsequent ESI LC-MS/MS.

### *UCH-L1 small interfering RNA gene silencing in human skin fibroblasts*

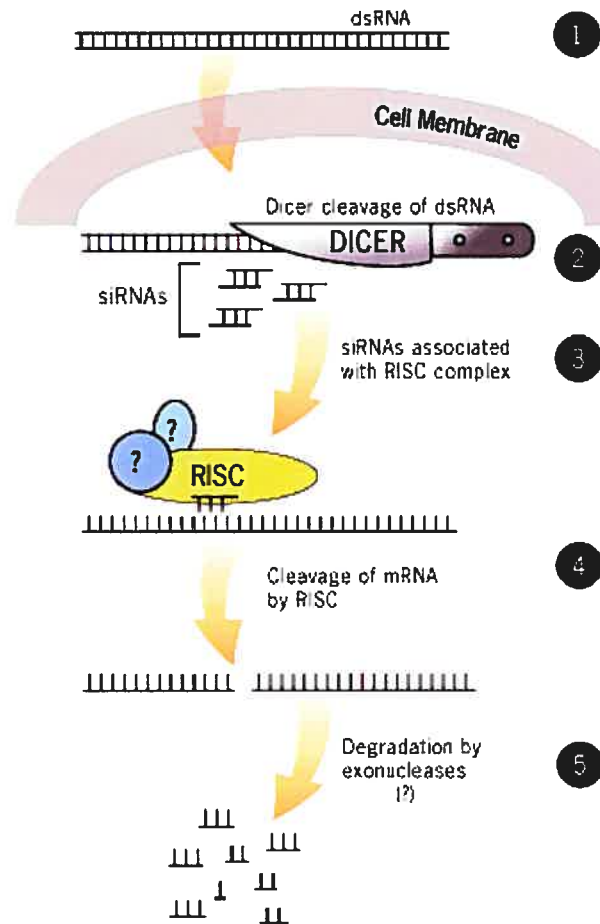
RNA interference can induce potent gene silencing through degradation of complementary mRNA (Fig. 4, p.52). Synthetic siRNAs transfected into mammalian cells can result in a transient decrease in expression of the target gene for 3-5 days. Silencer™ pre-designed siRNA targeting exons 4 and 5 of the human UCH-L1 gene (Table VII, p.50) were obtained from Ambion (Austin, TX).

**TABLE VII** siRNA primers used to downregulate UCH-L1 in cultured fibroblasts.

siRNA ID	Target sequence	Length	MW	% GC	Targeted exon(s)
14138	Sense: 5'-GGAAAAAGCAGAUUGAAGAtt-3'	21	6827.2	33	Targeted Exon(s): NM_004101: Exon 4 siRNA ID#: 14138 
	Antisense: 5'-UCUUCAAUCUGCUUUUUCctg-3'	21	6468.2	38	
14227	Sense: 5'-GGGACAAGAAGUUAGUCCUtt-3'	21	6733.2	43	Targeted Exon(s): NM_004101: Exon 4 siRNA ID#: 14227 
	Antisense: 5'-AGGACUAACUUCUUGUCCct-3'	21	6567.2	43	
14311	Sense: 5'-GGAUGGAUCAGUUCUGAAAAtt-3'	21	6734.2	38	Targeted Exon(s): NM_004101: Exon 4,5 siRNA ID#: 14311 
	Antisense: 5'-UUUCAGAACUGAUCCAUCtc-3'	21	6536.2	43	

Cultured skin fibroblasts were transfected with siRNA using the Lipofectamine Plus transfection kit (Invitrogen). GAPDH siRNA (Ambion) was used as a positive control for the optimization of transfection conditions. Prior to the experiments with normal control fibroblasts, siRNA efficacy was verified using human skin fibroblasts immortalized by transduction with retroviral vectors expressing the type 16 human papilloma virus E7 gene and the catalytic component of human telomerase (kindly provided by E. Shoubridge, Montreal Neurological Institute). The cells were harvested 24 and 48 hours after transfection with 3 UCH-L1 siRNAs and UCH-L1 protein level was assessed by Western blot and immunocytochemistry as described above. Total RNA purified from a separate pool of transfected cells was used to measure UCH-L1 mRNA level by real-time PCR. The most effective UCH-L1 siRNA (ID# 14311) was selected to perform the suppression experiments in normal skin fibroblasts.

48 h after transfection, normal skin fibroblasts treated with UCH-L1 siRNA (final concentration in culture medium was 50 nM) and mock-transfected fibroblasts were fixed and permeabilized as described above. 24 h after transfection, a subset of UCH-L1-transfected and mock-transfected cells was also treated for additional 24 h by 0.5 mM E-64. All cells were stained using a TUNEL kit as described above and counterstained for UCH-L1 protein as described above. Programmed cell death was also detected using the sulforhodamine multi-caspase activity kit from Biomol, containing a SR-VAD-FMK substrate of caspases 1-9. For this, 48 h after transfection, live cells were incubated for 1 h at 37°C with SR-VAD-FMK reagent as recommended by manufacturer, washed, fixed and counterstained for UCH-L1 protein.



<http://www.ambion.com/>

**FIGURE 4 Mechanism of RNA interference (RNAi).**

RNAi is a phenomenon in which the introduction of double-stranded RNA (dsRNA) into a diverse range of organisms and cell types (step 1) causes degradation of the complementary mRNA. On entry into cells, dsRNA is cleaved by Dicer ribonuclease into 21- to 23-nt siRNAs (step 2). SiRNAs containing overhangs of 2 to 3 nucleotides at both 3' ends of the sense (identical to target mRNA sequence) and antisense strands can also be transfected directly to the cell with possibility of achieving transient gene-specific silencing. To overcome the transient inhibitory effects of transfected RNA molecule synthesis *in vitro*, expression plasmids, mostly based on RNA polymerase III promoters, have been designed to achieve long-term or stable inhibition of the target genes. The siRNAs subsequently assemble with protein components into an RNA-induced silencing complex (RISC), which is able to unwind the siRNA and target it to bind the complementary sequence on the host mRNA transcript (step 3). The bound mRNA is cleaved (step 4) and sequence specific degradation of mRNA (step 5) results in gene silencing (reviewed in Dillin, 2003).

### ***Detection of pro- and anti-apoptotic proteins in UCH-L1***

#### ***siRNA-treated cells***

Fibroblasts transfected with UCH-L1 siRNA for 12, 24 and 48 h and mock-transfected controls were fractionated as described (Gobeil et al., 2003). Briefly, cells were suspended in lysis buffer (10 mM Tris-HCl, 10 mM NaCl, 3 MgCl<sub>2</sub>, 30 mM sucrose, pH 7.4) and homogenized with a glass homogenizer (300 strokes); lysate was centrifuged at 700 g for 10 min at 4°C to remove nuclei and debris, and the supernatant re-centrifuged at 10,000 g for 15 min to obtain mitochondria-containing pellet. The supernatant was centrifuged again at 120,000 g 1 h to obtain the S100 cytosolic fraction. The nuclear fraction was additionally purified by washing with the lysis buffer containing 0.120 % NP-40 and centrifuged at 800 g for 10 min. Protein extraction was performed as previously described (Sennlaub et al., 2003) using 50 mM Tris-HCl (pH 7.4), 1 % NP-40, 0.25% sodium-deoxycholate (Sigma), 150 mM NaCl, 1 mM EDTA, 2 mM Na<sub>3</sub>VO<sub>4</sub> (Sigma), 1mM NaF and protease inhibitor cocktail (Roche), for 30 min incubation at 4° C.

20 or 30 µg of protein from the total lysate, mitochondrial, nuclear or cytosol fractions were analyzed by SDS-PAGE. Proteins were transferred to PVDF membranes and probed with antibodies against Bax (clone 6A7 of Pharmingen and B-9 of Santa Cruz for the cleavage of Bax to generate p18 fragment), Bcl-2 (Pharmingen), p53 (clone Pab 240, NeoMarkers), cytochrome C (Pharmingen) and β-actin (Abcam). Intensities of the immuno-reactive bands were measured using Image Pro Plus software (version 4.1.00) from Media Cybernetics.

#### ***Statistical Methods***

Statistical analysis was performed using the two-sample Wilcoxon test.



## **RESULTS AND DISCUSSION**

### **UCH-L1 AND LYSOSOMAL STORAGE**

Oligonucleotide microarrays performed on normal skin fibroblasts and skin fibroblasts obtained from patients with LSDs such as sialic acid storage disease and sialidosis revealed a number of transcripts that were differentially regulated and that were common to both LSDs, independently of the kind of storage material accumulated in the lysosomes. Since one of the most easily observable features of cells with lysosomal storage is the overwhelming increase in the number of lysosomes and their size, we performed an immunocytochemical staining for the lysosomal integral membrane protein LAMP-2 in SIASD and sialidosis human skin fibroblasts. In confluent cultured skin fibroblasts, a 3-5-fold increase in lysosomal storage bodies was detected by immunohistochemical staining with anti-LAMP-2 antibodies (Fig. 5, p.55) as well as by staining with a lysosome-specific dye, LysoTracker Red (not shown).

Since the UCH-L1 gene was downregulated in SIASD and sialidosis disorders in conjunction with an increase in the lysosomal storage bodies, we proceeded in verifying if this deubiquitinating enzyme was also downregulated in other lysosomal disorders with different primary genetic defects. Cultured human skin fibroblasts were first used for this purpose in addition to brain tissues from mouse models of human Sandhoff disease with defective hexosaminidase-B gene.

#### ***Reduced UCH-L1 mRNA levels in fibroblasts from LSD patients and Sandhoff mouse brains***

In order to confirm the suppression of UCH-L1 expression detected by microarray experiments and to determine if UCH-L1 expression is altered in

cell lines obtained from patients affected with other LSDs, we analyzed the level of UCH-L1 mRNA by real-time PCR in cultured skin fibroblasts from 5 different healthy controls and from 11 patients affected with the following LSDs: SIASD (1 line), sialidosis (2 lines), galactosialidosis (1 line), GM1-gangliosidosis (2 lines), Morquio syndrome type A (1 line) and B (2 lines), and Gaucher disease (types I and II, one line each).

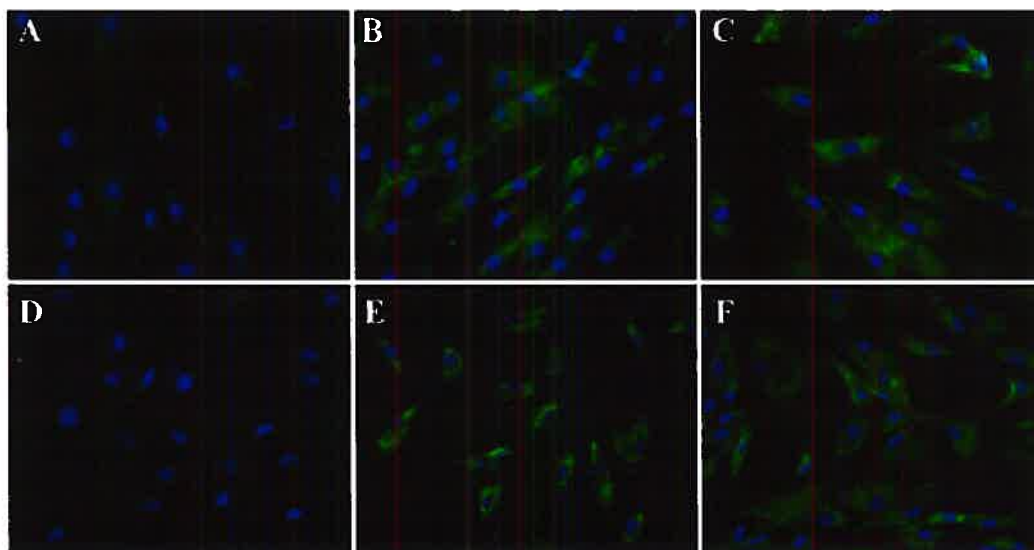


**FIGURE 5** Lysosomal storage bodies in the cells of patients affected with sialidosis and sialic acid storage disease (SIASD). Skin fibroblasts from normal controls (A, D) and from patients affected with sialidosis (B, E) and SIASD (C, F) were cultured to confluency, fixed, stained with a mouse monoclonal anti-human LAMP-2 antibody, and counterstained with oregon green 488-conjugated secondary antibodies. Cell nuclei were visualized with DAPI. Slides were studied on a Zeiss LSM510 inverted confocal microscope. Magnification 600x.

All cell lines were passed an equal number of times and had similar growth rates. These experiments (Fig. 6, p.56) demonstrated that the level of UCH-L1 mRNA in the affected cell lines was significantly reduced (mean 23.5 %, median 23 % of normal) compared to an internal control (18S mRNA). Some cell lines, although they have the same primary genetic defect, showed significant variability in the UCH-L1 mRNA levels between patients. For

example, sialidosis patient 1 (SL1) had almost twice higher UCH-L1 mRNA levels than sialidosis patient 2 (SL2) and similarly for Morquio syndrome type A (MA) patients. This finding should not be at all surprising since there is an evident genetic variability between individuals and that LSDs are heterogeneous in nature with varying residual enzyme activities (Grabowski and Hopkin, 2003).

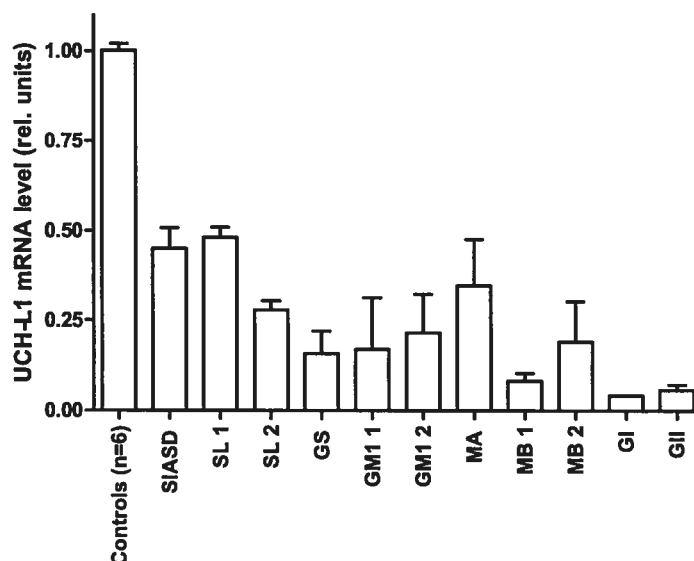


**FIGURE 6** Suppression of UCH-L1 in cultured fibroblasts obtained from LSD patients. UCH-L1 mRNA levels in control fibroblasts (Cont, n=5) and in cells from patients affected with sialic acid storage disease (SIASD), sialidosis (SL 1 and SL 2), galactosialidosis (GS), GM1-gangliosidosis (GM1 1 and GM1 2), Morquio syndrome type A (MA) and B (MB 1 and MB 2) and Gaucher disease types I (GI) and II (GII). The UCH-L1 mRNA was quantified by RT-PCR as described. UCH-L1 mRNA level is presented as a fraction of that in normal control cells (Cont). Values represent means  $\pm$  S.D. of triplicate experiments.

The alteration in UCH-L1 transcripts observed in cultured cells of patients was also confirmed in total brain extracts obtained from mice in which the lysosomal hexosaminidase B (HEXB) gene was inactivated by homologous recombination (Phaneuf et al, 1996). This constitutes a well-studied model of Sandhoff disease that replicates most of the aspects of its human counterpart. Consequently, homozygous HEXB null mice (HEXB<sup>-/-</sup>)

represent a reliable animal model of human Sandhoff disease and develop lysosomal storage bodies as well as a high rate of apoptosis in neurons, microglia and Purkinje cells (Huang et al, 1997). We found that UCH-L1 mRNA was reduced to about 30% in homozygous mutant mice (HEXB<sup>-/-</sup>) as compared to their wild type siblings (HEXB<sup>+/+</sup>) (Fig. 9, p.59). The mRNA level in heterozygous siblings (HEXB<sup>+/-</sup>) that were asymptomatic for LSD was not statistically different from transcript levels seen in their wild-type siblings.

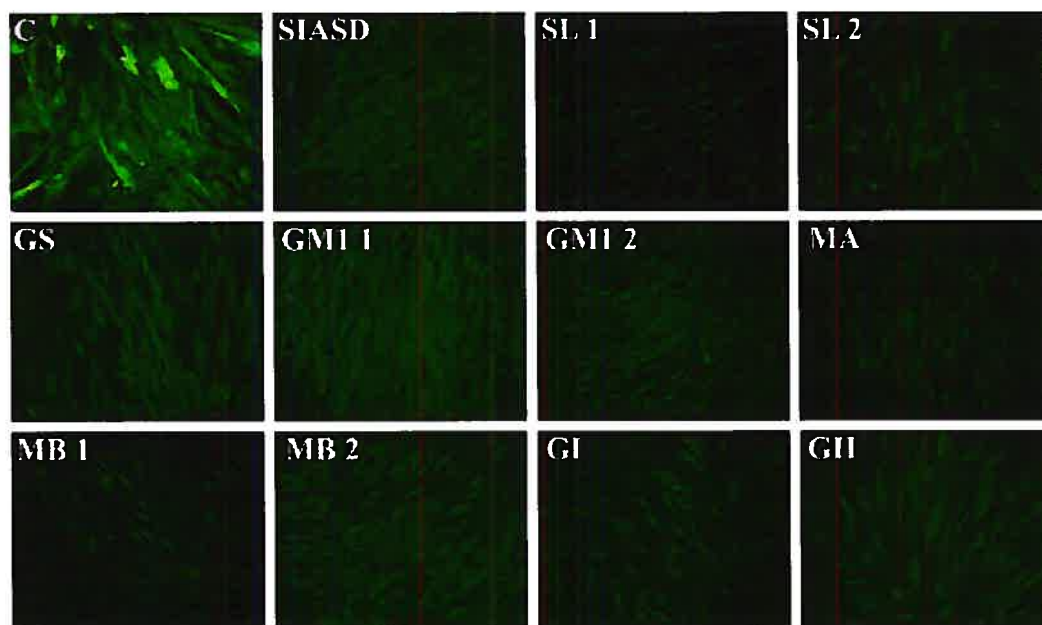


**FIGURE 7** Immunohistochemical detection of UCH-L1 in control cells (C) and cells obtained from LSD patients. Plates of confluent cells were fixed, stained with a mouse monoclonal anti-UCH-L1 antibody, and counterstained with oregon green 488-conjugated secondary antibodies. Slides were studied on a Zeiss LSM510 inverted confocal microscope. Magnification 400x.

***Reduced ubiquitin hydrolase activity and UCH-L1 protein levels in fibroblasts of LSD patients***

The results of these expression studies were confirmed by several biochemical experiments. First, we performed immunohistochemical staining of UCH-L1 in normal fibroblasts and in fibroblasts from LSD patients. Anti-UCH-L1 immunofluorescence in control skin fibroblasts showed a diffuse pattern consistent with the previously described intracellular localization of the enzyme, which is mainly cytosolic (Fig. 7, p.57). The cells of patients showed similar localization of UCH-L1, but the intensity of staining was significantly reduced in all lines reflecting lower protein levels (Fig. 7, p.57).

Second, we assayed ubiquitin hydrolase activity in the homogenates and found that it was significantly reduced in the cells of patients as compared to control fibroblasts (Fig. 8, p.58). Although the level of ubiquitin hydrolase activity somewhat correlates with the level of UCH-L1 mRNA in the patient cells, the ubiquitin hydrolase on average is reduced only to about 50% of normal control, suggesting human fibroblasts contain both UCH-L1 (Olerud et al., 1998) as well as other de-ubiquitinating enzymes.

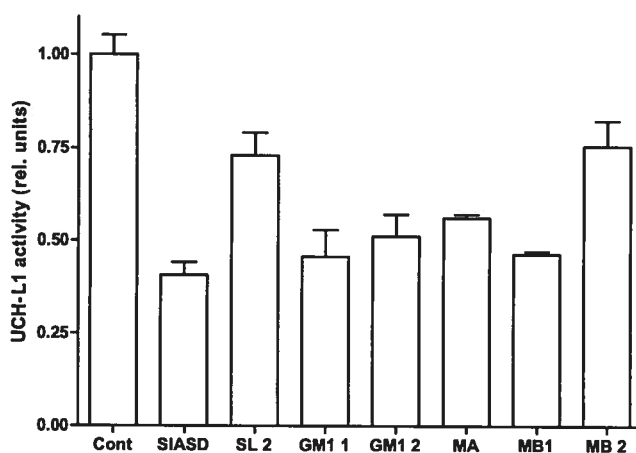


**FIGURE 8** Ubiquitin hydrolase activity in control cells and cells of LSD patients.

Plates of confluent cells were harvested and ubiquitin hydrolase activity in the total cell homogenate was measured with AMC-ubiquitin as described by Liu et al (2002). Specific ubiquitin hydrolase activity is presented as a fraction of that in normal control cells (Cont). Values represent means  $\pm$  S.D. of triplicate experiments.

### *Reduced UCH-L1 protein levels in Sandhoff mouse brains*

In order to determine whether the alteration in UCH-L1 expression levels observed in cultured cells of LSD patients might also accompany the neurodegeneration seen in LSDs, we assayed ubiquitin hydrolase activity and UCH-L1 protein in total brain extracts of Sandhoff mouse brains. As we showed that UCH-L1 mRNA levels were diminished in HEXB<sup>-/-</sup> mice in comparison with their wild-type siblings HEXB<sup>+/+</sup>, we subsequently found that UCH-L1 was also affected at the protein level. Ubiquitin hydrolase activity was reduced approximately 2-fold in the HEXB<sup>-/-</sup> mice when compared to wild-type animals (Fig. 9, p.59). Although the absolute values of ubiquitin hydrolase were significantly higher in mouse brains than those in human fibroblast homogenates, the degree of reduction was consistent between the two models.

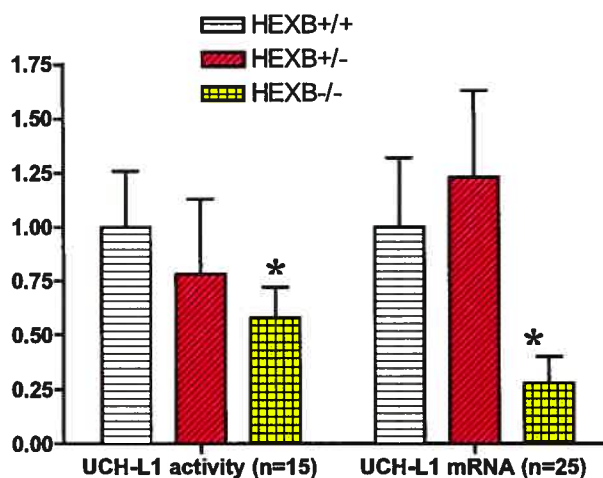


**FIGURE 9** Comparison of UCH-L1 cDNA and protein levels in total brains of Sandhoff mouse model (HEXB<sup>-/-</sup>, HEXB<sup>+/-</sup> and HEXB<sup>+/+</sup> siblings). \*  $p < 0.001$  as compared to wild-type HEXB<sup>+/+</sup> mice.

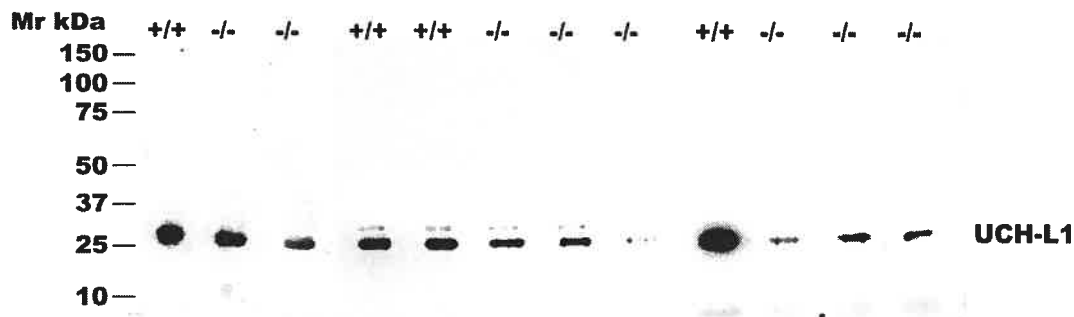
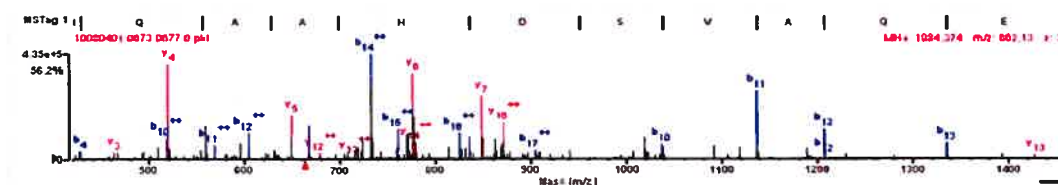


**FIGURE 10** Western blots for UCH-L1 in Sandhoff mouse brains. Western of brain lysates of HEXB<sup>-/-</sup> and HEXB<sup>+/+</sup> siblings of Sandhoff mouse model with monoclonal anti-UCH-L1 antibodies. 20  $\mu$ g of total protein was loaded per lane. Ponceau staining and  $\beta$ -actin were both used as loading controls (not shown). The position of UCH-L1 protein is shown on the right side of the blot.

Western blots also showed reduced levels of UCH-L1 protein in 5 of 8 homogenates tested (Fig. 10, p.60), but since results significantly varied between the different HEXB<sup>-/-</sup> mice, we decided to use a mass-spectrometry-based approach to quantify UCH-L1 protein directly in pooled whole brain extracts. Pooled extracts of HEXB<sup>-/-</sup> and pooled extracts of HEXB<sup>+/+</sup> mice were separated by SDS-PAGE. Gel pieces containing the UCH-L1 protein band as detected by western blot in extracts obtained from HEXB<sup>-/-</sup> and HEXB<sup>+/+</sup> mice were excised from gels, treated with trypsin and analyzed by tandem mass spectrometry coupled to liquid chromatography (LC-MS/MS).

Based on the differences in MS spectra intensity and in the number of unique UCH-L1 peptides detected in each sample (Fig. 11, p.61), we concluded that UCH-L1 protein levels were reduced approximately 2-fold in brain extracts of HEXB<sup>-/-</sup> animals when compared to wild-type animals. Recent data indicated that in the brains of patients affected with Alzheimer's

disease and Parkinson's disease, UCH-L1 undergoes post-translational modifications such as carbonylation, methionine oxidation and cysteine oxidation (Choi et al., 2004) which significantly alter its activity. Our experiments also detected the presence of the UCH-L1 isoforms with 3 oxidized methionine residues, but the ratio between modified and non-modified protein was similar for HEXB<sup>+/+</sup> and HEXB<sup>-/-</sup> animals.



HEXB <sup>-/-</sup> # spectra mean intensity	HEXB <sup>+/+</sup> # spectra mean intensity	Database Accession #	% AA Coverage	Distinct Peptides (#)	Distinct Summed MS/MS Search Score	Group #	Protein Name
14 4.5e+007	17 8.0e+007	18203410	36	6	85.60	7	Ubiquitin carboxyl-terminal hydrolase isozyme L1 (UCH-L1) (Ubiquitin thiolesterase L1)

#	Sequence	MH <sup>+</sup> Matched (Da)	HEXB <sup>-/-</sup> Score SP(%)	HEXB <sup>+/+</sup> Score SP(%)
1	(R)PSAVALCK(A)	895.4711	1.82e+007	1.83e+007
2	(K)LGVAGQWR(F)	886.4899	2.90e+007	2.90e+007
3	(R)MPLPVNHGASSEDSLQDAAK(V)	2214.0501	4.17e+008	5.01e+008
4	(-)MQLKPMENPEMLNK(V)	1815.9171	1.30e+008	3.69e+008
5	(K)NEAIQAHHDSVAQEGQCR(V)	1983.8943	1.90e+007	4.70e+007
6	(K)QEELKQGEVSPK(V)	1484.7960	2.82e+007	4.12e+007

1 MQLKPMENP EMLNKVLAKL GVAGQWR FAD VLGLEEETLG SVSPACALL LFLPLTAQHE NFRKKQHEEL KGOEVSPKVV 80  
81 FAIKQTIGNS GTIGLHAVA NNQDKLEFED GSVLKQFLSE TEKLSPEDRA KCFEKNEAIQ AAHDSVAQEG QRVDKQVNF 160  
161 HEILFNVDG HLYELDGRMP FPNHNGASSE DSSLQDAAKV CREFTEREQG EVRFSAVALC KAA 223

The matched peptides cover 37% (83/223 AA%) of the protein.

Protein Name: Ubiquitin carboxyl-terminal hydrolase isozyme L1 (UCH-L1) (Ubiquitin thiolesterase L1) (Neuron cytoplasmic protein 9.5) (PGP 9.5) (PGP9.5)

Species: MOUSE

NCBI nr\_mammals Accession #: 18203410

MS Digest Index #: 65272

pI of Protein: 5.14

Protein MW: 24838.4 Da

Amino Acid Composition: A20 C8 D11 E23 F13 G14 H6 I7 K16 L24 M5 N11 P9 Q13 R8 S12 T6 V16 W1 Y2

**FIGURE 11** Identification and quantification of UCH-L1 protein in brain lysates of (HEXB<sup>-/-</sup> and HEXB<sup>+/+</sup> siblings) Sandhoff mouse model by tandem mass spectrometry. **Upper panel** - tandem mass spectra of the triply-protonated precursor ion with m/z of 662.13 obtained from nanoLC-MS analysis of a 25-kDa UCH-L1 cross-reactive band. **Lower panel** - UCH-L1 peptides identified by Spectrum Mill software, their scores, relative abundance in brain homogenates of HEXB<sup>-/-</sup> and HEXB<sup>+/+</sup> mice and location in the UCH-L1 sequence. Analysis of relative  $\beta$ -actin spectral intensities and spiking with known amounts of recombinant UCH-L1-FLAG protein were used as loading controls.



### ***E-64-induced lysosomal storage results in reduced expression of UCH-L1***

In order to determine whether reduced levels of UCH-L1 mRNA and protein resulted directly from the accumulation of the storage materials in lysosomes, we induced this condition in normal cells by treating them with the cysteine protease inhibitor E-64 (epoxysuccinyl-leucylamido-(4-guanidino)butane). This compound enters cells by pinocytosis and inhibits lysosomal protein degradation, causing a significant increase in the number and volume of lysosomes as well as the formation of multivesicular dense bodies (Doherty et al, 1989; Laszlo et al, 1990), thus mimicking to a great degree the conditions of lysosomal storage.

In our experiments, 16-h incubation of normal control fibroblasts in the medium containing 0.5 mM of E-64 was sufficient enough to significantly cause an increase in the lysosome number and size as visualized by immunohistochemical staining with anti-LAMP-2 antibodies (Fig. 12A, p.63). These findings are almost identical to the LAMP-2 immunocytochemical staining patterns performed on fibroblasts derived from patients with LSDs such as SIASD, SL (Fig. 5, p.55), GS, GM1, MA, MB, GI and GII (not shown). Interestingly, these same organelles were also heavily stained with anti-ubiquitin antibodies as assessed by a strong colocalization (more than ~80%) of ubiquitin with Lysotracker dye, showing the accumulation of ubiquitinated proteins in the lysosomes (Fig. 12B, p.63). Parallely, we observed a diminished ubiquitin hydrolase activity of the order of ~30 % in the cell lysates of the same normal control fibroblasts after being treated with E-64 for 24 h (Fig 13, p.65). The UCH-L1 mRNA levels were equally depressed after a 24 h E-64 treatment, but the decrease was much more pronounced, almost half of the initial UCH-L1 transcript levels.

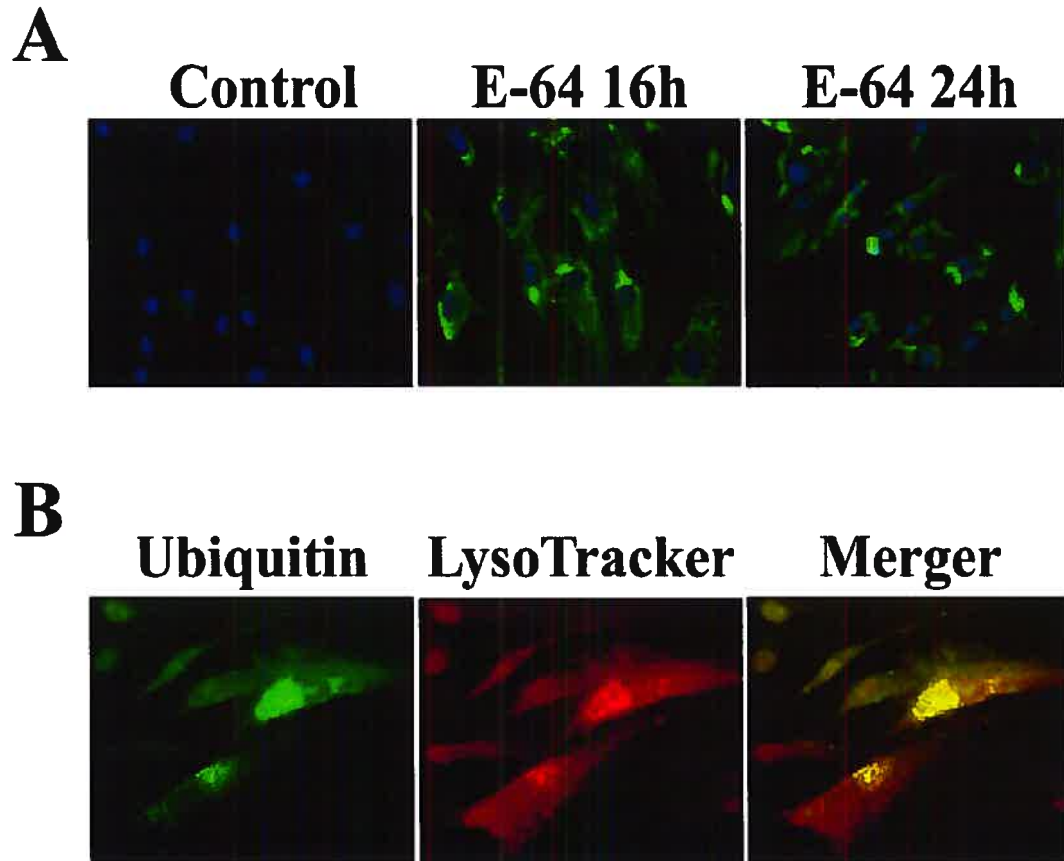


**FIGURE 12 Ubiquitinated lysosomal storage bodies in cultured skin fibroblasts treated with E-64.**

**A)** Lysosomal storage bodies in untreated normal fibroblasts (Control) or normal fibroblasts treated with 0.5 mM E-64 for 16 h (E-64 16h) or 24 h (E-64 24h). The cells were fixed, stained with a mouse monoclonal anti-human LAMP-2 antibody, and counterstained with oregon green 488-conjugated secondary antibodies. Cell nuclei were visualized with DAPI.

**B)** Immunohistochemical localization of ubiquitinated proteins in E-64-treated cells. Following incubation with 0.5 mM E-64 for 24 h, cells were probed with LysoTracker Red, fixed, stained with mouse monoclonal anti-ubiquitin antibodies, and counter-stained with oregon green 488-conjugated secondary antibodies. Panels show ubiquitin-related green immuno-fluorescence (Ubiquitin), LysoTracker-related red fluorescence (LysoTracker) and merged images. Magnification 600x (panel A) or 1000x (panel B).

## UBIQUITIN-PROTEASOME PATHWAY IN LYSOSOMAL STORAGE

As it was demonstrated in our experiments, the UCH-L1 transcripts, protein and activity were decreased in fibroblasts with different LSDs and in brains of Sandhoff mice. Since UCH-L1 is a predominant deubiquitinating enzyme important for regenerating the ubiquitin monomer, it was hypothesized to have an important regulatory role on the activity of the proteasome. Therefore, a deficiency of UCH-L1 enzyme secondary to lysosomal storage would result in impairment of deubiquitination processes and decrease in the recycling of free monomeric ubiquitin, possibly impacting the overall ubiquitin-dependent proteasomal activity. The idea of the presence of ubiquitinated protein aggregates observed earlier in fibroblasts treated with E-64 supported the aforementioned hypothesis (Fig. 12B, p.63), as an impairment of the proteasomal activity would lead to additional protein aggregate formation. The chymotryptic activity of the proteasome is most often used to measure the proteasomal activity in cells and tissues, however it has been shown that the three activities of the proteasome can be separately regulated and a single substrate may not accurately reflect the total proteasomal activity (Rodgers et al. 2003). In our case, proteasome substrates for the chymotryptic and tryptic activities, which were previously shown to display the greatest specificity for their respective activities, were employed to evaluate the overall state of the proteasome.

### *Decreased proteasomal activity in human fibroblasts with lysosomal storage*

Chymotryptic and tryptic activities measured in the 26S and 20S proteasomal fractions were both found to be significantly reduced in the cells of LSD patients (mean=55% of control and SD= $\pm$  12%) and in the E-64-treated control cells (mean= 30% of control and SD= $\pm$  3%) (Fig. 13B, p.65).

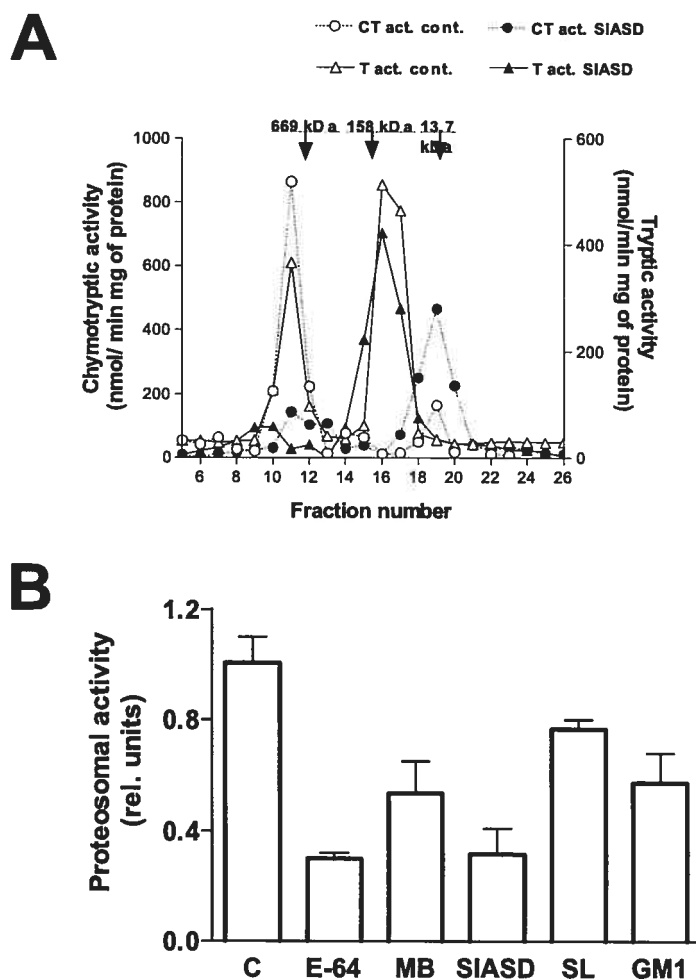


**FIGURE 13** Decrease of proteosomal activity in cultured skin fibroblasts from LSD patients.

A) Gel-filtration of the extracts of normal control skin fibroblasts and of cells from SIASD patients on FPLC Superose 6 column. Chymotryptic and tryptic proteolytic activities in fractions 10-12 corresponding to the expected elution volume of 26S and 20S proteasomes are significantly reduced. Positions of the elution of the Mr standards: thyroglobulin (669 kDa), aldolase (158 kDa) and ribonuclease A (13.7 kDa) are shown by arrows.

B) Proteosomal activity in normal control cells (C), in the cells from patients affected with Morquio syndrome type B (MB), SIASD (SIASD), sialidosis (SL), GM1-gangliosidosis (GM1) and in control cells treated for 24 h with 0.5 mM cysteine protease inhibitor E-64 (E-64). Cell extracts were analyzed by gel-filtration as described. Combined chymotryptic and tryptic activity in pooled fractions 10-12 is presented as a fraction of that in normal control cells (n=2). Values represent means  $\pm$  S.D. of triplicate experiments.

The proteosomal activity, however, was not affected in the cells treated with 0.5 mM E-64 for 2 h (i.e. before the beginning of apoptosis) or when 1 mM E-64 was added directly to the cell homogenates, indicating that the inhibition of the proteosomal activity was not caused by the unspecific action of E-64 on the proteasome itself or the proteasomal substrates in use. In support of the latter results are studies by Rodgers et al. (2003), where the 26S and 20S proteasome-rich gel-filtration fractions were only inhibited by less than 5% when 0.2 mM E-64 was directly added during the proteasome activity assays. The lower molecular weight gel-filtration fractions 15-20, in addition to remaining completely unaffected by lactacystin as opposed to the proteasome-rich fractions 10-12 (~80 % inhibition), showed no significant difference in the tryptic and chymotryptic activities between the controls and the cells with lysosomal storage (Fig. 13A, p.65).

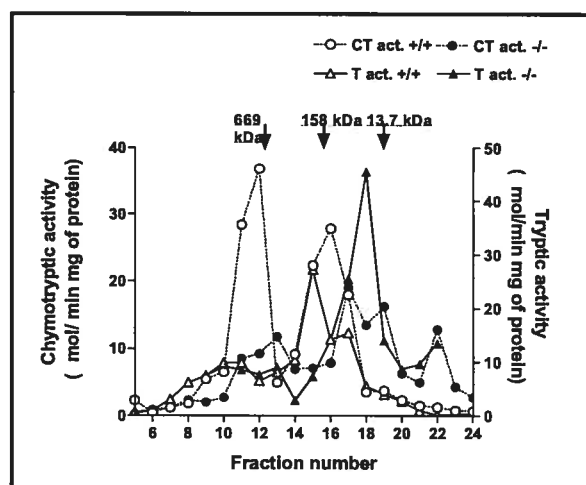


**FIGURE 14** Decrease of proteasomal activity in brain tissues of Sandhoff mice.

Gel-filtration of pooled brain extracts of HEXB<sup>-/-</sup> and HEXB<sup>+/+</sup> siblings of Sandhoff mice on FPLC Superose 6 column. Chymotryptic proteolytic activity is significantly reduced in fractions 10-12 corresponding to the expected elution volume of 26S and 20S proteasomes. Positions of the elution of the Mr standards: thyroglobulin (669 kDa), aldolase (158 kDa) and ribonuclease A (13.7 kDa) are shown by arrows.

### ***Impaired proteasomal activity in Sandhoff mouse brains***

The same trend was observed concerning the tryptic and chymotryptic proteasomal activities measured in total brain homogenates of Sandhoff HEXB<sup>-/-</sup> mice (Fig. 14, p.66). The proteasomal-rich fractions 10-12 of HEXB<sup>-/-</sup> mice demonstrated a marked decrease (almost 4 times less) in both the tryptic and chymotryptic activities when compared with wild-type, strongly suggesting that there is an impairment of the proteasome-mediated protein degradation, hinting for its involvement in the pathology of Sandhoff neurodegeneration.

### ***Lysosomal storage induces formation of ubiquitin protein aggregates and reduced level of free ubiquitin***

Since UCH-L1 is the major cellular ubiquitin hydrolase, we hypothesized that its suppression as a consequence of lysosomal storage should result in the accumulation of ubiquitinated protein conjugates in lysosomal dense bodies as well as in decreased intracellular levels of free ubiquitin. These changes would in turn be expected to impair the proteasomal ubiquitin-dependent protein degradation pathway, causing further cell deregulation and apoptosis. Previous studies have demonstrated that 20 to 30% of small and motor neurons of patients affected with Tay-Sachs disease, Niemann-Pick disease, and Hunter disease showed anti-ubiquitin immunoreactivity in contrast to the cells of normal controls (Zhan et al, 1992). The cells of animal models of MPS VII (Heuer et al, 2002), Niemann-Pick disease (Higashi et al, 1993) and prosaposin deficiency (Oya et al, 1998) also contained ubiquitinated protein aggregates. In our studies, 11 fibroblast lines from patients affected with different LSDs had lysosomal dense bodies that contained ubiquitinated protein aggregates. In addition, immunofluorescent

microscopy with a mouse monoclonal anti-ubiquitin antibody revealed that all the cells from LSD patients showed a predominantly perinuclear punctate staining pattern consistent with mainly lysosomal localization of ubiquitinated proteins (Fig. 15, p.68). Colocalization of ubiquitinated aggregates with lysosomal markers LAMP-2 and LysoTracker Red confirmed that the lysosomal dense bodies were heavily ubiquitinated. Western blots of total cell homogenates showed that the majority of cellular ubiquitin in LSD patient cells is associated with high-molecular weight protein aggregates: in contrast, the amount of free monomeric ubiquitin is significantly reduced (Fig. 16, p.69).

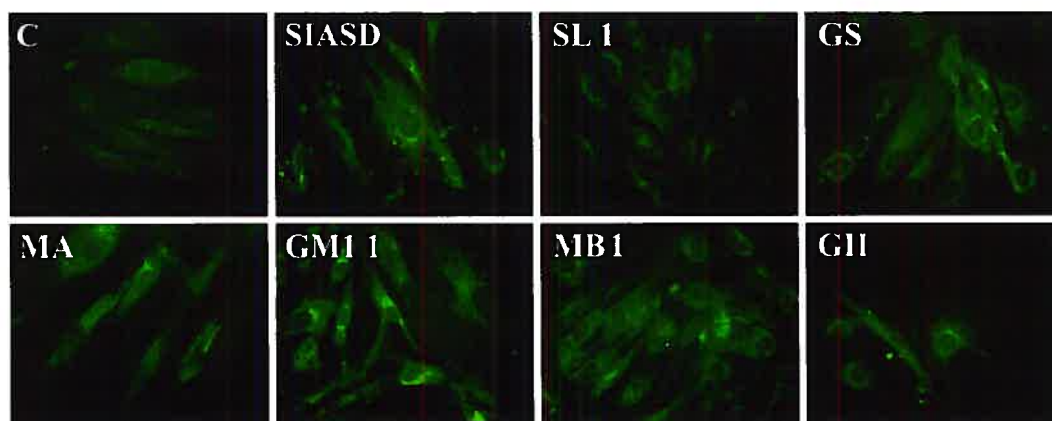


**FIGURE 15** Detection of ubiquitinated proteins in cells with lysosomal storage.

Immunohistochemical localization of ubiquitinated proteins in control fibroblasts (C) and in cells of patients affected with SIASD (SIASD), sialidosis (SL 1), galactosylalidosis (GS), Morquio syndrome type A (MA) and B (MB 1) and Gaucher disease type II (GII). Cells were stained with a mouse monoclonal anti-ubiquitin antibody, and counterstained with oregon green 488-conjugated secondary antibodies.

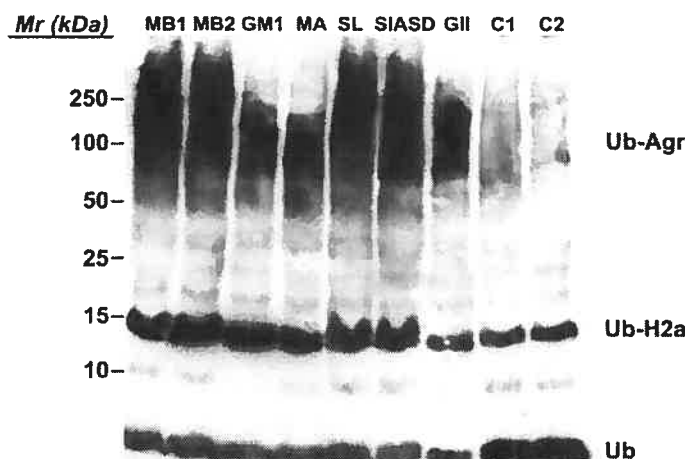


**FIGURE 16** Ubiquitin western blot of fibroblasts of LSD patients.

Western blots of lysates of control cells (C1 and C2) and cells obtained from patients affected with Morquio syndrome type A (MA) and B (MB1 and MB2), GM1-gangliosidosis (GM1), sialidosis (SL), SIASD (SIASD) and Gaucher disease type II (GII) with anti-ubiquitin antibodies. Each lane contains 40  $\mu$ g of total protein. Immunoblotting was performed with anti-ubiquitin rabbit polyclonal antibodies. The position of ubi-quitinated protein aggregates (Ub-Agr), ubiquitinated histone H2a (Ub-H2A) and free udiquitin (Ub) are shown on the right side of blot.

## APOPTOSIS AND LYSOSOMAL STORAGE

To further examine the relationship between lysosomal storage, UCH-L1 inhibition and the induction of programmed cell death, we treated normal fibroblasts with E-64 for 6-48 h. Parallel plates of cells were used to prepare RNA for real-time PCR studies as well as to measure the UCH-L1 hydrolytic activity and the activities of lysosomal  $\beta$ -N-acetyl hexosaminidase and caspase 3 (Fig. 17, p.70). Real-time PCR studies showed significantly decreased UCH-L1 transcript levels following 6 h incubation with E-64, which correlated with the formation of lysosomal storage vacuoles (increase of lysosomal  $\beta$ -N-acetyl hexosaminidase activity). This increase in lysosomal storage bodies upon E-64 treatment for 16h and 24h was as well observed by lysosomal LAMP-2 immunocytochemical staining (Fig. 12A, p.63). A decrease



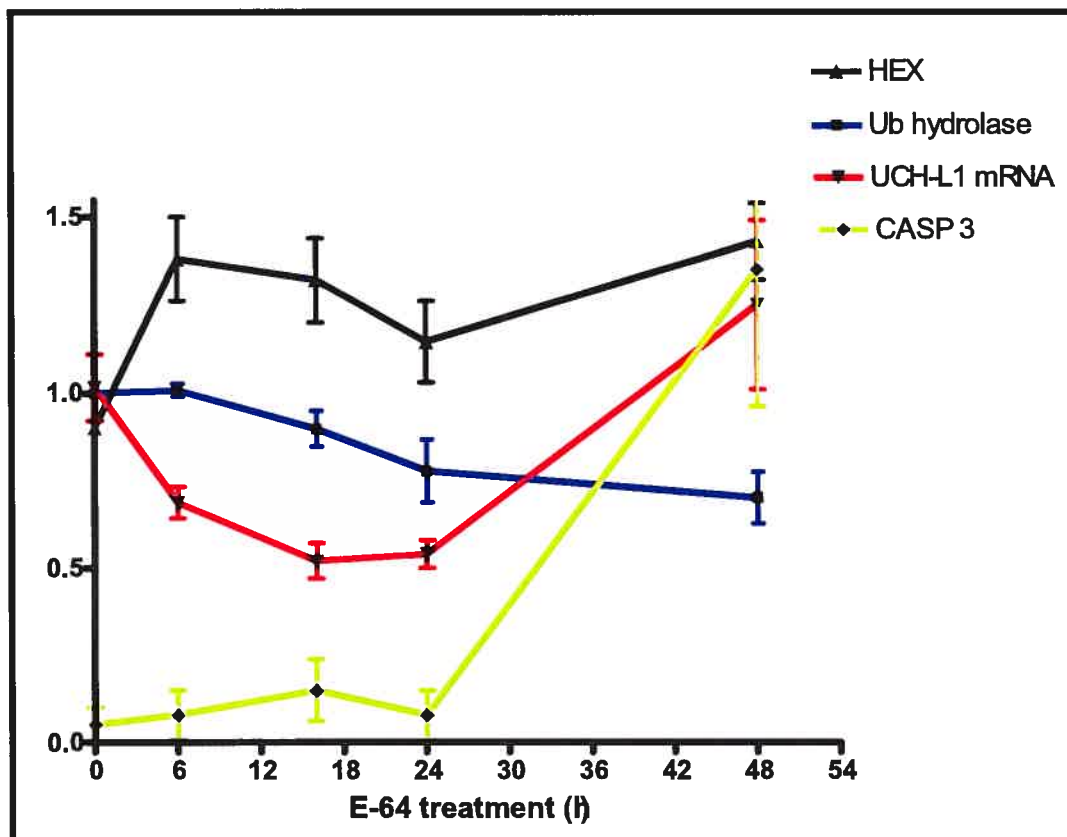


**FIGURE 17** Development of lysosomal storage, UCH-L1 deficiency and apoptosis in cultured skin fibroblasts treated with E-64. Cultured skin fibroblasts from normal controls were incubated with or without 0.5 mM E-64. The cells were harvested at the indicated time intervals and assayed for UCH-L1 mRNA level by RT-PCR (UCH-L1 mRNA), ubiquitin hydrolase activity (Ub hydrolase), lysosomal  $\beta$ -hexosaminidase activity (HEX) and caspase-3 activity (CASP 3) as described. Values represent means  $\pm$  S.D. of triplicate experiments.

of UCH-L1 activity lagged 6 hours after the decline of its mRNA (Fig. 17, p.70). After treatment of the cells with E-64 for 24h, immunofluorescent microscopy showed decreased levels of UCH-L1 protein (Fig. 18A, p.72). After 48-h treatment of cells with E-64, the UCH-L1 mRNA level increased; however, by this time the majority of cells had developed apoptosis as demonstrated by increased caspase 3 activity (Fig. 17, p.70), condensed nuclei (Fig. 18B, p.72) and DNA-fragmentation (Fig. 18C, p.72). This particular series of experiments demonstrates that, in the early stages of lysosomal storage, there is an accompanying decrease in UCH-L1 transcript levels, followed thereafter by a depression of UCH-L1 protein and activity, ending by an activation of caspase-3 and downstream events of apoptosis (DNA fragmentation and condensation).

***Fibroblasts with lysosomal storage display higher apoptosis rates***

We observed cells with condensed nuclei (data not shown) as well as TUNEL-positive cells in all studied fibroblast lines from LSD patients (Fig. 19, p.73). The number of apoptotic cells was variable, ranging from ~5 to ~95% (nuclei condensation assay) and from ~58 to ~100% cells (TUNEL positive cells). In contrast, control lines cultured under the same experimental conditions did not undergo apoptosis, showing that fibroblasts of LSD patients undergo apoptosis at high rate. Caspase 3 activity was detected in all LSD patient cell lines but not in control cells. Indeed, these findings closely resemble what was previously found when normal fibroblasts with E-64-induced lysosomal storage and UCH-L1 downregulation had undergone apoptosis (Fig. 17, p.70).

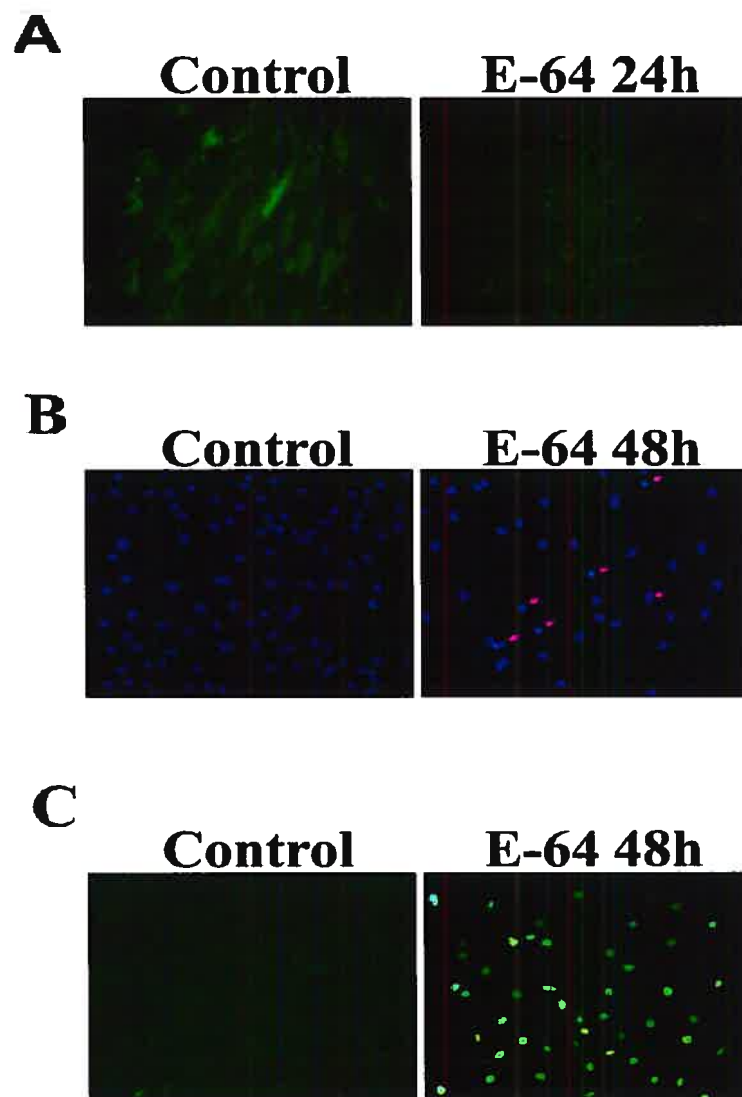


**FIGURE 18** E-64-treated fibroblasts show decreased UCH-L1 protein and increased apoptosis.

A) Immunohistochemical localization of UCH-L1 in control cells and cells treated with E-64 for 48 h. The cells were stained with a mouse monoclonal anti-UCH-L1 antibody, and counterstained with oregon green 488-conjugated secondary antibodies.

B) Epifluorescent microscopy of DAPI-stained control cells and those treated with E-64 for 48 h. Arrowheads show condensed nuclei in apoptotic cells.

C) Epifluorescent microscopy of TUNEL-stained control cells and those treated with E-64 for 48 h. Slides were studied on the Nikon Eclipse E6000 direct epifluorescence microscope. Magnification 400x.

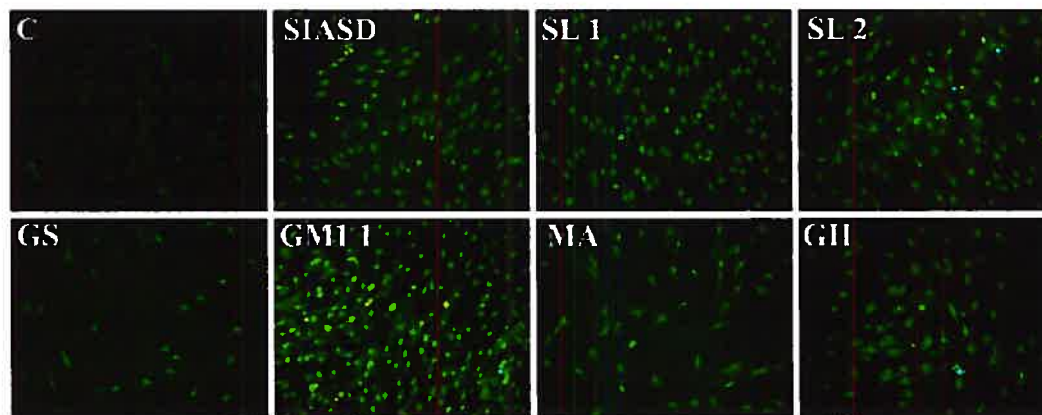


**FIGURE 19** Development of apoptosis in cultured skin fibroblasts from LSD patients. Normal control cells (C) and the cells of patients affected with SIASD (SIASD), sialidosis (SL 1; SL 2), galactosialidosis (GS), GM1-gangliosidosis (GM1 1), Morquio syndrome type A (MA) and Gaucher disease type II (GII) were stained for DNA fragmentation using a TUNEL fluorescence kit. Slides were studied on the Nikon Eclipse E6000 direct epifluorescence microscope. Magnification 400x.

*Overexpression of UCH-L1 in fibroblasts with lysosomal storage rescues them from apoptosis*

To establish the causal relationship between decreased UCH-L1 activity and apoptosis, we studied E-64-induced apoptosis in normal skin fibroblasts transfected with an expression vector coding for UCHL-1 containing a FLAG tag on the C-terminus (pCMV-UCHL-1-FLAG). Indeed, if a UCH-L1 deficiency secondary to lysosomal storage was driving these cells to programmed cell death, the supplementation of functional UCH-L1 would have the ability to partially rescue them. Separate experiments demonstrated that COS 7 cells transfected with pCMV-UCHL-1-FLAG expressed catalytically active UCH-L1. 24 hours after transfection with either pCMV-UCHL-1-FLAG or with pCMV-Tag 4a (mock), the fibroblasts were treated with E-64 for an additional 24 hours, then fixed, stained with anti-FLAG peptide antibodies and assayed for apoptosis using a TUNEL kit. As shown on **fig. 20 (p.75)**, FLAG-positive cells overexpressing UCH-L1 demonstrated a

significantly reduced rate of apoptosis under our experimental conditions. About 40% of control cells (E-64-treated fibroblasts) were TUNEL positive, whereas, only ~7% of FLAG-positive cells showed TUNEL staining (Fig. 20, p. 75). These results strongly support our hypothesis that a deficiency in UCH-L1 enzyme contributes to the increased apoptosis observed in cells with lysosomal storage.

*Suppression of UCH-L1 in normal fibroblasts induces caspase-mediated apoptosis*

Although we demonstrate that the overexpression of UCH-L1 in cells with lysosomal storage prevents cells from undergoing apoptosis, we cannot prove that UCH-L1 deficiency can directly cause apoptosis. In fact, as was previously reviewed, lysosomal storage disorders encompass a series of complex extralysosomal events, including the possibility that accumulated storage material like ceramide in Farber disease, may directly cause apoptosis, although this particular finding was recently invalidated (Ségui et al.). Thus, we transiently suppressed the expression of UCH-L1 in normal human skin fibroblasts (without lysosomal storage) by siRNA-mediated gene silencing, to discern the effects of UCH-L1 deficiency from those of lysosomal storage products in apoptosis.

When we used siRNA to inhibit the expression of UCH-L1 in normal control fibroblasts, we observed an important increase of apoptosis both in the presence and in the absence of E-64. Our preliminary experiments performed on immortalized fibroblasts showed that UCH-L1 siRNA 14311 completely inhibited synthesis of UCH-L1 protein in about 70% of cells (Fig. 21A, p.77). On average, the UCH-L1 mRNA level measured by RT-PCR was reduced more than 7-fold (Fig. 21C, p.77). Pronounced reduction of UCH-L1 protein was also detected by the Western blot (Fig. 21B, p.77).

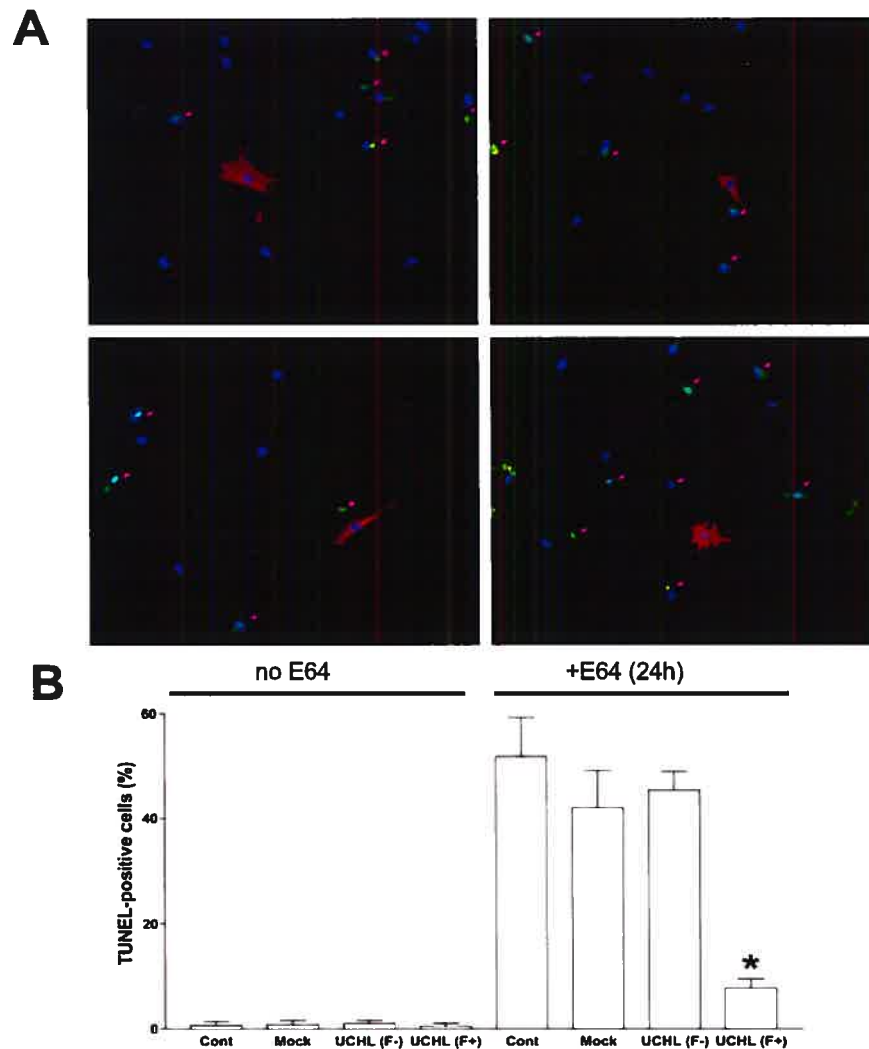


**FIGURE 20** Suppression of E-64-induced apoptosis in cultured skin fibroblasts.

Normal control fibroblasts (*Cont*) and fibroblasts transfected with pCMV-UCH-L1-FLAG plasmid (*UCHL*) or with pCMV-Tag 4a plasmid (*Mock*) were incubated in the presence of 0.5 mM E-64 for 24 h. Then the cells were fixed, and stained for the expression of UCH-L1-FLAG fusion protein with anti-FLAG peptide antibodies, and for DNA fragmentation using TUNEL assay. Nuclei were stained with DAPI. **A**) Epifluorescent microscopy of randomly selected representatives of pCMV-UCH-L1-FLAG-transfected cells treated with E-64 for 24 h. Pseudocolors show DAPI staining (blue) TUNEL staining (green) and anti-FLAG staining (red). Arrowheads show apoptotic TUNEL-positive cells. Slides were studied using a Nikon Eclipse E6000 direct epifluorescence microscope. Magnification 400x. **B**) A cumulative number of apoptotic deaths per 100 cells was counted based on TUNEL staining using epifluorescent microscopy. For pCMV-UCH-L1-FLAG-transfected cells apoptotic deaths were counted separately for FLAG-negative (*F-*) and FLAG-positive cells (*F+*). Values represent means  $\pm$  S.D. of triplicate experiments; from 200 to 300 cells were counted for each condition for each experiment. \*  $p < 0.001$  as compared to nontransfected cells, mock-transfected cells or FLAG-negative cells.

When normal control fibroblasts were treated with a similar concentration of UCH-L1 siRNA 14311 for 48 hours, the fraction of TUNEL-positive cells increased from 3-5% to ~60% (Fig. 22A, p.78). In the presence of E-64, the fraction of TUNEL-positive cells increased from 24% (mock-transfected cells) to 53% (siRNA-transfected cells) (Fig. 22C, p.78), showing that a further depression of UCH-L1 from the one caused by lysosomal storage (E-64 induction) results in greater apoptosis (additive effect). Similar results were obtained after staining the cells with a sulforhodamine multi-caspase activity kit, which detects active caspase enzymes 1-9 in live cells. Only 1-5% of mock-transfected cells showed positive staining in the absence of E-64, while 25% showed positive staining in the presence of E-64 (Fig. 22B, p.78). For siRNA-transfected cells, the fraction of caspase-positive cells in the absence of E-64 was 54% and in its presence 53% (Fig. 22C, p.78). Interestingly, double staining of the cells with pancaspase substrate and with anti-UCH-L1 antibodies or with anti-UCH-L1 antibodies and TUNEL kit showed that apoptosis was triggered exclusively in the cells depleted of UCH-L1 protein, suggesting that inhibition of UCH-L1 expression alone was sufficient to cause the cell death in cultured skin fibroblasts (Fig. 22B,C).

Special attention should be drawn to the fact that, aside the statistical differences or the negligible errors associated in the counting of apoptotic cells, both percentages of caspase activation and DNA fragmentation (TUNEL) are identical upon siRNA treatment, suggesting that they are related to the same event of apoptosis at the single-cell level. Due to technical limitations in combining TUNEL and multi-caspase activity assays, the latter assertion could not be fully verified. However, it can still be safely concluded that the UCH-L1 siRNA-induced apoptosis implicates caspase activation.

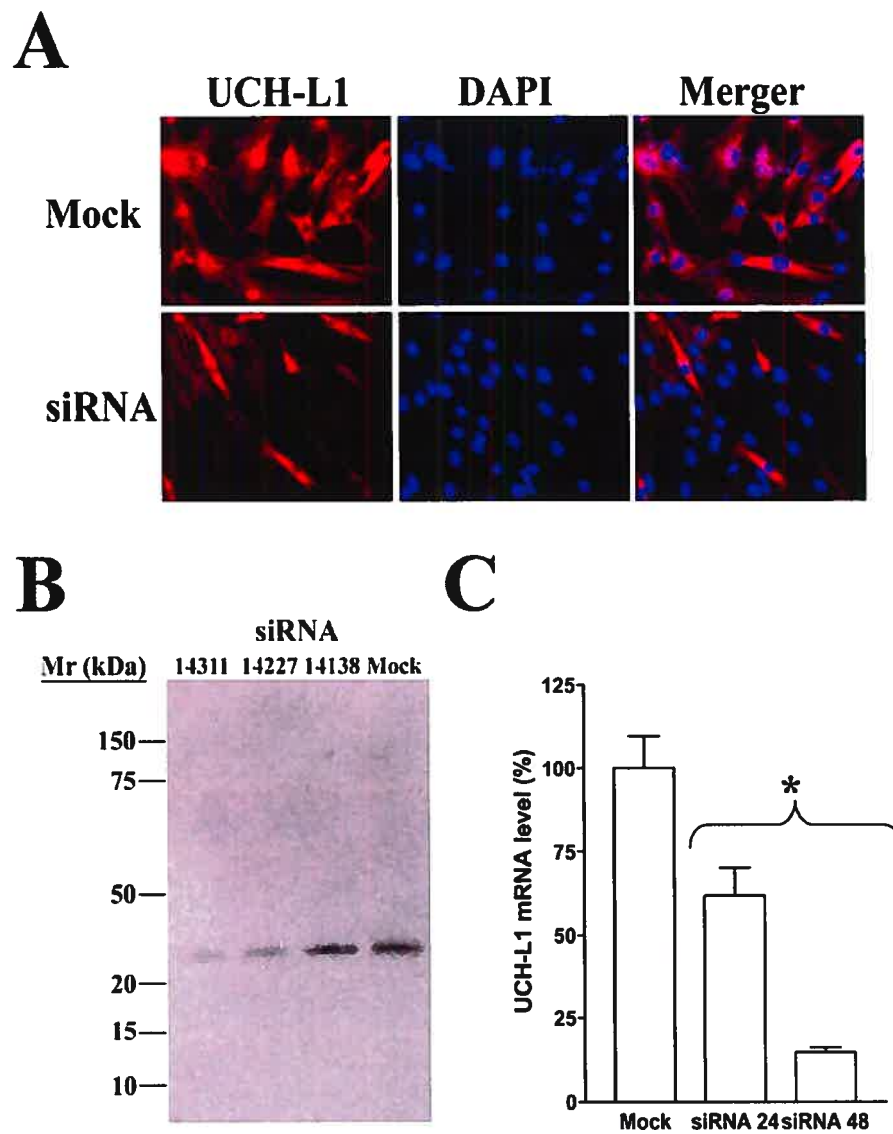


**FIGURE 21** Inhibition of UCH-L1 expression in cultured human skin fibroblasts by siRNA. Immortalized human skin fibroblasts were transfected with UCH-L1 siRNA as indicated. 24 and/or 48 hours after transfection the cells were harvested and UCH-L1 protein level was assessed by immunocytochemistry (A) and Western blot (B) as described in Materials and Methods. From a separate pool of transfected cells, total RNA was purified and used to measure UCH-L1 mRNA level by real-time PCR (C) Results shown represent at least 3 independent experiments performed in triplicates (n=9). \*  $p < 0.001$  as compared to mock-transfected cells.



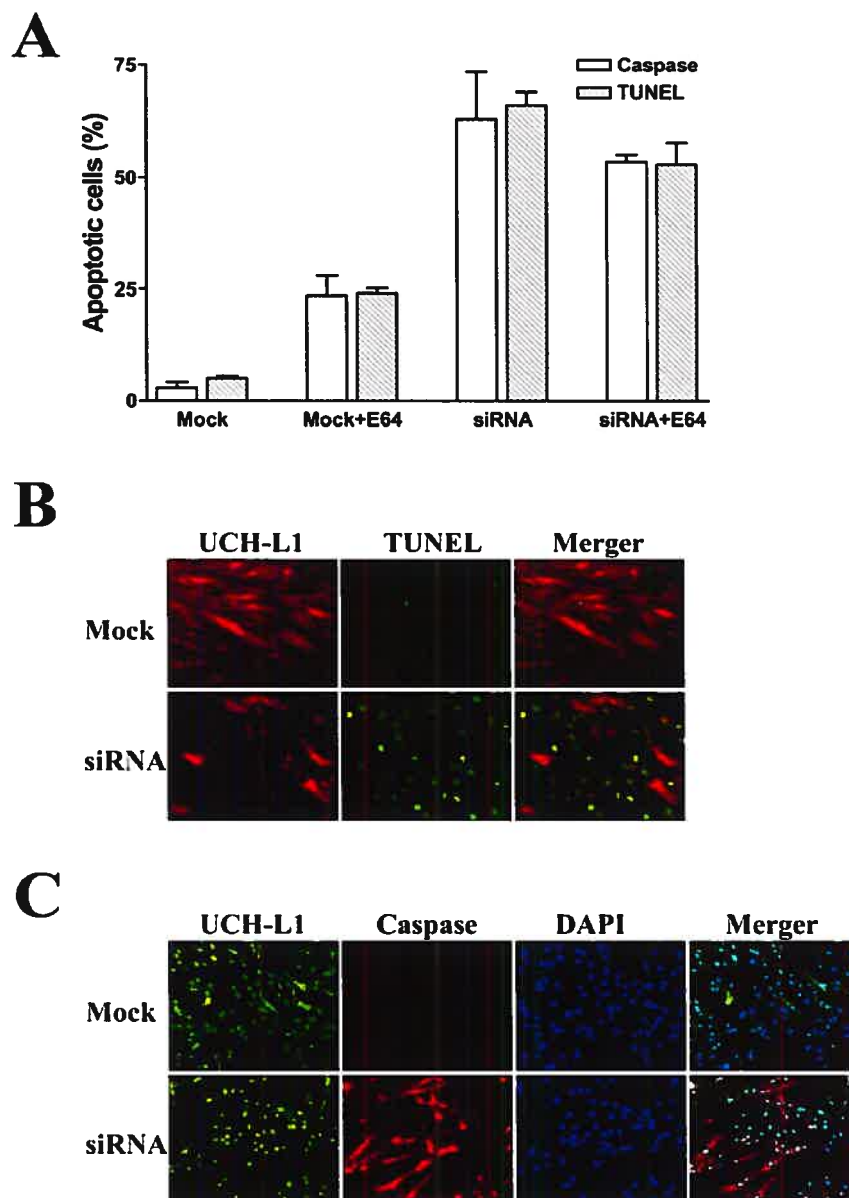


**FIGURE 22** Induction of apoptosis by siRNA-induced inhibition of UCH-L1 expression. Fibroblasts transfected with UCH-L1 siRNA (siRNA) and mock-transfected cells (Mock) were incubated in the absence and presence of 0.5 mM E-64 for 24 h. Then the cells were fixed, and stained for apoptosis using TUNEL kit or sulforhodamine multi-caspase activity kit. A cumulative number of apoptotic deaths per 100 cells was counted based on TUNEL or multi-caspase activity staining using epifluorescent microscopy (A). Values represent means  $\pm$  S.D. of triplicate experiments. Between 450 and 800 cells were counted for each condition in each experiment. In a separate experiment cells transfected with UCHL-1 siRNA were

stained for TUNEL (B) or multi-caspase (C) activity and counterstained for UCH-L1 protein as described above. Pseudo-colors show multi-caspase activity staining (red), TUNEL staining (green), DAPI staining (blue) and anti-UCH-L1 staining (red in B and green in C).

### *Apoptotic proteins bax, bcl-2 and p53 are increased in UCH-L1 suppressed fibroblasts*

In order to address the molecular mechanism by which a UCH-L1 deficiency triggers specific apoptotic pathways, we measured the level of pro- and anti-apoptotic proteins in cells treated with UCH-L1 siRNA 14311 for 12, 24 and 48 hours. After harvesting, nuclear, mitochondrial and cytosolic fractions were prepared by differential centrifugation. The subcellular fractions and the total homogenates were analyzed by western blots using antibodies directed against several known pro- and anti-apoptotic gene products. The expression of pro-apoptotic proteins Bax and p53 was significantly increased between 12 h and 48 h after treatment of the cells with siRNA (Fig. 23, p.81). Note that Bax was increased both in the cell lysate and the mitochondrial fractions, indicating in fact that bax translocates somehow to the mitochondria. The same cells showed a 2-fold increase of the cytosolic cytochrome C level, consistent with its translocation from the mitochondria to the cytoplasm through Bax-induced pore in the mitochondrial membrane. The concentration of pro-survival protein Bcl-2 was also slightly increased in siRNA-treated cells, but this did not stop them from undergoing apoptosis (Fig. 22A, p.78).

Numerous studies have shown that Bax as well as other apoptotic proteins such as Bcl-2 and p53, are targeted for degradation by the proteasome (Lee et al, 2003). In addition, the observed increase in nuclear p53 protein levels in the above experiments can possibly further upregulate the pro-apoptotic protein Bax by its transcriptional activity (Sadot et al, 2001). In cells where there is a transient UCH-L1 deficiency by siRNA treatment, it is

probable that the ubiquitin-dependent proteasomal degradation was negatively affected, with resulting increases in the stabilization of apoptotic proteins and cell cycle regulators, but this remains purely speculative until further experiments are performed. In GAD mice with defective UCH-L1 however, ubiquitinated protein inclusions were observed (Saigoh et al, 1999) denoting a decrease in proteasomal activity. Meanwhile, it is less probable that intralysosomal ubiquitinated storage bodies would be observed in UCH-L1 siRNA-treated normal fibroblasts since there is seemingly no inhibition of lysosomal degradation.

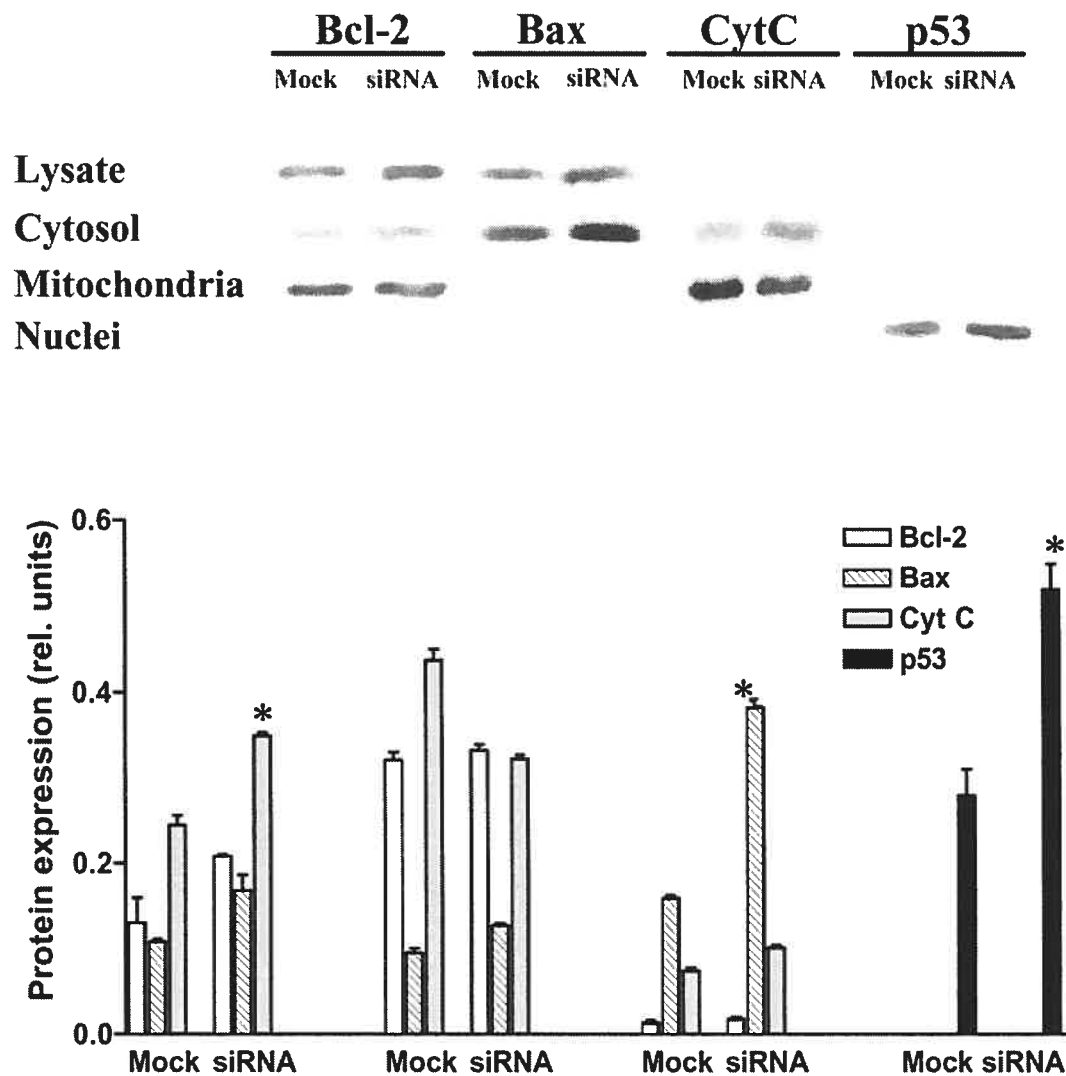


**FIGURE 23** Expression of pro- and anti-apoptotic proteins in cultured skin fibroblasts treated with UCH-L1 siRNA.

Cultured human skin fibroblasts were transfected with UCH-L1 siRNA (siRNA) and mock transfected cells (Mock). At the time periods indicated on the figure, cells were harvested and fractionated on nuclear, mitochondrial and cytosolic fractions by differential centrifugation. 20  $\mu$ g of total protein from cytosol and mitochondrial fractions and from the total homogenates and 30  $\mu$ g of total protein from nuclear fractions were analyzed by western blots using antibodies against p53, Bax, Bcl-2, cytochrome C and  $\beta$ -actin. **Upper panel:** representative images from four independent experiments are shown. **Lower panel:** relative intensities of pro- and anti-apoptotic proteins measured by western blots on the lysate, cytosol, mitochondria and nuclei (shown from left to right). Values represent means  $\pm$  S.D. of triplicate experiments. Intensities of immuno-reactive bands are normalized for the intensities of  $\beta$ -actin cross-reacting bands on the same lanes. \*  $p < 0.001$  as compared to mock-transfected cells.

## CONCLUSIONS AND PERSPECTIVES

The ubiquitin pathway is responsible for proteasome-mediated turnover of short-lived regulatory proteins as well as the degradation of misfolded, unassembled or damaged proteins that could be potentially dangerous for the cell (Hochstrasser & Varshavsky, 1990; Varshavsky, 1997). Ligation of activated ubiquitin to substrate proteins by ubiquitin protein ligases, targets them to proteosomes or lysosomes where proteolysis occurs. Previously, protein aggregation in cells transiently transfected with polyglutamine repeat-containing proteins was shown to directly cause near-complete inhibition of the ubiquitin-proteasome system (Bence et al, 2001). Our studies demonstrate that the impairment of the ubiquitin protein degradation pathway also takes place in the cells from LSD patients in which the lysosomal protein degradation system is overwhelmed by undegraded macromolecules.

We have shown that the expression of the most abundant cellular ubiquitin C-terminal hydrolase, UCH-L1, is dramatically inhibited in cells from LSD patients including those affected with sialidosis, SIASD, galactosialidosis,  $G_{M1}$ -gangliosidosis, Morquio disease type A and B, and Gaucher disease as well as in normal fibroblasts in which accumulation of lysosomal storage materials was induced by the cysteine protease inhibitor E-64. UCH-L1 was also inhibited in the brains of Sandhoff mice that showed neuronal lysosomal storage and accumulation. UCH-L1 is especially abundant in neurons and neuroendocrine cells where it represents 1-2% of total soluble protein (Wilkinson et al, 1989; Satoh & Kuroda, 2001a). Previous studies have shown that UCH-L1 deficiency is involved in the pathogenesis of several neurodegenerative disorders. In mice, mutation of the UCH-L1 gene results in gracile axonal dystrophy (GAD), a disorder characterized by axonal degeneration of the gracile tract: the affected animals display sensory

ataxia followed by posterior paralysis and death (Saigoh et al, 1999). Pathological examination of the GAD mice revealed ubiquitinated inclusion bodies, and dot-like deposits of proteasome immunoreactivity, indicating deposits of proteosomal substrates; similar observations were made in transgenic mice in which the double-knockout UCH-L1 and UCH-L3 genes resulted in posterior paralysis, dystrophic neurons, and increased neuronal death (Saigoh et al, 1999; Kurihara et al, 2001). In *Drosophila*, genetic screens have shown that an UCH homolog can enhance ataxia resulting from ablation of ataxin-1 function (Fernandez-Funez et al, 2000). In humans, a missense mutation (I93M) in UCH-L1 has been linked to Parkinson's disease. Further studies have identified a S18Y polymorphism in the UCH-L1 gene that is linked to decreased susceptibility to Parkinson's disease (Levecque et al, 2001; Maraganore et al, 1999; Momose et al, 2002; Satoh & Kuroda, 2001b; Wang et al, 2002; Liu et al, 2002). Subsequent studies have shown that UCH-L1 also catalyses a reverse ubiquityl ligase activity which is significantly reduced by a S18Y change (Liu et al, 2002).

Ubiquitinated protein aggregates have been observed in tissues of mice and humans affected with LSDs (Heuer et al, 2002; Higashi et al, 1993; Oya et al, 1998; Zhan et al, 1992), although Zhan et al (1992) viewed it as an unspecific epiphenomenon rather than a mechanism of biological significance. Our data suggest that intracellular storage of ubiquitinated aggregates seen in patients affected with LSDs is related to secondary UCH-L1 deficiency, which also results in lower levels of free monomeric ubiquitin, significantly decreased proteosomal activity and increased apoptosis and therefore contributes to tissue deterioration.

Previous studies have shown that ubiquitination is one of the major mechanisms for the regulation of key proteins of the cell apoptotic machinery, such as p53 (Haupt et al., 1997) and the molecules of Bcl-2 family

(reviewed in Lee and Peter, 2003; Yang and Yu, 2003). For example Ub-dependent degradation of pro-apoptotic Bcl-2 family members Bid (Breitschopf et al., 2000), Bax (Li and Dou, 2000) and Bak (Thomas and Banks, 1998) has been reported to promote cell survival. Moreover, recent studies on GAD and UCH-L3 knock-out mice suggest that through regulation of mUb level, UCH-L1 plays a role in balancing the expression of pro- and anti-apoptotic proteins (Osaka et al., 2003; Kwon et al., 2004). The majority of tumors and cancer cell lines contain significantly up-regulated UCH-L1 (Hibi et al., 1998; Tezel et al., 2000, Yamazaki et al., 2002; Otsuki et al., 2004).

In this study, we showed that the transient transfection of cells with UCH-L1 expression plasmid significantly reduced apoptosis in fibroblasts treated with the lysosomal cysteine protease inhibitor E-64, whereas siRNA-induced inhibition of UCH-L1 expression caused apoptosis both in the presence and in the absence of E-64. Almost 100% of siRNA-transfected cells were TUNEL-positive and showed activated caspase cascade. Since the same cells also showed presence of cytochrome C in the cytosol, and significantly induced levels of Bax and p53, we suggest that the execution phase of apoptosis involves translocation of Bax to the mitochondrial membrane, release of cytochrome C from the mitochondria and activation of the caspase cascade.

Less clear is the development of the upstream events. Recent studies (Osaka et al., 2003) have shown that UCH-L1 plays an important role in the maintenance of the intracellular monoubiquitin (mUb) level either by generating mUb through the hydrolysis of mono-ubiquitinated proteins intended for lysosomal degradation or/and by binding mUb and thus preventing its intra-lysosomal degradation (Fig. 24, p.85). In addition, the use of inhibitors of lysosomal function extended the Ub half-life and partially

diminished the effect of UCH-L1, suggesting to Osaka et al. (2003) that UCH-L1 may prevent ubiquitin degradation in lysosomes under normal conditions. Shih et al. (2000) found that Ub contains all the necessary signals for both targeting and degradation of monoubiquitinated proteins in the endosomal-lysosomal pathway. Therefore, direct UCH-L1 binding to Ub may prevent its shunting to the endosomal-lysosomal pathway.

Under conditions of lysosomal storage though, the degradation of Ub in the lysosome is also presumably impaired, as suggested by the observed accumulation of ubiquitinated material in the lysosomal dense bodies. It is tempting to speculate that down-regulation of UCH-L1 can be a part of

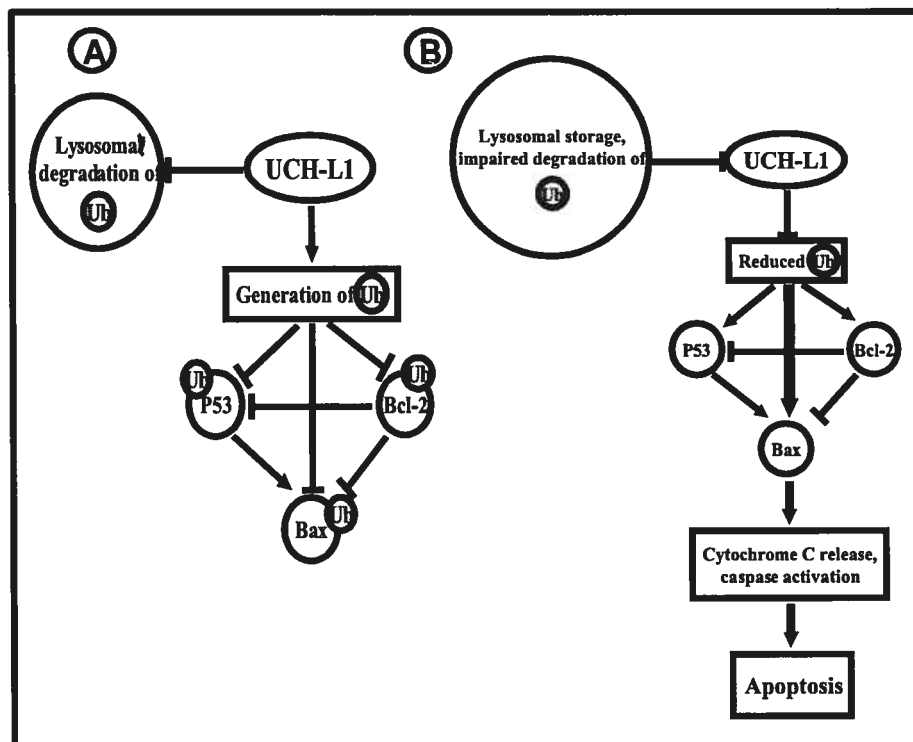


**FIGURE 24** Proposed scheme of UCH-L1-mediated apoptosis following lysosomal storage.

- A) In a normal cell, sufficient lysosomal degradation maintains the recycling of mUbi in conjunction with UCH-L1. UCH-L1 may prevent ubiquitin degradation in lysosome. Proteasomal degradation of critical cell cycle and apoptosis regulators is balanced.
- B) In a cell with lysosomal storage, lysosomal function is impaired with resulting intralysosomal accumulation of ubiquitin protein aggregates. Cellular mUbi levels drop and are somehow sensed, resulting in a downregulation of UCH-L1 and deregulation of the



ubiquitin-proteasome degradation pathway, driving the cell to apoptosis through the mitochondrial pathway.

the feedback mechanism to avoid a potential increase of the mUb level in the cytoplasm. However, the reduction of UCH-L1 also suppresses deubiquitination of monoubiquitinated proteins before their degradation within the endosomal-lysosomal pathway and causes an opposite effect: the mUb concentration in the cell drops below the critical level necessary to maintain the proteasomal activity (Fig. 24). Multiubiquitinated proteins have a propensity to aggregate and they have the potential to directly block the proteasome (Bence et al, 2001). In other words, a vicious cycle probably starts when accumulated proteins block the internal compartment of the proteasome, thereby further reducing proteasomal activity and initiating the cell death program. Although more experiments are needed to fully confirm this hypothesis, we believe that our results might provide an explanation for the increased apoptosis observed in many LSDs.

Interestingly, in our gene microarrays (Table V), secreted-frizzled related protein (SFRP1), dickkopf related protein-1 (DKK-1) and SOX-9, three types of inhibitors of the Wnt signaling pathway, were all significantly down-regulated in sialidosis skin fibroblasts compared to normals. Wnt signaling plays a major role in cell fate determination through the regulation of cell proliferation, differentiation and apoptosis (Cadigan et al, 1997). Recently, SFRP1 was found to have a protective effect on cultured human fibroblasts by decreasing the degree of ceramide-induced apoptosis (Xiaozhe et al, 2003). Moreover, in this same study, it was suggested that SFRP1 may regulate apoptosis through p53, caspases and bax (pro-apoptotic genes). Upon siRNA inhibition of SFRP1, they observed a significant upregulation of p53 and bax along with activation of casp-9 and casp-3. Since degradation of  $\beta$ -catenin involves the UPS, an impairment of UPS as in lysosomal storage, would cause

a greater stability of  $\beta$ -catenin. In the light of our UCH-L1 studies and our microarray results showing SFRP1 downregulation, it is possible that both an increase in  $\beta$ -catenin signaling and UCH-L1 down-regulation impinge on the same pathway (synergistic or additive effect), leading to the increased apoptosis observed in lysosomal storage cells. The main issue that still remains problematic in the studies pertaining to the field of LSDs is how lysosomal storage can precisely engender changes in gene expression levels. One valid opinion would be that the endo-lysosomal pathway is perturbed and that monoubiquitinated receptors on the cellular surface are not properly recycled, giving rise to a signal transduction cascade reaching the nucleus.

Taken together, our data suggest that decreased ubiquitin pathway activity caused by secondary UCH-L1 deficiency contributes to cellular deterioration in patients affected with LSDs. We propose that secondary UCH-L1 deficiency in LSDs results in the intracellular storage of ubiquitinated aggregates, lower levels of free monomeric ubiquitin, significantly decreased proteosomal activity and increased apoptosis. In contrast, transient transfection with a UCH-L1 expression plasmid successfully reduced the prevalence of apoptosis in cells treated with the lysosomal cysteine protease inhibitor E-64. On the other hand, siRNA suppression of UCH-L1 in normal fibroblasts precipitated them to undergo bax-mediated apoptosis. We believe that this mechanism provides a reasonable explanation for the increased programmed cell death observed in the different cell and tissue types in almost all LSDs regardless of the primary genetic and biochemical defect. Since the apoptosis-related tissue deterioration (including the neurodegeneration caused by the neuronal apoptosis) is the underlying pathology in most LSDs, we believe that our findings may help to develop new therapies that would target these disorders.

## REFERENCES

Adams, J. M. & Cory, S. (2001) *Life-or-death decisions by the Bcl-2 protein family*. Trends Biochem. Sci. 26: 61-66

FAChapter AAebersold R. and Mann M. (2003) *Mass-spectrometry-based proteomics*. Nature 422: 198-207

GACChapter AAlves-Rodrigues A., Gregori L., Figueiredo-Pereira ME. (1998) *Ubiquitin, cellular inclusions and their role in neurodegeneration*. Trends Neurosci. 21: 516-520

Arends, M.J. and Wyllie, A.H. (1991) *Apoptosis: Mechanisms and roles in pathology*. Intl Rev Exp Pathol 32: 223-254

Bence NF, Sampat RM, Kopito RR (2001) *Impairment of the ubiquitin-proteasome system by protein aggregation*. Science 292: 1552-1555

Broker L, Kruyt F, and Giaccone G. (2005) *Cell Death Independent of Caspases: a review*. Clin Cancer Res 11(9): 3155-3162

Buccoliero R, Bodennec J, Futerman AH (2002) *The role of sphingolipids in neuronal development: lessons from models of sphingolipid storage diseases*. Neurochem Res 27: 565-574

Burek C, Roth J, Koch HG, Harzer K, Los M, Schulze-Osthoff K (2001) *The role of ceramide in receptor- and stress-induced apoptosis studies in acidic ceramidase-deficient Farber disease cells*. Oncogene 20: 6493-6502

Cadigan, K.M. and Nusse, R. (1997) *Wnt signaling: a common theme in animal development*. GenesDev. 11: 3286-3305

Chipuk JE, Kuwana T, Bouchier-Hayes L, Droin NM, Newmeyer DD, Schuler M, Green DR. (2004) *Direct activation of Bax by p53 mediates mitochondrial membrane permeabilization and apoptosis*. Science 13: 1010-1014

Ciechanover, A. , Orian A., Schwartz AL. (2000) *Ubiquitin-mediated proteolysis: biological regulation via destruction*. Bioessays 22: 442-451

Cirman T, Oresic K, Mazovec GD, Turk V, Reed JC, Myers RM, Salvesen GS, Turk B. (2004) *Selective disruption of lysosomes in HeLa cells triggers*

*apoptosis mediated by cleavage of Bid by multiple papain-like lysosomal cathepsins. J. Biol Chem* 279: 3578-3587

Coenen, R., Gieselmann, V., and Lullmann-Rauch, R. (2001) *Morphological alterations in the inner ear of the arylsulfatase A-deficient mouse. Acta Neuropathol. (Berlin)* 101:491-498

Conconi, M., Szweda, LI., Levine, RL., Stadtman, ER. and Friguet, B. (1996) *Age-related decline of rat liver multicatalytic proteinase activity and protection from oxidative inactivation by heat-shock protein 90. Arch Biochem Biophys* 331: 232-240

Daugas, E., Nochy, D., Ravagnan, L., Loeffler, M., Susin, S.A., Zamzami, N., and Kroemer, G. (2000) *Apoptosis-inducing factor (AIF) :A ubiquitous mito-chondrial oxidoreductase involved in apoptosis. FEBS Lett* 476:118-123

Day, I. N. M.; Hinks, L. J.; Thompson, R. J. (1990) *The structure of the human gene encoding protein gene product 9.5 (PGP9.5), a neuron-specific ubiquitin C-terminal hydrolase. Biochem. J.* 268: 521-524

Day, I. N. M.; Thompson, R. J. (1987) *Molecular cloning of cDNA coding for human PGP 9.5 protein: a novel cytoplasmic marker for neurones and neuroendocrine cells. FEBS Lett.* 210: 157-160

Deveraux, Q.L. and Reed, J.C. (1999) *IAP family proteins – suppressors of apoptosis. Genes Dev* 13: 239-252

Dillin A. (2003) *The specifics of small interfering RNA specificity. Proc Natl Acad Sci U S A.* 100(11): 6289-6291

Dimmeler, S., Breitschopf, K., Haendeler, J. & Zeiher, A. M. (1999) *Dephosphorylation targets Bcl-2 for ubiquitin-dependent degradation: a link between the apoptosome and the proteasome pathway. J. Exp. Med.* 189: 1815-1822

Doherty FJ, Osborn NU, Wassell JA, Heggie PE, Laszlo J, Mayer RJ (1989) *Ubiquitin-protein conjugates accumulate in the lysosomal system of fibroblasts treated with cysteine proteinase inhibitors. Biochem J* 263: 47-55

Doran, J. F.; Jackson, P.; Kynoch, P.; Thompson, R. J. (1983) *Isolation of PGP 9.5, a new human neurone-specific protein detected by high resolution two-dimensional electrophoresis. J. Neurochem.* 40: 1542-1547

Drexler HC. (1997) *Activation of the cell death program by inhibition of proteasome function*. PNAS 94: 855-860

Ellinwood NM, Vite CH, Haskins ME. (2004) *Gene therapy for lysosomal storage diseases: the lessons and promise of animal models*. J. Gene. Med. 6: 481-506

Erickson RP, Bernard O (2002) *Studies on neuronal death in the mouse model of Niemann-Pick C disease*. J Neurosci Res 68: 738-744

Eskelinen E., Tanaka Y., Saftig P. (2003) *At the acidic edge: emerging functions for lysosomal membrane proteins*. Trends in Cell. Bio. 13 (3): 137-144

Fernandez-Funez P, Nino-Rosales ML, de Gouyon B, She WC, Luchak JM, Martinez P, Turiegano E, Benito J, Capovilla M, Skinner PJ, McCall A, Canal I, Orr HT, Zoghbi HY, Botas J. (2000) *Identification of genes that modify ataxin-1-induced neurodegeneration*. Nature 408: 101-106

Ferri KF, Kroemer G. (2001) *Organelle-specific initiation of cell death pathways*. Nat Cell Biol 3: E255- E263

Finn LS, Zhang M, Chen SH, Scott CR (2000) *Severe type II Gaucher disease with ichthyosis, arthrogryposis and neuronal apoptosis: molecular and pathological analyses*. Am J Genet 91: 222-226

Foghsgaard L, Wissing D, Mauch D, Lademann U, Bastholm L, Boes M, Elling F, Leist M, Jaattela M. (2001) *Cathepsin B acts as a dominant execution protease in tumor cell apoptosis induced by tumor necrosis factor*. J Cell Biol 153 (5): 999-1010

Grabowski GA, Hopkin RJ. (2003) *Enzyme therapy for lysosomal storage disease: principles, practice, and prospects*. Annu. Rev. Genomics Hum. Gen. 4: 403-436

Hacker, G. (2000) *The morphology of apoptosis*. Cell Tissue Res. 301: 5-17

Hannun, Y. A. and Bell, R. M. (1987) *Lysosphingolipids inhibit protein kinase C: implications for the sphingolipidoses*. Science 235: 670-674

Hengartner, M.O. (2000) *The biochemistry of apoptosis*. Nature 407: 770-776

Hesselink RP, Wagenmakers AJ, Drost MR, Van der Vusse GJ (2003) *Lysosomal dysfunction in muscle with special reference to glycogen storage disease type II*. Biochim Biophys Acta 1637: 164-170

Heuer GG, Passini MA, Jiang K, Parente MK, Lee VM, Trojanowski JQ, Wolfe JH (2002) *Selective neurodegeneration in murine mucopolysaccharidosis VII is progressive and reversible*. Ann Neurol 52: 762-770

Higashi Y, Murayama S, Pentchev PG, Suzuki K (1993) *Cerebellar degeneration in the Niemann-Pick type C mouse*. Acta Neuropathol 85: 175-184

Hinek A, Zhang S, Smith AC, Callahan JW (2000) *Impaired elastic-fiber assembly by fibroblasts from patients with either Morquio B disease or infantile GM1-gangliosidase is linked with deficiency in the 67-kD spliced variant of beta-galactosidase*. Am J Hum Genet 67: 23-26

Hochstrasser M, Varshavsky A (1990) *In vivo degradation of a transcriptional regulator: the yeast alpha 2 repressor*. Cell 61: 697-708

Honig LS, Rosenberg RN. (2000) *Apoptosis and neurologic disease*. Am J Med 108: 317-330

Huang JQ, Trasler JM, Igdoura S, Michaud J, Hanal N, Gravel RA (1997) *Apoptotic cell death in mouse models of GM2 gangliosidosis and observations on human Tay-Sachs and Sandhoff diseases*. Hum Mol Genet 6: 1879-1885

Igdoura S, Morales C, Tranchemontage J, Potier M (1994) *Ultrastructural and immunocytochemical study of skin fibroblasts from normal and sialidosis patients*. Cell Tissue Res 278: 527-534

Im DS, Heise CE, Nguyen T, O'Dowd BF, Lynch KR (2001) *Identification of a molecular target of psychosine and its role in globoid cell formation*. J Cell Biol 153: 429-434

Jatana M, Giri S, Singh AK (2002) *Apoptotic positive cells in Krabbe and induction of apoptosis in rat C6 glial cells by psychosine*. Neurosci Lett 330: 183-187

Jeyakumar M, Thomas R, Elliot-Smith E, Smith DA, van der Spoel AC, d'Azzo A, Perry VH, Butters TD, Dwek RA, Platt FM (2003) *Central nervous system inflammation is a hallmark of pathogenesis in mouse models of GM1 and GM2 gangliosidosis*. Brain 126: 974-987

Johnston, J., Ward, C., and Kopito, R. (1998) *Aggresomes: A cellular response to misfolded proteins*. J. Cell Biol 143: 1883-1898

Kaufmann, S.H. and Hengartner, M. (2001) *Programmed cell death: alive and well in the new millenium*. Trends Cell Biol 11: 526-534

Kitada, T., Asakawa, S., Hattori, N., Matsumine, H., Yamamura, Y., Minoshima, S., Yokochi, M., Mizuno, Y. and Shimizu, N. (1998) *Mutations in the parkin gene cause autosomal recessive juvenile parkinsonism*. Nature 392: 605-608

Kornfeld, S., and Mellman, I. (1989) *The biogenesis of lysosomes*. Annu. Rev. Cell Biol. 5: 483-525

Kurihara LJ, Kikuchi T, Wada K, Tilghman SM (2001) *Loss of Uch-L1 and Uch-L3 leads to neurodegeneration, posterior paralysis and dysphagia*. Hum Mol Genet 10: 1963-1970

Kurihara, L. J.; Semenova, E.; Levorse, J. M.; Tilghman, S. M. (2000) *Expression and functional analysis of Uch-L3 during mouse development*. Molec. Cell. Biol. 20: 2498-2504

Lane, S. C., Jolly, R. D., Schmechel, D. E., Alroy, J., and Boustany, R. M. (1996) *Apoptosis as the mechanism of neurodegeneration in Batten's disease*. J. Neurochem. 67: 677-683

Laszlo L, Doherty FJ, Osborn NU, Mayer RJ (1990) *Ubiquitinated protein conjugates are specifically enriched in the lysosomal system of fibroblasts*. FEBS 261: 365-368

Lee JC, Peter ME. (2003) *Regulation of apoptosis by ubiquitination*. Imm. Rev. 193: 39-47

Lennox, G., Lowe, J., Morrell, K., Landon, M. and Mayer, R.J. (1989) *Anti-ubiquitin immunocytochemistry is more sensitive than conventional techniques*

*in the detection of diffuse Lewy body disease. J Neurol Neurosurg Psychiatry* 52 : 67-71

Leroy E, Boyer R, Auburger G, Leube B, Ulm G, Mezey E, Harta G, Brownstein MJ, Jonnalagada S, Chernova T, Dehejia A, Lavedan C, Gasser T, Steinbach PJ, Wilkinson KD, Polymeropoulos MH (1998) *The ubiquitin pathway in Parkinson's disease. Nature* 395: 451-452

Leroy, E.; Boyer, R.; Polymeropoulos, M. H. (1998) *Intron-exon structure of ubiquitin C-terminal hydrolase-L1. DNA Res.* 5: 397-400

Lincoln, S.; Vaughan, J.; Wood, N.; Baker, M.; Adamson, J.; Gwinn-Hardy, K.; Lynch, T.; Hardy, J.; Farrer, M. *Low frequency of pathogenic mutations in the ubiquitin carboxy-terminal hydrolase gene in familial Parkinson's disease. Neuroreport* 10: 427-429, 1999.

Levecque C, Destee A, Mouroux V, Becquet E, Defebvre L, Amouyel P, Chartier-Harlin MC (2001) *No genetic association of the ubiquitin carboxy-terminal hydrolase-L1 gene S18Y polymorphism with familial Parkinson' disease. J Neural Transm* 108: 979-984

Liu Y, Fallon L, Lashuel HA, Liu Z, Lansbury PT Jr (2002) *The UCL-L1 gene encodes two opposing enzymatic activities that affect alpha-synuclein degradation and Parkinson's disease susceptibility. Cell* 111: 209-218

Lozano J, Morales A, Cremesti A, Fuks Z, Tilly JL, Schuchman E, Gulbins E, Kolesnick R (2001) *Niemann-Pick disease versus acid sphingomyelinase deficiency. Cell Death Differ* 8: 100-103

Maraganore DM, Farrer MJ, Hardy JA, Lincoln SJ, McDonnell SK, Rocca WA (1999) *Case-control study of the ubiquitin carboxy-terminal hydrolase L1 gene in Parkinson's disease. Neurology* 53: 1858-1860

March PA, Thrall MA, Wurzelmann S, Brown D, Walkley SU. (1997) *Dendritic and axonal abnormalities in feline Niemann-Pick disease type C. Acta Neuropathol (Berl)* 94: 164-172

McNaught, K.S. and Jenner, P. (2001) *Proteasomal function is impaired in sub-stantia nigra in Parkinson's disease. Neurosci Lett* 297: 191-194



Momose Y, Murata M, Kobayashi K, Tachikawa M, Nakabayashi Y, Kanazawa I, Toda T (2002) *Association studies of multiple candidate genes for Parkinson's disease using single nucleotide polymorphisms*. *Ann Neurol* 51: 133-136

Neufeld EF, Muenzer J. (2001) *The mucopolysaccharidoses*. In *The Metabolic & Molecular Bases of Inherited Diseases*, ed. Scriver, Beaudet, Valle, Sly, Childs, Kinzler, Vogelstein. p. 3421-52. New York: McGraw-Hill

Novak JP, Sladek R, Hudson TJ. (2002) *Characterization of variability in large-scale gene expression data: implications for study design*. *Genomics* 79: 104-113

Orlowski, R. Z. (1999) *The role of the ubiquitin-proteasome pathway in apoptosis*. *Cell Death Differ.* 6: 303-313

Orr H.T., Nusse R. (2000) *Reversing Neurodegeneration: A Promise Unfolds*. *Cell* 101: 1-4

Oya Y, Nakayasu H, Fujita N, Suzuki K, Suzuki K (1998) *Pathological study of mice with total deficiency of sphingolipid activator proteins (SAP knockout mice)*. *Acta Neuropathol* 96: 29-40

Park, M., Helip-Wooley, A., and Thoene, J. (2002) *Lysosomal cystine storage augments apoptosis in cultured human fibroblasts and renal tubular epithelial cells*. *J. Am. Soc. Nephrol.* 13: 2878-2887

Parton RG, Simons K, Dotti CG (1992) *Axonal and dendritic endocytic pathways in cultured neurons*. *J Cell Biol* 119: 123-137

Phaneuf D, Wakamatsu N, Huang JQ, Borowski A, Peterson AC, Fortunato SR, Ritter G, Igdoura SA, Morales CR, Benoit G, Akerman BR, Leclerc D, Hanai N, Marth JD, Trasler JM, Gravel RA (1996) *Dramatically different phenotypes in mouse models of human Tay-Sachs and Sandhoff diseases*. *Hum Mol Genet* 5: 1-14

Pshezhetsky AV, Potier M (1996) *Association of N-Acetylgalactosamine-6-sulfate Sulfatase with the Multienzyme lysosomal Complex of  $\beta$ -Galactosidase, Cathepsin A and  $\alpha$ -Neuraminidase: possible implication for intralysosomal catabolism of keratan sulfate*. *J Biol Chem* 271: 28359-28365

Renlund M, Kovanen PT, Raivio KO, Aula P, Gahmberg CG, Ehnholm C (1986) *Studies on the defect underlying the lysosomal storage of sialic acid in Salla disease. Lysosomal accumulation of sialic acid formed from N-acetyl-mannosamine or derived from low density lipoprotein in cultures mutant fibroblasts.* J Clin Invest 77: 568-574

Rodgers KJ, Dean R (2003) *Assessment of protease activity in cell lysates and tissue homogenates using peptide substrates.* Int J Biochem Cell Biol 35: 716-727

Ross, C. (1995) *When more is less: Pathogenesis of glutamine repeat neurodegenerative disease.* Neuron 15: 493-496

Ross CA and Poirier MA. (2004) *Protein aggregation and neurodegenerative disease.* Nature Med. 10: supplement p. S10-S17

Ryan, K. M., Phillips, A. C. & Vousden, K. H. (2001) *Regulation and function of the p53 tumor suppressor protein.* Curr. Opin. Cell Biol. 13: 332-337

Sadot, E., Geiger, B., Oren, M. & Ben-Ze'ev, A. (2001) *Down-regulation of  $\beta$ -Catenin by activated p53.* Mol. Cell Biol. 21: 6768-6781

Saigoh K, Wang YL, Suh JG, Yamamishi T, Sakai Y, Kiyosawa H, Harada T, Ichihara N, Wakana S, Kikuchi T, Wada K (1999) *Intragenic deletion in the gene encoding ubiquitin carboxy-terminal hydrolase in gad mice.* Nat Genet 23: 47-51

Salvesen, G.S. and Duckett, C.S. (2002). *IAP proteins: Blocking the road to death's door.* Mol Cell Biol 3: 401-410

Conzelmann E., Sandhoff K. (1983/84) *Partial enzyme deficiencies: residual activities and development of neurological disorders.* Dev Neurosci 6: 58-71

Satoh J, Kuroda Y (2001a) *Ubiquitin C-terminal hydrolase-L1 (PGP9.5) expression in human neural cell lines following induction of neuronal differentiation and exposure to cytokines, neurotrophic factors or heat stress.* Neuropathol Appl Neurobiol 27: 95-104

Satoh J, Kuroda Y (2001b) *A polymorphic variation of serine to tyrosine at codon 18 in the ubiquitin C-terminal hydrolase-L1 gene is associated with a reduced risk of sporadic Parkinson's disease in Japanese population.* J Neurol Sci 189: 113-117

Schwartz LM, Myer A, Kosz L, Engelstein M, Maier C. (1990) *Activation of polyubiquitin gene expression during developmentally programmed cell death.* Neuron 5: 411-419

Segui B, Bezombes C, Uro-Coste E, Medin JA, Andrieu-Abadie N, Auge N, Bouchet A, Laurent G, Salvayre R, Jaffrezou JP, Levade T. (2000) *Stress-induced apoptosis is not mediated by endolysosomal ceramide.* FASEB J. 14(1): 36-47

Seyrantepe V, Landry K, Trudel S, Hassan JA, Morales CR, Pshezhetsky A (2004) *Neu4, a novel human lysosomal lumen sialidase confers normal phenotype to sialidosis cells.* J Biol Chem 279: 37021-37029

Shih, S.C., Sloper-Mould, K.E. and Hicke, L. (2000) *Monoubiquitin carries a novel internalization signal that is appended to activated receptors.* EMBO J., 19: 187-198

Simonaro CM, Haskins ME, Schuchman EH (2001) *Articular chondrocytes from animals with a dermatan sulfate storage disease undergo a high rate of apoptosis and release nitric oxide and inflammatory cytokines: a possible mechanism underlying degenerative joint disease in the mucopolysaccharidoses.* Lab Inv 81: 1319-1328

Snyder, H., Mensah, K., Theisler, C., Lee, J.M., Matouschek, A., and Wolozin, B. (2003) *Aggregated and Monomeric  $\alpha$ -Synuclein bind to the S6' Proteasomal Protein and Inhibit Proteasomal Function.* J Biol Chem (epub ahead of print)

Suh, J. G.; Yamanishi, T.; Matsui, K.; Tanaka, K.; Wada, K. (1995) *Mapping of the gracile axonal dystrophy (gad) gene to a region between D5Mit197 and D5Mit113 on proximal mouse chromosome 5.* Genomics 27: 549-551

Suzuki K (1976) *Neuronal storage diseases: a review* in: Progress in Neuropathology, Zimmerman HM (ed.), Volume 3, pp.173-202, Grune & Straton: New York

Suzuki K. and Mansson JE. (1998) *Animal models of lysosomal disease: an overview.* J. Inh. Metab. Dis. 21: 540-547

Swerdlow PS, Finley D, Varshansky A (1986) *Enhancement of immunoblot sensitivity by heating of hydrated filters*. Anal Biochem 156: 147-153

Taniike, M., Mohri, I., Eguchi, N., Irikura, D., Urade, Y., Okada, S. and Suzuki, K. (1999) *An apoptotic depletion of oligodendrocytes in the twitcher, a murine model of globoid cell leukodystrophy*. J. Neuropathol. Exp. Neurol. 58: 644-653

Tohyama, J., Oya, Y., Ezoe, T., Vanier, M. T., Nakayasu, H., Fujita, N., and Suzuki, K. (1999) *Ceramide accumulation is associated with increased apoptotic cell death in cultured fibroblasts of sphingolipid activator protein-deficient mouse but not in fibroblasts of patients with Farber disease*. J. Inherit. Metab. Dis. 22: 649-662

Varshavsky A (1997) *The ubiquitin system*. Trends Biochem Sci 22: 383-387

Wada, R., Tiffet, C. J., and Proia, R. L. (2000) *Microglial activation precedes acute neurodegeneration in Sandhoff disease and is suppressed by bone marrow transplantation*. Proc. Natl. Acad. Sci. USA 97:10954-10959

Walkley SU. (1998) *Cellular pathology of lysosomal storage disorders*. Brain Path. 8: 175-193

Walkley SU (1987) *Further studies on ectopic dendrite growth and other geometrical distortions of neurons in feline GM1 gangliosidosis*. Neuroscience 21: 313-33176

Walkley SU (1988) *Pathobiology of neuronal storage disease*. Int Rev Neurobiol 29: 191-244

Walkley SU, Baker HJ, Rattazzi MC, Haskins ME, Wu J-Y. (1991) *Neuroaxonal dystrophy in neuronal storage disorders: Evidence for major GABAergic neuron involvement*. J Neurol Sci 104:1-8

Wang J, Zhao C-Y, Si Y-M, Liu Z-L, Chen B, Yu L (2002) *ACT and UCH-L1 polymorphisms in Parkinson's disease and age of onset*. Mov Dis 17: 767-771

Wilkinson KD. (1997) *Regulation of ubiquitin-dependent processes by deubiquitinating enzymes*. FASEB 11: 1245-1256

Wilkinson KD, Lee KM, Deshpande S, Duerksen-Hughes P, Boss JM, Pohl J (1989) *The neuron-specific protein PGP 9.5 is a ubiquitin carboxyl-terminal hydrolase*. Science 246: 670-673

Winchester B., Vellodi A., Young E. (2000) *The molecular basis of lysosomal storage diseases and their treatment*. Bioch. Society Transactions 28 (part 2): 150-153

Wing S. *Deubiquitinating enzymes :the importance of driving in reverse along the ubiquitin-proteasome pathway*. (2003) Intern. J. Bioch. and Cell bio. 35: 590-605

Wu, Y. P., Kubota, A., and Suzuki, K. (1999) *Neuronal death and reactive glial changes in the brain of Niemann-Pick disease type C mouse*. Soc. Neurosci. Abstr. 25: 1118

Xiaozhe H., Salomon A. (2004) *Secreted Frizzled-related Protein 1 (SFRP1) Protects Fibroblasts from Ceramide-induced Apoptosis*. JBC 279; 4: 2832-2840

Yamazaki, K.; Wakasugi, N.; Tomita, T.; Kikuchi, T.; Mukoyama, M.; Ando, K. (1988) *Gracile axonal dystrophy (GAD), a new neurological mutant in the mouse*. Proc. Soc. Exp. Biol. Med. 187: 209-215

Yuan, J. & Yankner, B. A. (2000) *Apoptosis in the nervous system*. Nature 407: 802-809

Yoshimori T. (2002) *Toward and beyond lysosomes*. Cell Struct. and function 27: 401-402

Zhan S-S, Beyreuther K, Schmitt HP (1992) *Neuronal ubiquitin and neurofilament expression in different lysosomal storage disorders*. Clin Neuropathol 11: 251-255

Zhou J, Cox NR, Ewald SJ, Morrison NE, Basker HJ (1998) *Evaluation of GM1 ganglioside-mediated apoptosis in feline thymocytes*. Vet Immunol Immunopathol 66: 25-42